NANOPARTICLE OXIDES AS CATALYST SUPPORTS FOR THE OXIDATIVE COUPLING OF 4-METHYLPYRIDINE OVER PALLADIUM

By

LUKE MICHAEL NEAL

A DISSERTATION PRESENTED TO THE GRADUATE SCHOOL
OF THE UNIVERSITY OF FLORIDA IN PARTIAL FULFILLMENT
OF THE REQUIREMENTS FOR THE DEGREE OF
DOCTOR OF PHILOSOPHY

UNIVERSITY OF FLORIDA

2008

To my Mom and Dad

ACKNOWLEDGMENTS

Many people have helped me arrive at this point in my research. First, I thank my advisor, Dr. Helena Hagelin-Weaver, for her technical guidance and patient support of my research. My committee Dr. Gar Hoflund, Dr. David Hahn, and Dr. Kirk Ziegler also provided important guidance in my research and writing. Group members Sam Jones, Mike Everett, Justin Dodson and Daniel Hernandez provided valuable assistance to me in the lab over the years. The American Chemical Society Petroleum Research Fund supported portions of this research. I am grateful to Prof. Angela Lindner (Environmental Engineering Sciences, EES) for her fruitful collaboration and for providing equipment used to initiate experiments during this research. Dr. David Mazyck (EES) provided an activated carbon sample used during the research project. Melani Withana and Charlotta Brodin performed the initial work on this research project. The Particle Engineering Research Center and the Major Analytical Instrumentation Center at the University of Florida and their staff, particularly Gill Brubaker and Dr. Kerry Siebein provided valuable assistance. I also thank my former colleagues and supervisors at the USDA National Center for Agriculture Utilization Research (NCAUR) in Peoria, Illinois for their encouragement in my pursuit of additional studies and research in the field of chemical engineering. Finally, I thank my parents for their unwavering support throughout my years of study.

TABLE OF CONTENTS

page

LIST OF TABLES

LIST OF FIGURES

Abstract of Dissertation Presented to the Graduate School of the University of Florida in Partial Fulfillment of the Requirements for the Degree of Doctor of Philosophy

NANOPARTICLE OXIDES AS CATALYST SUPPRTS FOR THE OXIDATIVE COUPLING OF 4-METHYLPYRIDINE OVER PALLADIUM

By

Luke Michael Neal

December 2008

Chair: Helena E. Hagelin-Weaver
Major: Chemical Engineering

The use of nanoparticles as supports for palladium catalysts was studied for application to the oxidative coupling of 4-methylpyridine via C-H activation and C-C coupling. The product of this oxidative coupling is 4,4'-dimethyl-2,2'-bipyridine which is a useful but expensive chelating agent. Although palladium on alumina are traditionally poor catalysts in this reaction, an excellent palladium on nanoparticle alumina catalyst was developed which exceeds the activities of the traditional palladium on carbon catalyst. This nanoparticle catalyst only gives high activities when prepared by precipitation. Other nanoparticle oxide supports were found that give highly active palladium catalyst for the oxidative coupling reaction, including nanoparticle magnesia and zirconia. Additionally, some traditional porous supports were found to result in active catalysts, including gamma-alumina, titania, and silica, but only the porous titania had activities comparable to the best performing nanoparticle-supported catalysts. It was also determined that zirconia and ceria are effective additives in several of the palladium catalysts.

In general, oxides with strong palladium-support interactions, and/or very high surface areas were the most active. This is attributed to electrophilic palladium oxide particles that can form on supports with strong metal-support interactions or to the numerous low-coordination

edge or corner sites of the high surface area supports. The electrophilicity of these particles was determined by x-ray photoelectron spectroscopy (XPS). It was also shown that basic sites on the support are not necessary for forming an active catalyst, but that a high concentration of acidic support sites tends to give more active catalysts.

Optimization studies of the catalysts were also performed. It was determined that 2.5, 5, and 10% loadings of palladium on nanoparticle alumina give the same product yield per unit weight of catalyst, which indicates a structure sensitive reaction. Lowering the Pd loading to 1% decreases the yield palladium loadings of ~ 2.5% were, thus, determined to be optimal on the nanoparticle alumina support. Additionally it was shown that titration to a pH of 11 gives more consistent results compared with titration to a simple stoichiometric excess (based on the amount of palladium(II) nitrate used).

CHAPTER 1
INTRODUCTION

1.1 Overview

The oxidative coupling of 4-methylpyridine over palladium via C-H activation and C-C coupling (Figure 1-1) is a useful system for the study of nanoparticle oxide catalyst supports. Early research has shown that palladium on carbon (Pd/C) is a reasonably good catalyst for this reaction [1-4], and that palladium on alumina is a poor catalyst [1]. The reason for the large differences in activities between the carbon and alumina supported catalyst is not fully explained in literature, as the carbon support's advantage is mainly high surface area with concurrent propensity to give high metal dispersion. It has been suggested that palladium oxide is the active phase [5] and commercial alumina catalysts are often prereduced. As such, it was predicted that palladium supported on nano-alumina would be active due to the oxidized palladium of prepared catalysts, and the unique properties of nanoparticles, including relatively high surface areas. In this research, the use of nanoparticle alumina and other nano-oxides, as well as porous oxides, as supports for palladium catalysts was studied in the oxidative coupling reaction. Additionally the properties of these catalysts were probed to determine what contributes to the activity of a palladium catalyst for this reaction system.

1.2 Background

1.2.1 Nanoparticle Oxide Supports

Nanoparticles are particles with diameters of less than 100 nm particularly those with diameters in the size range of 0.5-20 nm. Due to their small size, they can have very high surface areas per unit mass. Additionally, they have a high density of edge and corner sites, which have low coordination [6]. With these low coordination sites, nanoparticle oxide supports are expected to interact more strongly with the active catalyst phase(s) than the traditionally used

porous oxides. These interactions may result in high dispersions and/or significantly alter the electronic environment of the palladium/palladium oxide particles.

1.2.2 Palladium Catalysts

In heterogeneous catalysis palladium (Pd) is typically dispersed onto a high surface area support. This increases the metal surface area available to catalyze the reaction and helps prevent sintering of the small palladium particles. This is particularly important due to palladium's high cost. However, in addition to maintaining a high palladium surface area, the support can also interact strongly with palladium. Therefore, different supports can give palladium catalysts with somewhat different properties. Consequently, palladium catalysts can be tailored to a wide array of reaction systems. Palladium on carbon (Pd/C), one of the most widely used Pd catalysts, is efficient in hydrogenation reactions. There are, however, numerous palladium catalysts studied for oxidation reactions, in particular low temperature and selective oxidations, that may be better suited for oxidative coupling. Palladium on alumina is a typical oxidation catalyst [7], and is of particular interest for oxidation of methane [8] as the mechanism involves the activation of methane's very strong C-H bonds [9-11]. Pd/tin oxide is also an effective low-temperature methane oxidation catalyst [12,13]. Pd/titania is used in selective hydrogenation such as partial hydrogenation of alkadienes to alkenes [14]. Titania is also of interest as a support as it has been reported to have strong metal support interactions in palladium catalysts which change the CO and H_2 uptake of the palladium phase, with the strength of the interaction depending upon the titania structure (anatase or rutile) and the heat treatment of the catalyst [14]. Reactions activated by acidic sites such as oxidation of ethane [15] proceed well on palladium supported on silica and modified silica. Pd/ceria and Pd/ceria-zirconia have interesting redox properties that make them good catalysts for CO to CO_2 oxidation [16-18]. Pd/zirconia and Pd/magnesia are also of interest in a coupling reaction as they catalyze the

aromatization of hexane to aromatic compounds [19]. If the high dispersion properties of Pd/C can be obtained on a nanoparticle oxide, there would be great potential to find a more suitable support for the oxidative coupling reaction.

1.2.3 Bipyridines: Applications and Synthesis

Bipyridines are excellent chelating agents that form useful transition metal complexes [20]. The interesting properties of these complexes make them suitable for a range of catalytic and photochemical systems. Ruthenium/bipyridine complexes adsorb visible light and exhibit electron transfer and chemiluminescence properties [21,22,], making them promising for use in artificial photosynthesis [23] and chemiluminescence detection systems [24]. Copper/bipyridine catalysts are widely used in atom transfer radical polymerization (ATRP) reactions [25]. Iron and cobalt/bipyridine complexes can catalyze the reduction of CO_2 [26]. Palladium/bipyridine complexes are applied in numerous organic reactions including oxidative carbonylations [27], the Kumada-Corriu reaction [28], and the Suzuki cross-coupling reaction [29].

Of the bipyridines, 4,4'-dimethyl-2,2'-bipyridine is particularly useful as it can be derivatized in the 4 positions [30]. However, it is also prohibitively expensive for industrial scale use. The methods of synthesizing this bipyridine are expensive and time consuming, which results in very high prices (more than $5,200/kg, [31]). Some bipyridine synthesis methods include building a second pyridine ring onto a substituted pyridine precursor, and coupling of halogenated pyridines precursors have also been used [32-34]. Unfortunately, these processes are complex, use expensive and environmental unfriendly starting materials, and require involved subsequent purification steps.

Of the synthesis pathways, the coupling of pyridine is the simplest. This coupling can be accomplished with over Raney nickel or palladium [1-4]. Although Raney nickel (or skeletal nickel) is a common and relatively inexpensive catalyst, it requires complicated pretreatments

and special handling due to its pyrophoric nature, making it undesirable as catalyst. Oxidative coupling of 4-methylpyridine to 4,4'-dimethyl-2,2'-bipyridine over palladium, on the other hand is a simple one-step reaction (Figure 1-1), in which the only products are water, the bipyridine, and a small amount of terpyridine byproduct. The Pd catalyst is relatively safe and requires no special handling. However, this reaction is slow, and the catalyst loses activity during reaction [5]. Finding an improved palladium catalyst for this reaction would make use of 4,4'-dimethyl-2,2'-bipyridine more viable economically.

1.2.4 Catalyst Characterization Techniques

In the research presented here numerous techniques were used to characterize the supports. Detailed descriptions of the technique can be found in several textbooks and hand books such as Masel [35], Cullity [36] and the Handbook of X-ray Photoelection Spectroscopy [37]. However, a brief overview is in order.

1.2.4.1 Brunauer-Emmett-Teller (BET) surface area measurements

The surface areas of the catalysts and catalyst supports were determined using BET adsorption isotherms, which are described in detail in Masel [35]. Briefly, in the instrument used in these studies (Quantachrome Nova 1200) nitrogen is adsorbed onto the catalyst or support surface by pulsing nitrogen gas into an evacuated sample cell that contains the catalyst or support and is immersed in liquid nitrogen (Figure 1-2). An isotherm (constant temperature ~123 K) plot that relates the cell pressure (P) to the volume of gas pulsed into the cell (V) is created (Figure 1-3). By finding the slope of the isotherm plot and its zero pressure intercept, the volume of nitrogen necessary to adsorb one-monolayer (V_M) of nitrogen molecules on the surface can be calculated:

$$V_M = \frac{1}{Slope + Intercept} \quad [36]$$

Because the cross-sectional area of nitrogen can be determined (16.2 $Å^2$) [35] the amount of area one monolayer of nitrogen covers can be calculated. This area is approximately equal to the surface area of the adsorbent (catalyst/support) surface.

1.2.4.2 Chemisorption measurements

Masel [35] also describes the chemisorption phenomena in detail. Chemisorption measurements are powerful techniques for probing the sample surface. Carbon monoxide (CO) chemisorption is commonly used to determine the surface area of palladium metal on a catalyst support. CO adsorbs to metal atoms on surfaces and if the stoichiometry of CO to Pd surface atoms is known then the number of Pd atoms on the surface can be calculated. Additionally with estimates of the shapes of Pd particles on the support surface, the surface area of palladium and palladium crystallite sizes can be calculated. These calculations are described in a detailed in chapter 3. By using an acidic or basic gas, such as CO_2 or NH_3, the number of basic and acidic sites on a support can also be measured.

In the studies presented here chemisorption measurements were performed on a ChemBET 3000. This instrument works by titrating a known amount of adsorbate gas (such as CO, CO_2 or NH_3) gas into a stream of inert makeup gas (such as helium) (Figure 1-3). The titrated stream then flows over the sample surface, where the active gas is adsorbed onto the surface until the surface is saturated. The amount of unabsorbed titrate gas in the makeup stream is then measured with a thermal conductivity detector (TCD).

1.2.4.3 X-ray photoelectron spectroscopy (XPS)

An excellent overview of XPS can be found in The Handbook of X-pay Photoelectron Spectroscopy [37]. In this technique a solid surface is exited with an X-ray source (Figure 1-4). Electrons from the surface and near surface region of a solid are ejected into a vacuum by this excitation. If these ejected photoelectrons escape without other effects, they have an energy

equal to the exciting x-ray source less the energy required to remove the electron (binding energy) from the solid and the work function of the spectrometer. This binding energy is partially dependent upon the energy of the near surface atoms before (initial state) and after (final state) the electron is removed. The binding energies of electrons from various orbitals are different not only for different elements, but for different oxidation states of the same element, as well as the electronic environment of the atom. In XPS the kinetic energy of the ejected photoelectron is then measured. Since the energy of the exciting x-ray is known (typically magnesium or aluminum $K_{\alpha 1,2}$) and the work function of the spectrometer is corrected for by use of a standard, the binding energy of the electron can be calculated. This allows for the elemental composition of the surface as well as the oxidation state of the surface atoms to be determined. Since this is a surface technique it is a very powerful tool for probing catalysts, where their behavior is determined by surface atoms. However, this is an ultra high vacuum (UHV) (pressures less than 10^{-9} Torr) technique, requiring special equipment.

1.2.4.4 X-ray diffraction (XRD)

X-ray diffraction (XRD) is covered in detail in numerous textbooks such as Cullity [36]. In XRD an x-ray beam is directed at a solid sample. If the sample is crystalline than a diffraction pattern will emerge due to the planes of the crystal. The angel of diffraction is dependent upon the wavelength (λ) of the incident light and the distance between the parallel planes (d_{hkl}) of diffraction (Figure 1-5) as described by the Bragg equation:

$$n\lambda = 2d_{hkl} \cdot \sin(\theta)$$

(Where n must be an integer for a reflection to be observed)

If the composition of the sample is known then the crystal phases present can be determined by comparing the diffraction pattern to known standards. Additionally in powder

XRD where the sample is polycrystalline the average diameter of the crystals (d_{av}) can be determined from the peak widths (full width at half maximum or *FWHM*) and the angle of the reflection (θ) diffraction patterns by the Scherrer equation:

$$d_{av} = K \cdot \lambda \; / \; (FWHM \cdot \cos(\theta))$$

(*K* is a prefactor determined by the instrument, but is typically assigned a value of unity)

However, care must be taken when using XRD to characterize catalysts. The attenuation depth of diffracted x-rays in the samples can be several micrometers, which is several orders of magnitude greater than the thickness of surface atom layers. Powder XRD is thus a bulk technique in terms of catalysts. Additionally, the active surface phase can be amorphous and would thus not be detected by XRD. Consequently it may be impossible to probe the active surface phase in many catalysts with XRD. And the XRD patterns obtained may be for inactive phases far removed from the catalyst surfaces. Nonetheless, knowing these limitations and when used in conjunction with surface techniques, powder XRD can give important information.

1.3 Objectives

In this work palladium on nanoparticle oxide supports are studied for the use in the synthesis of 4,4'-dimethyl-2,2'-bipyridine. Prior to this research the highest yields reported for a catalyst (5% Pd/C) is ~2 g product per gram of catalyst, i.e. 40 g/g Pd [38], with lower yields being typical [4,39,40].

In the research presented here a palladium on nanoparticle alumina catalyst was developed and studied for this reaction as a proof of concept. Additional nanoparticle and porous oxide supports were then studied to find the most active and economical support materials. Once prospective supports were developed, the use of promoters was studied to increase yields further. Additionally an extensive characterization of these catalysts was undertaken to determine the

important properties responsible for catalyst activity. Finally, optimization was undertaken to develop the best possible catalyst by the simplest means.

The objectives of this research were: 1) showing that nanoparticle oxides are viable supports for palladium catalysts in the production of 4,4'-dimetyl-2,2'-bipyridine via oxidative coupling of 4-methylpyridine, 2) determining what support/catalyst properties are responsible for activity, and 3) developing an economically viable catalyst.

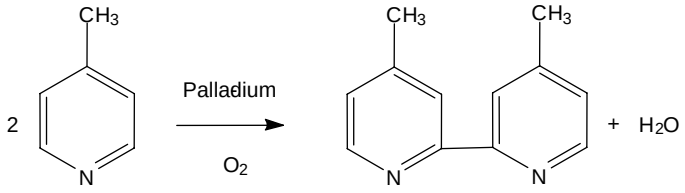

Figure 1-1 Palladium-catalyzed oxidative coupling of 4-methylpyridine.

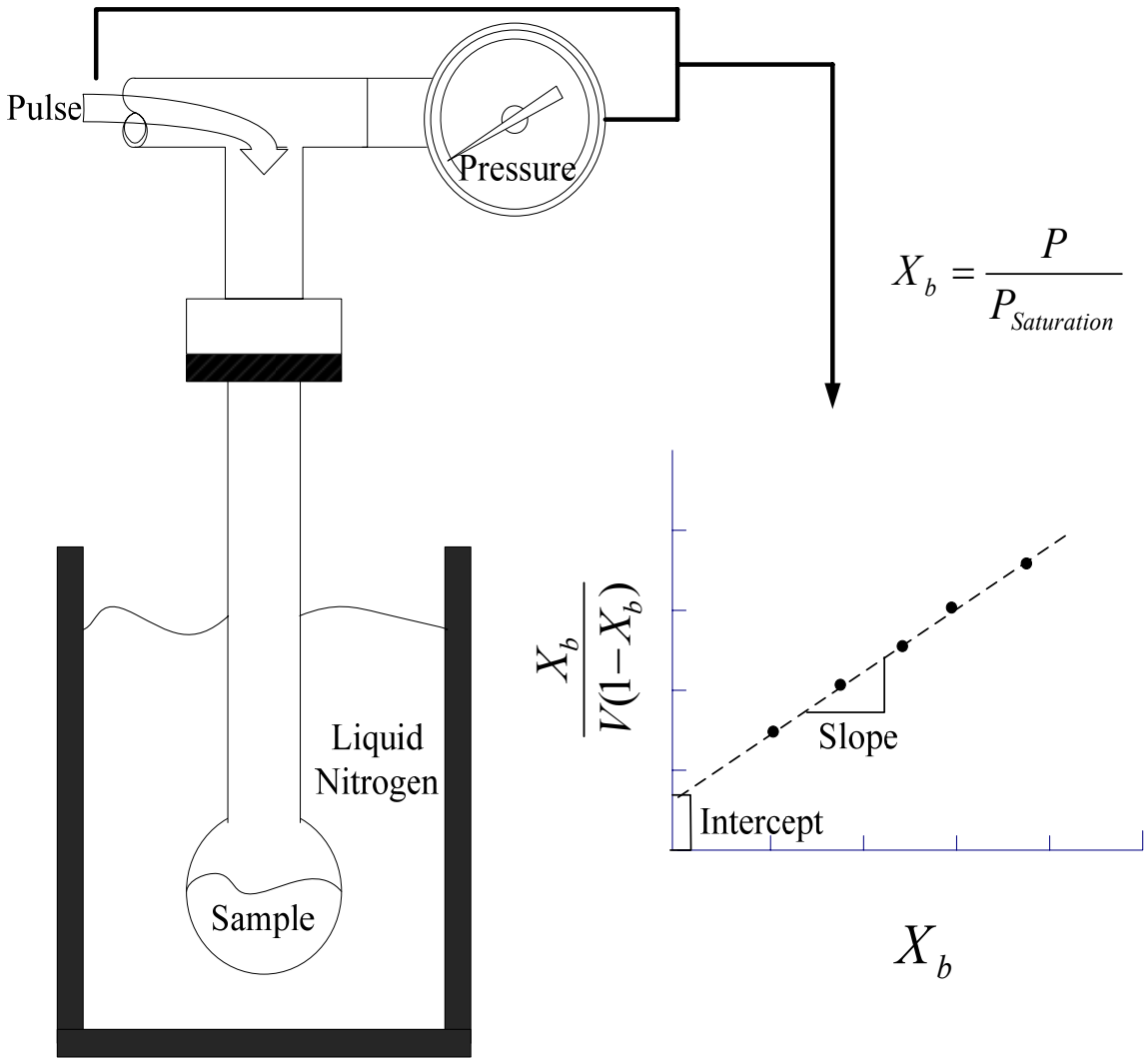

Figure 1-2 Brunauer-Emmett-Teller (BET) measurement and BET isotherm

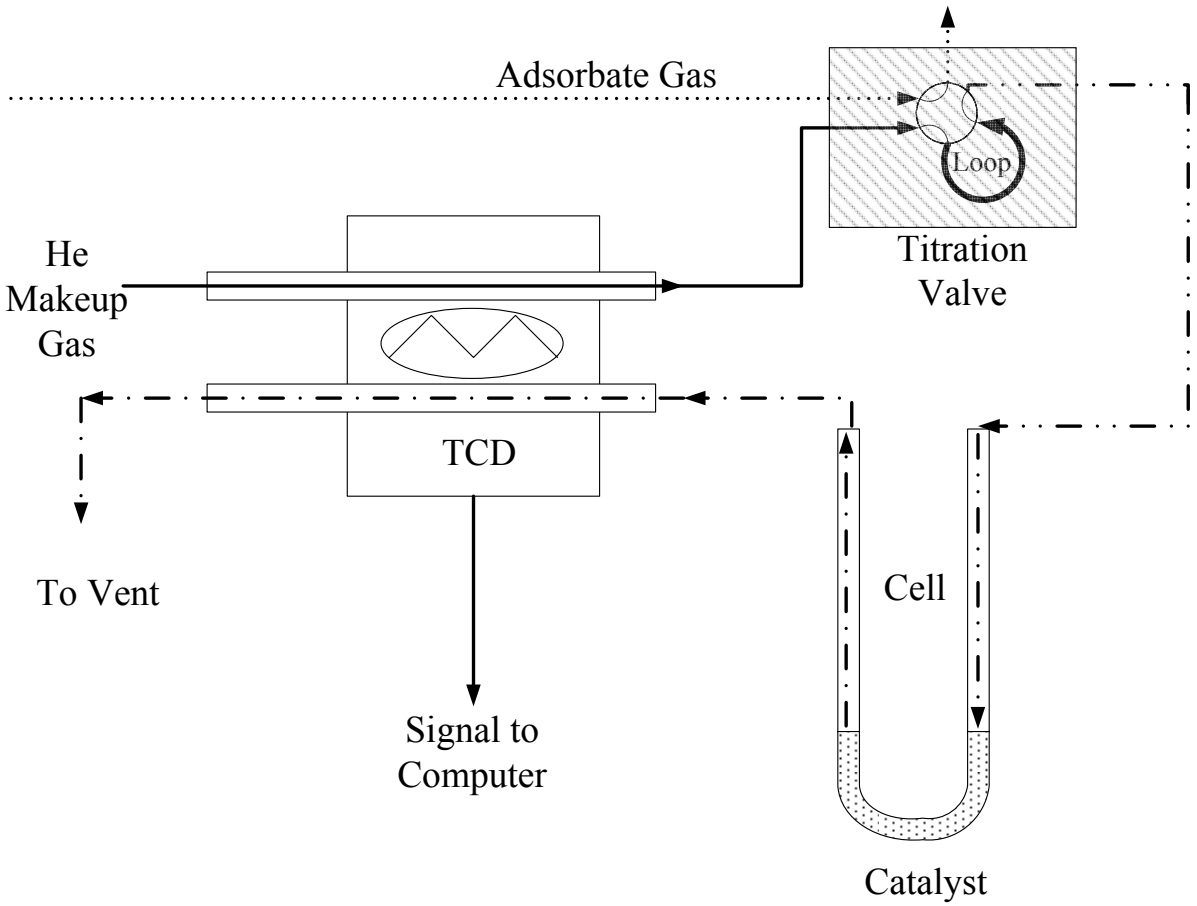

Figure 1-3 ChemBET chemisorption measurement

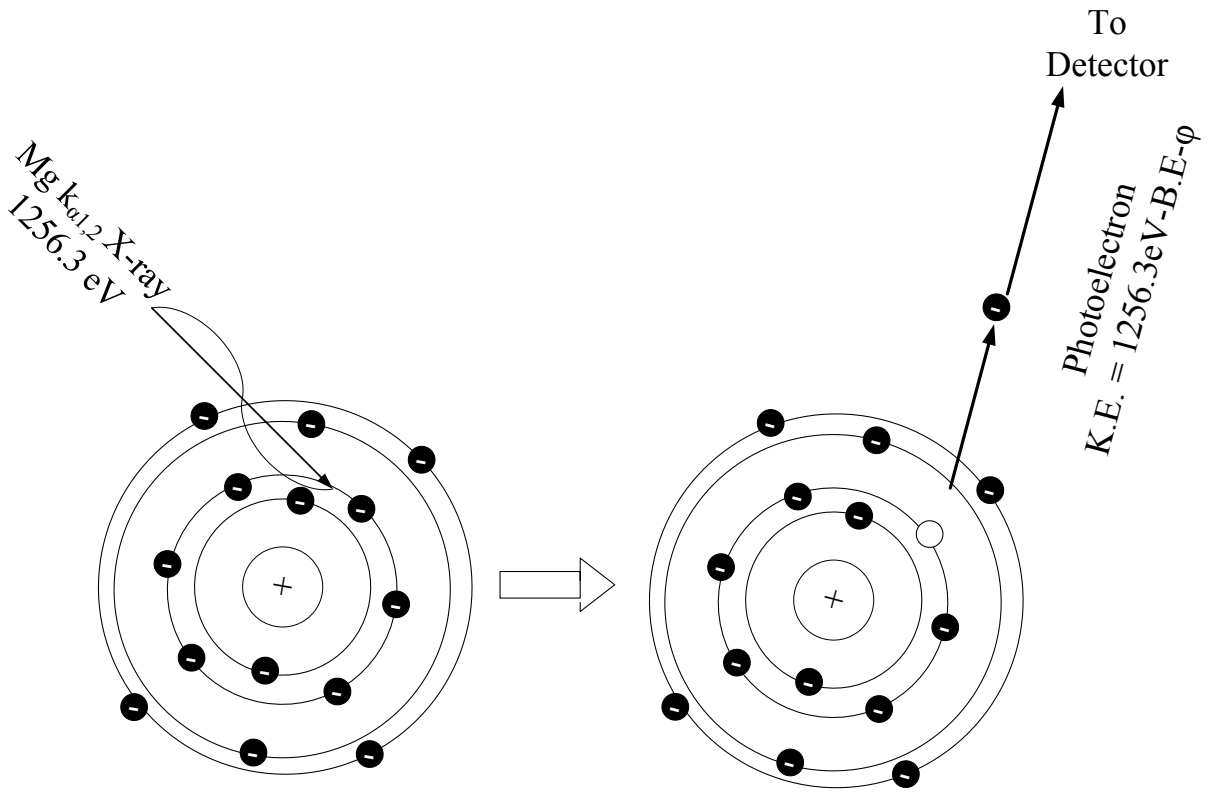

Figure 1-4 X-ray photoelectron spectroscopy (XPS)

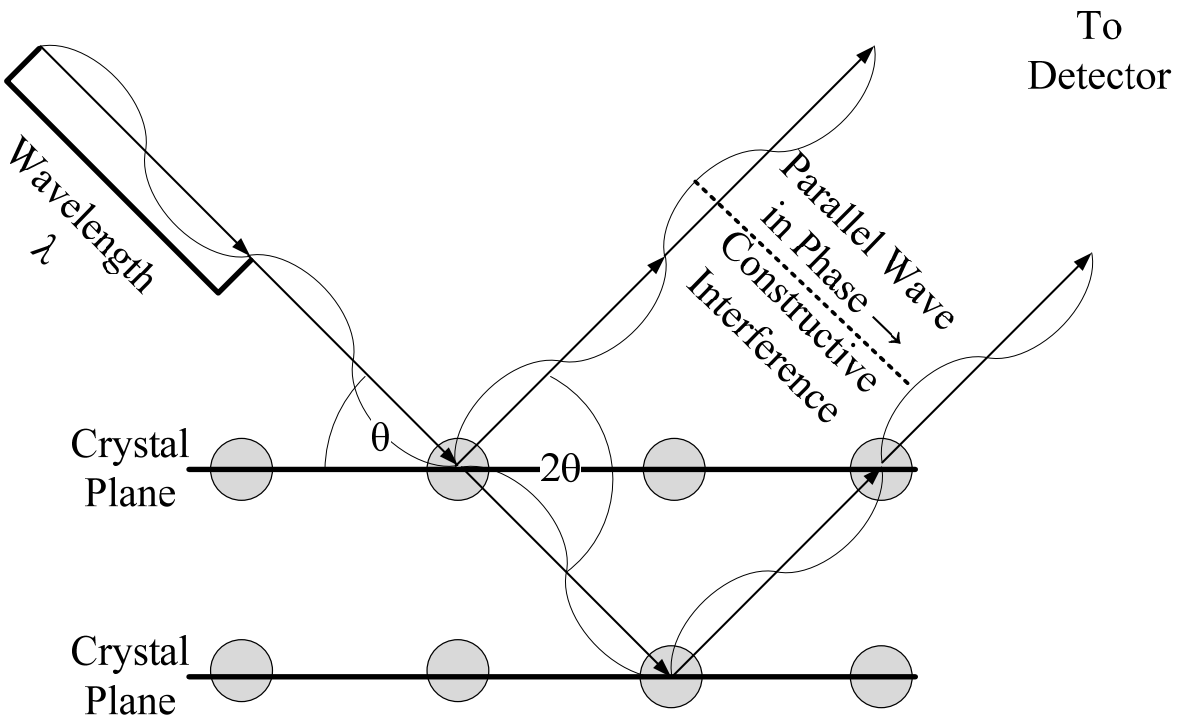

Figure 1-5 X-ray Diffraction (XRD)

CHAPTER 2
C-H ACTIVATION AND C-C COUPLING OF 4-METHYLPYRIDINE USING PALLADIUM SUPPORTED ON NANOPARTICLE ALUMINA[1]

2.1 Introduction

Bipyridines are receiving increasing attention in the literature due to their ability to coordinate to transition metal cations and form complexes with interesting properties [20]. The importance of metal complexes containing bipyridine ligands has been revealed in several reviews that have been published in the past fifteen years on the synthesis of bipyridines, as well as on properties of metal-bipyridine complexes and their applications [21,22,41-43]. Of the transition metals, bipyridine complexes of ruthenium are by far the most commonly studied systems [21,43]. This is due to their unique photo- and electrochemical properties. Ruthenium-bipyridine complexes can absorb photons in the visible light region and have unique redox properties that can lead to electron transfer and chemiluminescence, which make them suitable for application in solar energy conversion (e.g. in solar cells and artificial photosynthesis systems [43,44]), in organic light-emitting diodes [23] and in chemiluminescence detection systems [24]. Bipyridines are also commonly used as ligands to metals in various catalyst systems. For example, many copper-based atom transfer radical polymerization (ATRP) catalysts contain bipyridine units [25]. Iron and cobalt complexes of bi- or ter-pyridines have been shown to catalyze the reduction of CO_2 and O_2 [26]. Palladium bipyridine complexes have been used as catalyst in several reactions, such as oxidative carbonylation [27], the Kumada-Corriu reaction [30], and the Suzuki cross-coupling reaction [29]. Of the bipyridines, 4,4'-dimethyl-2,2'-bipyridine is of particular interest, since this compound can easily be modified by reactions with

[1] Reprinted from Journal of Molecular Catalysis A: Chemical Vol. 284 pp. 141–148, Luke M. Neal, Helena E. Hagelin-Weaver (2008) with permission from Elsevier

the methyl groups in the 4-positions. However, due to the poor yields in the coupling reaction of 4-methylpyridine, the production of 4,4' dimethyl-2,2'-bipyridine is prohibitively expensive for large scale processes. A kilogram quantity sells for more than $4,500, [45] while smaller quantities sell for significantly higher prices per unit weight.

Bipyridines can be formed via a number of pathways. Some include building the second pyridine ring from a substituted pyridine, while other methods rely on the coupling of halogenated pyridines using transition metal catalysts [32-34]. The disadvantages with these processes are the low yields of multi-step processes, the cost of the halogenated precursors and the environmental impact of the waste streams of halide salts and other byproducts that result from these reactions. Furthermore, these processes require a high level of subsequent purification for applications that are sensitive to halogens, such as catalysis. Consequently, a one-step process in which the bipyridine is formed directly from the pyridine reactant is desirable. The oxidative coupling of 4-methylpyridine to 4,4'-dimethyl-2,2'-bipyridine using palladium on carbon as the catalyst meets this criterion (Figure 2-1). This reaction requires only a catalyst plus the reactant and the only by-products of the reaction are water and the terpyridine (Figure 2-1). Furthermore, compared to its halogenated derivatives (the most active bromo-derivative is available through reaction with commercially available 2-amino-4-methylpyridine at ~$200/kg [34, 46]), 4-methylpyridine is relatively inexpensive (less than $40/kg [47]) with lower environmental impact. The disadvantages of this reaction are the slow reaction rate and the deactivation of the catalyst [5].

Early research has shown that 2,2'-bipyridines can be formed via coupling of pyridine derivatives over catalysts such as Raney nickel and palladium on carbon (Pd/C) [1-4]. The results from these early experiments reveal that while palladium on carbon is a reasonable

catalyst in the coupling reaction of pyridine derivatives, palladium on alumina exhibits poor activity [1]. No explanation as to why alumina is an inferior support has been given in the literature. The early research also indicated that low-valent palladium is the active form of the Pd/C catalysts. However, more recent results revealed that the active catalyst actually contains a Pd(II) species [5] and that the variation in catalytic activity between batches of Pd/C catalysts could be reduced by simply oxidizing the catalyst before reaction. However, despite previous improvements of the catalyst, the reaction is slow and suffers from catalyst deactivation. One of the major limitations of the reaction appears to be reoxidation of Pd in these solution experiments, since the catalyst after exposure to the reaction conditions is in a reduced form [5]. The maximum isolated yield reported for a 5% Pd/C is ~2 g product per gram of catalyst, i.e. 40 g/g Pd [38]. However, yields of 1.5-2 g/g for a 10% Pd/C catalysts are more common [5, 39, 40]. Comparing these product yields to reactions using a homogeneous catalyst complex or halogenated precursors in solution is difficult. The yields reported as converted reactant tend to be higher for reactions in solution with halogenated precursors [33, 34, 48], while the yield per gram of palladium generally is higher in reactions where 4-methylpyridine is the reactant and no solvent is used (See summary of literature yields in Table 2-1). Furthermore, the higher conversion of reactant for the reactions using solvent and halogenated precursors can be outweighed by the lower yields per gram of palladium, the formed byproducts (halide salts) and the use of solvent. Furthermore, the unreacted 4-methylpyridine can easily be recovered in the reactions with no solvent and a heterogeneous catalyst and there is a potential for recycling and regeneration of the heterogeneous catalyst. Therefore, there are significant advantages of synthesizing 4,4'-dimethyl-2,2'-bipyridine using a heterogeneous catalyst and no solvent, particularly if the yields can be increased. Naturally, the converted reactant yield can also be

increased in reactions with no solvent by simply increasing the catalyst-to-reactant ratio, although more terpyridine byproduct will be formed in these cases.

Our hypothesis is that palladium supported on nanoparticle oxide supports has potential to be a very efficient catalyst. This hypothesis is based on the fact that nanoparticles have a large surface area compared to their bulk analogues. Furthermore, nanoparticles have a high degree of low coordination sites, such as corners and edges [6]. These low coordination sites may cause a stronger interaction between the support oxide and the active metal deposited onto the nanoparticles compared with more conventional supports. In addition to potentially higher dispersions of the active metal, these interactions may result in unique catalytic properties. It is possible that this is the reason for the high activity observed at low temperatures in the palladium-catalyzed oxidation of methane when nanoparticle oxides are used as supports [49]. Consequently, not only the large surface area, but also the intrinsic properties of nanoparticle oxides can result in unique catalytic activities of nanoparticle-supported catalysts.

The main objective in this work is to determine if palladium supported on nanoparticle alumina can be an efficient catalyst in the coupling of pyridines despite previous research showing that commercial palladium on alumina is a poor catalyst in this reaction. Part of the objective is also to determine the effects of catalyst preparation on the catalytic activity and if the active species is likely to be a dissolved homogeneous complex instead of heterogeneous palladium surface species.

2.2 Experimental

2.2.1 Catalysts Preparation

The catalysts were prepared using commercially available alumina nanoparticles [50]. Two catalyst preparation methods were used; wet impregnation and precipitation. In the wet impregnation method the support powders were dispersed in an aqueous solution of palladium

nitrate (Fluka or Alfa Aesar). The water was then boiled off until a paste consistency was achieved. This paste was dried in a muffle furnace at 105°C overnight. The dried samples were ground and calcinated at 450°C for 3 hours to decompose the palladium nitrate and form palladium oxide on the support.

In the precipitation method, the support was dispersed into a solution of palladium nitrate. The mixture was then titrated with a NaOH solution, which formed $Pd(OH)_2$ on the support [51]. The amount of NaOH used in these experiments corresponds to 50% stoichiometric excess. The resulting mixture was aged overnight at room temperature before it was filtered. The recovered catalyst was rinsed by stirring in water overnight, followed by another filtration. As for the catalysts prepared via the wet impregnation method, the precipitated samples were dried over night at 105°C and calcinated at 450°C for 3 hours.

Several commercial catalyst supports and catalysts were also used for catalyst preparation, or used as received, and tested for activity in the coupling reaction of 4-methylpyridine. These include 5% Pd/C (Alfa Aesar, surface area [SA]: 695 m^2/g), 5% Pd/Al_2O_3 (Alfa Aesar Pd/γ-alumina, SA: 155 m^2/g), γ-Al_2O_3 (Alfa Aesar high surface area bimodal, SA: 260 m^2/g) and activated carbon (Calgon F 400, SA: 765 m^2/g).

2.2.2 Reaction Conditions

The 4-methylpyridine (Aldrich or Across) was distilled over KOH or NaOH prior to use. In a typical reaction run 1 g of catalyst was placed in a round bottom flask along with 10 g of the distilled 4-methylpyridine. The reaction mixture was evacuated and an oxygen atmosphere introduced before it was heated to the boiling point (145°C). The reaction proceeded under reflux for 72 hours. After a complete reaction the flask contents were filtered using a glass

micro-fiber filter and washed with chloroform to dissolve the product. The chloroform, water and unreacted 4-methylpyridine were removed using a rotary evaporator.

Selected samples were purified via sublimation. These experiments indicate that at least 75% of the raw yield is the desired product. This, however, is a low number since only about 85% of the original sample mass is recovered in the sublimate and residue due to the difficulty in removing all of the product from the sublimation apparatus. Consequently, the yields are reported as raw yields in the paper. The sublimate, residue, and raw products were characterized using NMR. The only significant product found was the bipyridine. The residue did not redissolve well into the chloroform. The soluble fraction of the sublimation residue showed little evidence of organic compounds other than the product. Based upon NMR it is likely that the major portion of the non-sublimated impurities is inorganic residues from the catalysts.

2.2.3 Catalyst Characterization

Brunauer-Emmett-Teller (BET) surface area measurements were performed on a Quantachrome NOVA 1200 instrument. Fresh catalysts were outgassed under vacuum for 3 hours at room temperature before the measurements. Catalysts that had been stored for longer times were outgassed at 105°C for at least an hour before the BET analysis. The N_2 adsorption was performed over five isotherms, which gave roughly linear fits.

To determine the dispersion of Pd on the catalysts carbon monoxide chemisorption experiments were performed. The fresh catalysts were reduced for 2 hours at 170 °C using a 5% hydrogen in nitrogen gas mixture. The samples were then out-gassed for 1 hour in helium before the pulse titration experiments with CO at 25 °C and 1 atm. The low reduction temperature was used to avoid excessive sintering or spalling of the Pd particles during the reductive treatment and was chosen to be close to reaction temperature.

2.3 Results and Discussion

2.3.1 Effects of Catalyst Preparation Method

In the first set of experiments 10% (by weight) of palladium was deposited onto the NanoActive Aluminum Oxide Plus support [Pd/nano-Al_2O_3(+)] using the wet impregnation method. This catalyst was tested for activity in the coupling reaction of 4-methylpyridine. As expected for a palladium on alumina catalyst, this nano-particle supported catalyst did not exhibit any significant activity in the reaction (Table 2-2, Entry 1). When the precipitation method was used, however, a 10% Pd/nano-Al_2O_3(**+**) catalyst yielded a significant amount of the 4,4'-dimethyl-2.2'-bipyridine (Table 2-2, Entries 2 and 3). In fact, the 20-25 g product per g of palladium corresponds to 2-2.5 g product per gram of catalyst, which is equal to or higher than the maximum yield reported from a palladium on carbon catalyst [5]. It was also shown that the Pd content can be reduced to 5% Pd on alumina without substantially reducing the product yield (Table 2-2, Entry 4). In other words, the yield per gram of palladium can be doubled by going from a 10% to a 5% Pd/nano-Al_2O_3(+). Consequently, a yield of 50 g raw product per gram palladium can be obtained with this catalyst. The 5% Pd/nano-Al_2O_3(**+**) catalyst is more active than the commonly used Pd/C catalyst despite the inactivity reported for commercial Pd/Al_2O_3 catalysts. It is also interesting to note that the catalytic activity is very dependent on the catalyst preparation method. While the precipitation method yields a catalyst with the highest observed catalytic activity to date, the impregnation technique results in a very low activity or an inactive catalyst. Both the impregnated and the precipitated catalysts have specific surface areas in the range of 150-200 m^2/g (Table 2-2, Entries 1-4). Therefore, the support surface areas cannot explain the differences in activities between these catalysts. As can be seen in Table 2, the results are reproducible (Entries 4, 11 and 26). In fact, the yields obtained from different preparations of precipitated Pd/nano-Al_2O_3(+) catalysts are more reproducible than the yields

obtained from different runs on the same batch of commercial Pd/C (Table 2-2, Entries 5 and 25). This is likely due to variations in the PdO concentration on the "as received" Pd/C catalysts [5]. Since our catalysts are calcined in air and not reduced before reaction, the amount of PdO on the Pd/nano-Al_2O_3(**+**) catalysts is almost certainly more constant compared to the commercial "Pd(0)"/C.

To test whether or not the differences in the catalytic activity between catalysts prepared by the impregnation and precipitation methods only applies to alumina supports, impregnated and precipitated palladium on activated carbon catalysts where prepared. The precipitated catalyst gave a modest yield (15.1 g/g Pd, Entry 22, Table 2-2), which is comparable to the commercial Pd/C catalyst, while the impregnated Pd/C catalyst gave a low yield (6.6 g/g Pd, Entry 23, Table 2-2). This indicates that the precipitation method is superior to the impregnation method regardless of the support used, although the difference is more drastic for the nanoparticle alumina support.

2.3.2 Catalyst Support Effects

As expected, the commercial 5% Pd/Al_2O_3 catalyst exhibited poor activity and resulted in little, if any, product under the reaction conditions of the experiments. This is most likely due to the fact that the commercial 5% Pd/Al_2O_3 catalyst consists mainly of Pd(0), in contrast to commercial Pd/C catalysts which appear to have a relatively high, albeit varying, surface Pd(II) content. The yield of the commercial 5% Pd/C catalyst agrees with previous results [5]. It is lower than the highest yield observed using this catalyst, due to the fact that the catalyst was used as received without oxidation treatment. To determine if it is the nature of the nanoparticle alumina support or the preparation method that is responsible for the high catalytic activity, a 5% Pd/Al_2O_3 catalyst was prepared with a commercial alumina support using the precipitation method. The yield for this catalyst varied widely (Table 2-2, Entries 15, 21 and 24). On average

the catalyst does exhibit a fair activity, but it is not as active as the nanoparticle-supported Pd/Al_2O_3 catalyst. Another catalyst was prepared using the precipitation method and a second nanoparticle alumina sample [NanoActive Aluminum Oxide, nano-Al_2O_3(-)] as support. The surface area of this alumina sample (275 m^2/g) is lower than the NanoActive Aluminum Oxide Plus sample (695 m^2/g), but on the same order as the commercial γ-alumina support (260 m^2/g) [See Table 3]. The catalytic activity of this catalyst is significantly lower than that obtained on the commercial Pd/C catalyst and the palladium on the NanoActive Aluminum Oxide Plus or commercial γ-alumina supports. Consequently, there is a significant difference in the catalytic activities of the catalysts prepared with the two NanoActive Aluminum Oxide supports. It is interesting to note that the catalyst supported on the nano-Al_2O_3(-) gives a lower yield than the catalyst prepared using the commercial γ-alumina despite the fact that the surface areas of these supports are similar. The catalysts prepared via precipitation onto these three alumina supports all have surface areas between 150 and 205 m^2/g. These results indicate that neither the surface area of the bare support nor the final surface area of the prepared catalysts is the sole determining factor of the catalytic activity.

A further indication that the initial support surface area is not the main factor in determining the catalytic activity can be seen when comparing alumina and carbon supported catalysts. While a catalyst prepared via precipitation of palladium onto NanoActive Aluminum Oxide Plus (695 m^2/g, Table 2-3) gives a product yield of ~50 g/g Pd, a catalyst prepared using the same method but with an activated carbon support (surface area: 765 m^2/g, Table 2-3) only gives a yield of 15 g/g Pd. Thus, despite the slightly higher surface area of the activated carbon it does not result in a catalyst as active as the one supported on nano-Al_2O_3(+).

Aside from giving the best activity of any of the supports tested, the nano-Al_2O_3(+) catalysts exhibited better reproducibility than any of the catalysts including the commonly used commercial palladium on carbon. The only major activity variations seen for the catalysts supported on nano-Al_2O_3(+) can be attributed to reactant quality.

2.3.3 Palladium Surface Areas

The palladium surface areas were determined after reduction of the PdO on the catalyst surfaces using CO adsorption and the volume of adsorbed CO is given in Table 4 for selected catalysts. Performing CO titration measurements on reduced catalysts do not necessarily result in a good measure of the catalytically active surface area since the active phase on these catalysts is PdO and not Pd metal. This is particularly the case when the catalyst before reduction consists of Pd metal or a mixture of PdO and Pd, as in the case of the commercial Pd/C and Pd/Al_2O_3 catalysts. However, in cases where the original catalysts consist solely of PdO (as is the case for the nanoparticle-supported catalysts) and if the same mild reduction conditions are used for all catalysts, it should be possible to observe trends and obtain qualitative results from the Pd surface area measurements. CO chemisorption measurements on supported Pd catalysts are further complicated by the dependence of the Pd:CO stoichiometry on the dispersion since CO can adsorb in linear, bridge and hollow binding modes on the surface [52]. Literature data indicate that a stoichiometry of two Pd surface atoms per CO molecule adsorbed is appropriate for high dispersions and a surface atom density (C_m) of 1.42×10^{15} /cm^2 based on the cubo-octahedral geometry is reasonable for small Pd crystallites [53]. While the exact Pd:CO stoichiometry may deviate slightly from the 2:1 ratio used here, the assumptions made in calculating the Pd surface area should give sufficient accuracy for comparisons between the different catalysts in the study, particularly considering that the active phase is PdO rather than Pd on these catalysts.

The 5% precipitated nano-Al_2O_3(+) has a very high Pd surface area compared to the other catalysts in this study (Table 2-4). In fact, the Pd surface area of this catalyst is more than two times that of the commercial 5% Pd on activated carbon catalyst, which is the commercial catalyst with the highest Pd surface area. The commercial 5% Pd/Al_2O_3 catalyst also has a high dispersion but, as mentioned, this catalyst exhibits a low activity due to a low PdO concentration rather than a lack of Pd surface area. The 5% impregnated nano-Al_2O_3(+) has a surprisingly high Pd dispersion considering its low activity. The high yields per Pd surface area for the impregnated palladium on carbon and the palladium precipitated on nano-alumina(-) catalysts is likely an artifact of impurities in the product and the low dispersions of the catalysts. For low yields (~0.1 g for 0.7 g catalyst or 2.9 g/g Pd) trace impurities from the reactant and catalyst can be a significant portion of the raw product mass and due to the nanoparticle supports used, it is difficult to separate these impurities from the products. Even though the same is partly true for the precipitated palladium on carbon catalyst, i.e. the reported yield per surface area is unrealistically high, it appears that this catalyst does give a decent yield despite the low dispersion. The Pd surface areas of the precipitated Pd/C and Pd/nano-Al_2O_3(-) are on the same order, but the yield is higher for the Pd/C catalyst. In fact, the data suggest that the palladium on the surface of the precipitated Pd/C catalyst is more active than the palladium on the surface of the commercial Pd/C. Comparing the data in Tables 2 and 4 it is evident that the modest yields obtained from the precipitated Pd/nano-Al_2O_3(-) and the precipitated and impregnated Pd/C catalysts can be explained in part by low dispersions. Another surprising result is the relatively high Pd surface area of the 10% precipitated nano-Al_2O_3(+). It has roughly twice the metal surface area of the 5% catalyst but exhibits no increase in yield. The most striking result, however, is that the Pd surface area of the 5% Pd precipitated on commercial γ-Al_2O_3 is very low

despite the relatively good yield. The low dispersion of this catalyst is the main reason for the very high yield reported per palladium surface area. These results strongly indicate a structure sensitive reaction, i.e. only a portion of the surface Pd atoms are active. Consequently, the catalytic activity does not correlate with the measured Pd surface areas. This can be a result of the fact that the surface areas are determined on reduced catalysts, while the active catalyst is the unreduced form. While the support is important to give catalysts with high Pd surface areas, it is evident that this is not a sufficient criterion for an active catalyst. The Pd, or rather PdO, on the surface must also have the correct structure.

2.3.4 Impact of Reactant Quality

As mentioned, the catalysts prepared using the nanoparticle alumina(+) support for the most part exhibited good reproducibility. There were slight variations in the specific surface areas and yields for repeated samples as seen in Table 2-2 (Entries 4, 11, 13 and 26). However, the results are very sensitive to the quality of the 4-methylpyridine used. The 4-methylpyridine must be distilled over KOH (Distillates 1 and 3-5 in Table 2-2) to give good results, preferably doubly distilled. The product yields obtained with a reactant that had been distilled over a small amount of NaOH (Distillate 2) were markedly lower than the yields for reactants distilled over KOH (compare Entries 8 and 11 in Table 2-2). It was noticed that Distillate 2 discolored more quickly over time compared with the other distillates. In addition, Distillate 3, which was treated with KOH over night and then distilled over the same KOH, turned cloudy or turbid over time. This may explain the lower yields obtained for Entries 15 and 16 in Table 2-2, since those were the last two runs using Distillate 3. The best and most reproducible results are obtained if the 4-methylpyridine is treated with KOH over night then decanted and distilled over fresh KOH. This treatment results in a clear liquid, which will not discolor or turn opaque over a reasonable time (on the order of months). These results tend to indicate that an impurity is present in the lower

quality reactants (Distillate 2 and 3) and that this impurity inhibits the reaction. As the primary purpose of adding KOH to the sample during distillation is for drying, it seems possible that water is the impurity. To test this hypothesis, parallel reactions were run with the same catalyst preparation [5% Pd precipitated onto nano-Al_2O_3(+)] and the same reactant distillate. To one of these reactions 0.3 g of water per g of catalyst was added to the reactant. The water-free specimen gave a typical yield of 52 g/g Pd (Entry 26, Table 2-2). The sample with the added water yielded 31 g/g catalyst (Entry 27, Table 2-2). While this reveals that water exhibits an inhibiting effect on the reaction, it does not explain the considerably lower yields (18.2 g/g Pd) obtained from Distillate 2 (cf Entries 8 and 27 in Table 2-2). Furthermore, at a product yield of 50 g/g Pd the amount of water formed is slightly lower than the added 0.3 g/g catalyst. Consequently, the presence of water cannot be solely responsible for the inhibiting effects seen in the lower quality distillates.

The palladium nitrate source also had an effect on the catalytic activity. Catalysts prepared using the palladium nitrate from Fluka resulted in higher catalytic activities than catalysts prepared using the palladium nitrate from Alfa Aesar. During the catalyst preparation it was observed that the palladium nitrate from Alfa Aesar did not dissolve as well in the deionized water as the Fluka $Pd(NO_3)_2$. In fact, the residual solids from the Alfa Aesar palladium nitrate did not dissolve even after addition of acid (HNO_3 to a pH of 1.0). XRD analysis of both materials indicated the presence of a palladium oxide or related phase in the palladium nitrate from Alfa Aesar. The Fluka $Pd(NO_3)_2$ did not contain these phases. Consequently, it is important to check the catalyst precursor quality before preparing supported palladium catalysts.

2.3.5 Homogeneous Versus Heterogeneous Catalysis

With palladium-pyridine systems there is a natural question of whether supported catalysts are truly heterogeneous, or if the actual active species is dissolved into the solution. Palladium(II) ions coordinate easily to the nitrogen of 4-methylpyridine and perhaps even more strongly to the bipyridine product formed in the reaction. Consequently, it is possible that the surface palladium is simply a precursor, or a source, to active palladium ions in solution. Other palladium-catalyzed coupling reactions, such as the Heck reaction, do exhibit palladium leaching when heterogeneous catalysts are used [54,55], and there is still a debate as to whether these heterogeneous palladium catalysts are active catalysts or simply precursors to a dissolved active species [56]. Therefore, a set of experiments was designed to probe if a dissolved palladium species is active in this reaction. If palladium is dissolved into the reaction mixture and this palladium is catalytically active, it would be expected that the reaction proceeds after the heterogeneous catalyst (support) has been removed. One reaction was taken out of the oil bath after 24 hours and the reaction mixture was filtered hot to remove the solid catalyst. The filtrate was then returned to reflux under oxygen for an additional 72 hours. The product yield recovered from a 24-hour experiment is lower than the product yield after a 72-hour reaction (17 g/g Pd versus 50 g/g Pd, Entry 1, Column 3 in Table 2-5). This reveals a slow reaction rate and the need for a 72-hour reaction time. Furthermore, the product recovered after 24 hours with solid catalyst plus 72 hours without solid catalyst (i.e. after returning the filtrate to the reaction conditions) is very close to the yield of a 24-hour reaction (22 g/g Pd). This is evidence that the reaction is heterogeneous, or at least that the presence of a heterogeneous catalyst is necessary for the reaction to proceed.

A set of similar experiments were run by reacting a catalyst-reactant mixture for 24 hours and then use the recovered catalyst in a subsequent reaction. The recovered catalyst from a 24-

hour reaction was washed with chloroform, dried and then reloaded with fresh 4-methylpyridine. After 72 hours at the reaction conditions, 24 g of product was recovered per gram of the reloaded catalyst [Pd/nano-Al_2O_3(+), Entry 1, Column 4 in Table 2-5]. This is significantly less product compared to a fresh catalyst, however, the combined product yield from the 24-hour and the 72-hour reactions is consistent with an uninterrupted 72-hour experiment (there is very little product formed after the initial 72 hours at the reaction conditions). While the results clearly show that a recovered catalyst is still active, it is evident that the recovered catalyst has a lower activity compared to a fresh catalyst. One of the main reasons for the lower activity of a catalyst after exposure to the reaction conditions for 24 hours or more, is probably reduction of the active Pd(II) species. However, it is also possible that some leaching does occur, even though any palladium in solution does not appear to be an active catalyst. From the experiments on commercial Pd/C it is evident that the 24-hour product yield is higher (~30 g/g Pd) than for the Pd/nano-Al_2O_3(+) catalyst (~ 20 g/g Pd), even though the 72-hour yield is considerably higher for the nano-Al_2O_3(+)-supported catalyst. However, the recovered catalyst is much less active (Table 2-5). This indicates that the reaction is faster on Pd/C, but the catalyst also deactivates faster than the Pd/nano-Al_2O_3(+) catalyst.

Even though the above results imply that no catalytically active species is present in solution, there are indications of palladium leaching from the support. Previous results have indicated that the palladium surface concentration is lower after reaction [5]. In these reaction runs a palladium mirror could be observed in some experiments. However, generally the active Pd/nano-Al_2O_3(+) catalyst prepared via precipitation displayed little or no Pd mirror on the reaction flask after a completed reaction. In contrast, significant Pd mirrors were seen on several of the poorly performing catalysts, such as the Pd/nano-Al_2O_3(+) catalyst prepared via

impregnation. Some mirroring was observed also in the commercial Pd/C catalyst. If the catalytic action of these catalysts was reliant solely upon a dissolved palladium species, it might be expected that palladium mirroring (which is evidence of palladium leaching from the support) would accompany a significant catalyst activity. In contrast, palladium dissolution is observed mainly for catalysts with poor activity. Thus, this can be taken as another indication that the active species is on the surface of the heterogeneous catalyst and not dissolved into the solution.

2.3.6 Precipitation Base

NaOH or KOH were used as the base to force palladium precipitation onto the support. Both these bases resulted in highly active catalysts with similar yields (Entries 11 and 13, Table 2-2). To determine if the presence of trace amounts of base was responsible for the activity of the precipitated samples, KOH was added to a reaction with an impregnated catalyst. This catalyst system showed no significant increase in activity. If the base is crucial for the activity it is possible the Na or K is required in the deposition stage, i.e. a closer interaction between the Pd and the Na or K is necessary.

2.4 Conclusions

While the palladium impregnated on nano-Al_2O_3(+) exhibits little or no activity in the coupling reaction of 4-methylpyridine, nano-Al_2O_3(+)-supported catalysts prepared via the precipitation method give significant yields. Despite the fact that commercial Pd/Al_2O_3 is not an active catalyst in this reaction, the nano-Al_2O_3(+) was shown to be a viable support for the coupling reaction. The yield obtained from the palladium precipitated onto nano-Al_2O_3(+) is significantly higher, the highest reported for this reaction system, and more reproducible compared to the yields obtained from commercial Pd/C catalysts, which are the commonly used catalysts in this reaction. Additionally, it was found that traditional alumina-supported catalysts can be active for this reaction if prepared by precipitation. However, the yields are not as

reproducible or as high as those obtained for the nano-Al_2O_3(+) support. The sensitivity to catalyst preparation indicates that the activity of this catalyst is not based solely upon the surface area of the support. The lack of correlation between the measured Pd surface and the catalyst yields strongly suggests a structure sensitive reaction. Furthermore, experiments reveal that the differences in activities between catalysts prepared via precipitation and impregnation is not due to the presence of bases (NaOH or KOH) in the reaction mixture. To ensure high product yields the 4-methylpyridine must be distilled over KOH. Purification by sublimation followed by NMR measurements verifies that the product is 4,4' dimethyl 2,2' bipyridine and that the raw yields are at least 75% or more of the desired product. Experiments also reveal that a heterogeneous phase is necessary for the reaction to proceed at a significant rate.

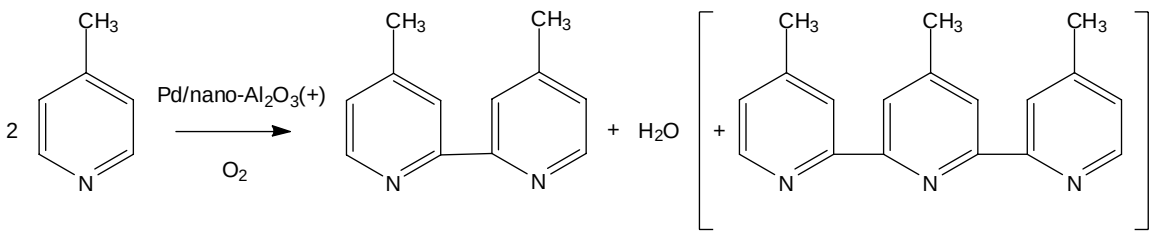

Figure 2-1 Oxidative coupling of 4-methylpyridine using a palladium catalyst.

Table 2-1 Reported literature yields for 4,4'-dimethyl-2,2'-bipyridine forming reactions

Starting material	Amount Reactant [mol]	Catalyst	Amount Catalyst [g]	Yield [%]	Yield [g/g Pd]	Reference
2-Br-4-methylpyridine	$2 \cdot 10^{-3}$	5% Pd/C, Zn	0.3	19	2.3	[34]
2-Br-4-methylpyridine	$2 \cdot 10^{-3}$	5% Pd/C, Zn	0.11	19	6.6	[34]
2-Br-4-methylpyridine +	$23 \cdot 10^{-3}$	$Pd(PPh_3)_4$	0.95	67	32.5	[35]
2-$SnBu_3$-4-methylpyridine	$27 \cdot 10^{-3}$					[35]
2-Br-4-methylpyridine	$5 \cdot 10^{-3}$	$NiBr_2$	0.07	47	10.5 [Ni]	[50]
2-Br-4-methylpyridine	$5 \cdot 10^{-3}$	$NiBr_2$	0.3	93	4.9 [Ni]	[50]
4-methylpyridine	1.03	10% Pd/C	4	7	17.3	[40]
4-methylpyridine	2.06	5% Pd/C	8.93	9	40.0	[39]
4-methylpyridine	7.19	10% Pd/C	28	6	14.3	[41]
4-methylpyridine	$75 \cdot 10^{-3}$	5% Pd/C	0.7	26	52	This work

[Ni] Nickel Catalyst Used

Table 2-2 Product yields and catalyst surface areas of various catalysts prepared and tested in the coupling reaction of 4-methylpyridine. Reaction conditions are given in the Experimental Section.

Entry	Catalyst Description [a]	4-Methyl-Pyridine [b]	Raw Product [g/g Pd] [c]	Specific Surface Area [m^2/g]
1	10% Pd Impregnated on nano-Al_2O_3(+)	1	<1 [d]	155
2	10% Pd Precipitated on nano-Al_2O_3(+)	1	25.4	205
3	10% Pd Precipitated on nano-Al_2O_3(+)	1	20.0	165
4	5% Pd Precipitated on nano-Al_2O_3(+)	1	48.6	180
5	5% Pd/C Commercial	1	16.4	695
6	5% Pd/Al_2O_3 Commercial	1	2.6 [d]	155
7	5% Pd Impregnated on nano-Al_2O_3(+)	2	1.4 [d]	170
8	5% Pd Precipitated on nano-Al_2O_3(+)	2	18.2	170
9	5% Pd/C Commercial	2	7.6	695
10	5% Pd/Al_2O_3 Commercial	2	2.4 [d]	155
11	5% Pd Precipitated on nano-Al_2O_3(+)	3	52.6	165
12	5% Pd/C Commercial	3	14.4	695
13	5% Pd Precipitated (KOH) on nano-Al_2O_3(+)[e]	3	55.2	165
14	5% Pd Precipitated on nano-Al_2O_3(-)	3	8.2	155
15	5% Pd Precipitated on Commercial γ Al_2O_3[f]	3	4.2	200
16	5% Pd Precipitated on activated carbon	3	2.4	
17	5% Pd Impregnated on nano-Al_2O_3(+) +KOH[g]	3	2.6	
18	5% Pd Precipitated on nano-Al_2O_3(+) (Alfa)[h]	4	14.0	
19	5% Pd Precipitated on nano-Al_2O_3(+)	4	44.0	
20	5% Pd Precipitated on nano-Al_2O_3(-)	4	5.8	
21	5% Pd Precipitated on Commercial γ-Al_2O_3[f]	4	24.0	
22	5% Pd Precipitated on Activated Carbon	4	15.1	
23	5% Pd Impregnated on Activated Carbon	4	6.6	
24	5% Pd Precipitated on Commercial γ-Al_2O_3[f]	4	34.0	
25	5% Pd/C Commercial	5	36.0	
26	5% Pd Precipitated on nano-Al_2O_3(+)	5	52.0	
27	5% Pd Precipitated on nano-Al_2O_3(+) + H_2O[i]	5	31.0	

[a] nano-Al_2O_3(+): nanoparticle alumina (NanoActive Aluminum Oxide Plus), nano-Al_2O_3(-): nanoparticle alumina (NanoActive Aluminum Oxide). Unless otherwise stated the palladium(II) nitrate source is Fluka.

[b] 4-Methylpyridine distillates: 1: 4-methylpyridine distilled over KOH, 2: 4-methylpyridine distilled over NaOH, 3: 4-methylpyridine treated with KOH over night before distilling over the same KOH, 4 and 5: 4-methylpyridine treated with KOH over night then decanted and distilled over fresh KOH.

[c] Product: 4,4'-dimethyl-2,2'-bipyridine. Raw yield contains a small amount of the terpyridine byproduct: 4,4',4"-trimethyl-2,2',6'2"-terpyridine as the only byproduct.

[d] There is very little 4,4'-dimethyl-2,2'-bipyridine product in these runs. The solids recovered appear to be mostly catalyst and organic byproducts.

[e] Catalyst prepared via precipitation using KOH instead of NaOH.

[f] Alfa Aesar high surface area bimodal γ-alumina. [g] 0.09 g of KOH was added to the reaction mixture.

[h] Palladium(II) nitrate source was Alfa Aesar not Fluka. [i] 0.3 g of H_2O was added to the reaction mixture.

Table 2-3 BET surface areas of the supports used in the catalyst preparations.

Catalyst Support	Surface Area [m^2/g]
Nano Active Alumina Plus	695
Nano Active Alumina	275
Commercial γ-Alumina bimodal (Alfa Aesar)	260
Activated Carbon (Calgon F 400)	765

Table 2-4 Results from CO chemisorption measurements of selected catalysts prepared and tested in the coupling reaction of 4-methylpyridine.

Catalyst	CO Adsorbed (μl/g cat)	Pd Surface Area[a] (m^2/g catalyst)	Product Yield (g/m^2 Pd)
Nano-Al_2O_3(+)	0	0.0	N/A
10% Pd Precipitated on nano-Al_2O_3(+)	8480	29.4	0.08
5% Pd Precipitated on nano-Al_2O_3(+)	4550	15.8	0.17
5% Pd Impregnated on nano-Al_2O_3(+)	1530	5.3	0.06
5% Pd Precipitated on nano-Al_2O_3(-)	280	1.0	0.29
5% Pd/Al_2O_3 Commercial	1880	6.5	0.02
5% Pd/C Commercial	2530	8.8	0.20
5% Pd Precipitated on Activated Carbon	310	1.1	0.68
5% Pd Impregnated on Activated Carbon	240	0.8	0.41
5% Pd Precipitated on Commercial γ-Al_2O_3[f]	140	0.5	3.4

[a] The Pd surface area has been calculated assuming a Pd:CO stoichiometry of 2:1 and a surface atom density of 1.42 x 10^{15} atoms/cm^2.

Table 2-5 Results from experiments at different reaction times to probe homogeneous versus heterogeneous catalysis.

Entry	Catalyst Description [a]	Raw Yield [g/g Pd] [b] 1st Day	Raw Yield [g/g Pd][b]
	Recovered Catalyst [c]		
1	5% Precipitated Pd/nano-Al_2O_3(+) (1st day and 4th day)	17	24
2	5% Pd/C Commercial (1st day and 4th day)	32	5
	Recovered Reactant Mixture [d]		
3	5% Precipitated Pd/nano-Al_2O_3(+) (1 day with and 3 days without catalyst)	N/A	22
4	5% Pd/C commercial (1 day with and 3 days without catalyst)	N/A	30

[a] nano-Al_2O_3(+): nanoparticle alumina (NanoActive Aluminum Oxide Plus).

[b] Raw yield of 4,4'-dimethyl-2,2'-bipyridine, which contains a small amount of the terpyridine byproduct: 4,4',4"-trimethyl-2,2',6'2"-terpyridine as the only byproduct.

[c.] The 1-day yield is the product recovered during filtration after the first 24 hours. The 4-day yield is the product obtained from a recovered 1-day catalyst after reaction with fresh 4-methylpyridine for three additional days.

[d] Reaction was run for 24 hours with catalyst. The reaction mixture was filtered and the catalyst removed. The filtrate was then returned to the reaction conditions for an additional 72 hours.

CHAPTER 3
NANOPARTICLE- AND POROUS-METAL-OXIDE-SUPPORTED PALLADIUM CATALYST FOR THE OXIDATIVE COUPLING OF 4-METHYLPYRIDINE[2]

3.1 Introduction

Palladium is a transition metal that has the ability to induce C-H activations in hydrocarbons and aromatic systems [57]. The efficacy with which palladium inserts into the C-H bond of methane, which is the strongest of C-H bonds, is evident in the large number of publications involving palladium-catalyzed methane oxidation [9,11,12]. While partial and complete oxidation reactions of hydrocarbons are very important, reactions that can lead to C-C coupling after a C-H activation step are of particular interest [58]. Naturally, C-H activation and C-C coupling of CH_4 would be a highly desirable method to produce chemicals directly from methane. However, C-C coupling of aromatic compounds after a direct C-H activation step is also of significance in the synthesis of fine chemicals and pharmaceuticals. An important example is the oxidative coupling of 4-methylpyridine to 4,4'-dimethyl-2,2'-bipyridine. This is a simple one-step process in which the bipyridine is formed directly from the pyridine reactant and the only by-products are water and the terpyridine. Consequently, this is an environmentally friendly reaction since no solvent or halogenated compounds are needed. In addition to reducing halogenated byproduct salts or compounds, halogenated derivatives are usually more expensive, with 2-bromo-4-methylpyridine available through reaction with commercially available 2-amino-4-methylpyridine at ~$200/kg [46], compared to the non-halogenated analogue, 4-methylpyridine, which is relatively inexpensive at less than $40/kg [47]. The disadvantages of

[2] Luke M Neal, Daniel Hernandez, Helena Weaver, Manuscript in preparation to be submitted in the near future, Unpublished copyright (2008).

this reaction are the slow reaction rate and the deactivation of the catalyst [5]. The low yields of bipyridine product over the palladium (or Raney nickel) catalysts [1-4] or the high prices of halogenated reactants results in prices of 4,4' dimethyl-2,2'-bipyridine in excess of $5,300 [31]. This prohibits large scale use of the 4,4' dimethyl-2,2'-bipyridine, and its transition metal complexes. This is unfortunate since transition metal complexes with bipyridine ligands have many interesting photo- and electrochemical [20,21,23,24,43,45] or catalytic [25-29] properties. The oxidative coupling of 4-methylpyridine is thus a useful "probe" reaction on which to test new catalyst formulations to find more efficient catalysts.

In heterogeneous catalysts the active metals are normally supported on some type of high surface area support. This is done to increase the surface area of the active metal and to reduce sintering of the active metal. It has also been shown that the support can interact with the active metal and alter the catalytic activity of the resulting catalyst. Consequently, a large number of different supports have been used for palladium catalyst systems and some important palladium-support interactions have been identified. For example, carbon-supported palladium catalysts are commonly used for hydrogenation reactions, while alumina-supported catalysts are normally used for complete oxidation reactions [7], including methane oxidation [8]. Silica and modified silica supports are utilized for reactions dependent upon acidic sites such as ethane oxidation to acetic acid [15] and NO reduction [60]. Pd/ZrO_2 and Pd/MgO have been used for aromatization of hexane [19]. Palladium on TiO_2 has been studied for selective oxidation of acetylene to ethylene [61] and the selective hydrogenation of alkadienes [14]. The type of phase of titania (anatase or rutile) has been reported to affect the CO and H_2 uptake of palladium catalyst with similar Pd sizes [14]. Pd/ZnO has been studied for use in steam reforming applications [62], and has been shown to have longer catalyst life than Cu catalysts in methanol reformation [63].

Pd-Sn catalysts are used for denitration of contaminated water [64] and Pd/SnO_2 have been studied in the low-temperature oxidation of methane [12,13]. Pd/CeO_2 are efficient low-temperature CO oxidation catalysts [16,17]. This is likely due to strong Pd-CeO_2 interactions, which can supply oxygen to Pd at Pd-CeO_2 interfaces and affect the reduction and oxidation properties of Pd by lowering the temperature of Pd oxidation. As a result, oxidation reactions are facilitated on Pd/CeO_2 catalysts compared to palladium supported on non-reducible oxides [65]. The use of ZrO_2 and ZrO_2/CeO_2 in Pd catalysts has demonstrated similar properties [11,18,19]. The oxygen mobility of reducible oxides may be very beneficial in the oxidative coupling of 4-methylpyridine, since the catalysts are known to reduce during the reaction [5]. Considering the number of supports that have been used effectively in palladium-catalyzed reactions, we are interested in how the properties of the catalysts can be altered by using different catalyst supports. In particular, we are interested in nanoparticle oxides supports and if these supports lead to catalytic properties that are different from traditional high surface area, porous supports.

While early research indicated that palladium on alumina exhibits poor activity [1], more recent results have demonstrated that palladium precipitated onto alumina nanoparticles [n-Al_2O_3(+)] is not only active, but one of the best catalysts found for this reaction [66]. The maximum isolated yield reported for a commercial 5% Pd/C is ~2 g product per g of catalyst [38], with yields of 1.5-2 g/g for 10% Pd/C catalysts being more common [5,39,40]. In contrast, the 5% Pd/n-Al_2O_3(+) catalyst gave yields in excess of 2.5 g/g of catalyst [5]. In addition to the excellent n-Al_2O_3(+)-supported catalyst, previous work revealed that 5% Pd precipitated onto a traditional porous alumina support is an active catalyst but with only half the yield compared to the n-Al_2O_3(+) catalyst. Our hypothesis is that the high activity of the 5%Pd/n-Al_2O_3 catalyst is due to the high number of low coordination sites, such as corners and edges [6] that many

nanoparticles and some traditional high surface area, porous supports have. These low coordination sites may cause a stronger interaction between the support oxide and the deposited active metal than with most conventional supports, which in turn can alter the catalytic activity of the resulting catalyst. In the alumina-supported catalysts, no favorable strong palladium-support interactions are expected. We therefore decided to prepare palladium catalysts supported on nanoparticle ZrO_2, CeO_2, ZnO, CuO, SnO_2, since these oxides have revealed favorable interactions with palladium (see preceding literature review). Traditional supports (porous SiO_2 and TiO_2) were also included as well as their nanoparticle analogues and MgO plus CaO nanoparticle oxides, to probe different acidic and basic support properties as well as the differences between traditional and nanoparticle oxide supports. Considering that the nanoparticle alumina is a relatively expensive support at a price of nearly $700/kg on a kg purchase basis (NanoScale NanoActive Alumina Plus), it is also important to search for a less expensive support that can give comparable yields to find an economically viable catalyst.

The main objectives in this work are to 1) determine the effects of the support on the catalytic activity of palladium supported on porous and nanoparticle oxides, 2) determine if the acidic or basic properties of the supports are important for the preparation of an active catalyst, and 3) identify any catalyst supports competitive with the n-Al_2O_3(+) support in terms of cost and/or activity.

3.2 Experimental

3.2.1 Catalyst Preparation

The catalysts were prepared using commercially available nanoparticle oxides supplied by NanoScale Materials Inc. [67] and Nanostructured & Amorphous Materials, Inc (NanoAmor) [68] as well as some commercially available traditional supports [69]. The properties of these support oxides are given in Table 3-1.

The catalysts where prepared by precipitation. In this method, the support was dispersed into a solution of palladium nitrate. Porous oxides pellets were ground before dispersion. The mixture was then titrated with a NaOH solution, which formed $Pd(OH)_2$ on the support [51]. The amount of NaOH used in these experiments corresponds to 50% stoichiometric excess based on the amount of palladium nitrate used. The resulting mixture was aged overnight at room temperature before it was filtered. The recovered catalyst was rinsed by stirring in water overnight, followed by another filtration. The catalyst was then dried overnight at 105°C and calcined at 350°C or 450°C for 3 hours.

3.2.2 Reaction Conditions and Product Recovery

The 4-methylpyridine (Aldrich or Across) was doubly distilled over KOH prior to use. In a typical reaction run 0.7 g of catalyst was placed in a round bottom flask along with 7 g of the distilled 4-methylpyridine. The reaction mixture was evacuated and an oxygen atmosphere introduced before it was heated to the boiling point (145°C). The reaction proceeded under reflux for 72 hours. After a complete reaction the flask contents were filtered using a glass micro-fiber filter and washed with chloroform to dissolve the product. The chloroform, water and unreacted 4-methylpyridine were removed using a rotary evaporator.

The standard deviation was estimated from 5% Pd precipitated onto n-Al_2O_3(+) (6 samples) and p-TiO_2 (5 samples). These were found to have average yields of 2.5 ± 0.15 g / g catalyst for n-Al_2O_3(+) and 2.6 ± 0.25 g / g catalyst for p-TiO_2 (from this and previous work (See chapter 2). This amounts to a % standard deviation of ~6.5% and ~%10 respectively. These numbers are typical for the catalysts used in this study, except for the commercial Pd/C catalyst. In the case of the Pd/C catalyst, the variation was closer to 20%, which in this case is due to the fact that the PdO:Pd ratio varies on this catalyst. Since the 6.5% and 10% are typical values of the standard deviation the more conservative 10% value was used in the research. The variation

in yield is believed to be caused by variations in palladium precursor and reactant distillate qualities, as well as (to a lesser extent) variations in support and extraneous variables, such as varying chlorine contents. It was found in previous work (See chapter 2) that the palladium-nitrate precursor and the quality of the 4-methlypyridine distillate had large effects upon the yields, and are, perhaps, the most important parameters to assure reproducible results.

3.2.3 Catalyst Characterization

The surface areas of supports as received and the prepared catalysts were characterized by multipoint BET isotherms using a Quantachrome Nova 1200 instrument. Chemisorption measurements to characterize active surface area of the catalysts and the number of acidic and basic sites of the supports were performed on a ChemBET 3000 from Quantachrome Instruments. Reduction in hydrogen followed by CO titration was used to characterize the active palladium surface area. Since PdO is believed to be the active phase, or a necessary precursor for this reaction [5], measuring the Pd surface area after reduction of the PdO phase is not necessarily a good measure of the active surface area. This is particularly the case when the surface consists of a mixture of Pd and PdO phases. However, in our prepared catalysts the palladium phase after calcination is PdO in all cases and no partially reduced PdO has been observed. Furthermore, reductions are performed using mild conditions (170°C in a stream of 5% hydrogen) to minimize sintering of the formed Pd phase. A temperature of 170°C was chosen to be close to the temperatures experienced by the catalyst during reaction.

The Pd particle size was calculated using: [53]

$$\Phi_{av} = \frac{1}{V_g S_{av}} \frac{k V_m C_m}{N_a \rho_m}$$

S_{av} Average stoichiometry; CO/Pd = 1. This value was selected to be conservative and report a lower Pd surface area (or dispersion) rather than one that may be higher than the true value.

Some research has indicated that a 1:2 CO:Pd stoichiometry may be more accurate for small particles [53], and this would give higher surface areas than those reported here.

k Shape factor. A value of 5 was used in the current study. It corresponds to a cube with one side attached to the support. This is reported to be a reasonable approximation for Pd crystals in this size range [53].

V_m Molar volume

N_a Avogadro's number

ρ_m Metal density

V_g Volume of gas adsorbed

Φ_{av} Average particle size

C_m Surface density of metal atoms. Values between 1.27×10^{15} and 1.44×10^{15} atoms/cm^2 have been reported in the literature [53]. The 1.44×10^{15} atoms/cm^2 assumes roughly spherical particles and was thus used in the current study.

The formula can be rearranged to give metal surface area:

$$A_m = \frac{V_g S_{av}}{V_m C_m N_a}$$

The basic sites of the supports were probed by titration with CO_2, and acidic sites were probed by titration with anhydrous ammonia in a stream of helium. Prior to titration, the support samples were outgassed in a flow of nitrogen at 105°C for an hour. Although some of the more basic supports may have adsorbed atmospheric CO_2 that does not desorb at 105°C, the possibility of sintering precludes the use of higher temperatures during out-gassing.

3.3 Results and Discussion

3.3.1 Catalytic Activity

All prepared catalysts were subjected to catalytic activity measurements. The results from these experiments are summarized in Table 3-2. Entries 1 and 2 have been added for comparison. Entry 1 reports a typical yield for the commercial Pd/C catalyst and Entry 2 is the result from a nanoparticle alumina catalyst, and is the best yield reported for this reaction to date [66]. As can be seen in Table 3-1, the surface areas of the various supports included in this study covers a wide range from ~700 down to 35 m^2/g. If the only function of the support is to provide the surface area onto which the palladium is dispersed, the yields would be expected to decrease with the surface area of the support. This is indeed observed for some of the supports used in this study (see Figure 3-1A). In particular, catalysts supported on n-Al_2O_3(+), n-MgO, n-SiO_2, γ-Al_2O_3 and n-SnO_2 give yields that appear to be a linear function of the support surface area. Fitting this data to a straight line gives a regression coefficient of 0.99 (Line equation: $Y_x = 0.058 \pm 0.004 + 7.9 \pm 2.2 \cdot SA_x$, where Y_x is the yield obtained over support x and SA_x is the surface area of that support). The n-TiO_2 support also is also close to this line and including the yields obtained from the Pd/n-TiO_2 catalyst gives a linear regression coefficient of 0.98.

Evidently, there are also a number of catalysts that result in higher yields than expected from the support surface areas. This may be expected in cases where there are strong palladium-support interactions, since favorable interactions can induce, for example, higher Pd surface areas, or a more catalytically active Pd species, compared to non-interacting supports. Consequently, strong palladium-support interactions are most likely the reason why the yields obtained from the catalysts supported on n-ZrO_2+CeO_2, n-ZrO_2, n-ZnO and n-CeO_2 are high, or reasonably high, despite their low support surface areas (70 m^2/g and below). These oxides have been shown to exhibit strong interactions with palladium in other catalysts [11,19,65]. In the

light of this, it is unexpected that the CuO and SnO_2 do not result in catalysts with higher activities, since Cu(II) and Sn(II) are often added as co-catalysts to palladium in homogeneous reaction systems [70-73]. In fact, the Sn(II)/Pd(II) pair has been shown to be effective in homogeneous C-H activation and C-C coupling reactions [74].

The yields obtained from the catalysts supported on n-CaO and the n-Al_2O_3(-) are also unexpectedly low, which appears to indicate some unfavorable interactions between the palladium and these supports. In contrast, the yields obtained from the catalysts supported on n-$Al(OH)_3$ and the traditional supports p-SiO_2 and p-TiO_2 are higher than predicted from their corresponding surface areas according to the equation derived above. In this case, it appears that there again are some favorable interactions between the palladium and the support. However, in the case of SiO_2 and $Al(OH)_3$ no specific palladium-support interactions have to our knowledge been reported.

3.3.2 Catalyst and Metal Surface Areas

Since the support surface area does not necessarily correlate with the amount of palladium available at the surface, it is important to determine the palladium surface areas of the catalysts. For reactions that are not structure sensitive it is expected that there is a linear correlation between the catalytic activity and the palladium surface area. Carbon monoxide adsorption measurements were therefore performed on reduced catalysts to determine the palladium surface areas of all catalysts. The results are presented in Table 3-3. From these measurements the dispersions of the catalysts, i.e. the fraction of Pd atoms at the surface (compared to all palladium atoms on the catalyst), were calculated. The palladium dispersions obtained on several of the prepared catalysts are high, ranging from 20 to over 40% (Table 3-3). By comparison, the dispersion on the commercial 5% Pd/C is 23%. It is noteworthy that such high dispersions (relative to the commercial Pd/C catalyst) can be obtained from a simple

precipitation method. This indicates strong promise for use of nanoparticles as catalyst supports also in other reaction systems.

When analyzing the data it is important to keep in mind that PdO and not Pd metal is the active site on these catalysts. This is not necessarily detrimental since the temperatures were kept low during the reductive pretreatment to avoid palladium particle growth. However, it is possible that different oxide supports could exhibit different amounts of palladium sintering during the reduction process. This together with structure sensitivity can lead to deviations from a linear correlation between the activity and the Pd surface area.

When plotting the Pd dispersion versus the support surface areas (Figure 3-1B) and comparing this to the plot of yield versus support surface areas (Figure 3-1A), some of the high and low catalyst yields can be explained. For example, the low yields obtained from catalysts supported on CuO, CaO and n-Al_2O_3(-) are evidently due to very low palladium surface areas on these catalysts. The palladium surface area on the n-SnO_2 support is also lower than expected if this support indeed would induce metal-support interactions. As expected, the n-ZrO_2+CeO_2, n-ZrO_2, n-ZnO and n-CeO_2 supports do result in catalysts with high palladium surface areas, compared to the respective support surface area. The palladium surface area as a fraction of the total surface area ranges from 10-19% on these catalysts. By comparison the palladium surface areas of the n-Al_2O_3(+)-supported catalyst and the commercial palladium on carbon catalyst are 10% and 1% of the total surface areas, respectively. While the reported dispersion on the Pd/n-CeO_2 appears abnormally high, this is likely the result of strong metal-support interactions. Since the CeO_2 is a reducible oxide, it is possible that some of the CeO_2 is reduced in the reduction process due to the Pd-CeO_2 interactions. Evidence of oxygen mobility on CeO_2 and transfer of oxygen from CeO_2 to palladium has been observed in, for example methane oxidation

over Pd/CeO_2 [18]. The Pd/CeO_2 system could also be similar to CuO/CeO_2 catalysts where it has been reported that surface CeO_2 can be reduced at low temperatures (less than 200ºC) [75]. It was verified that no CO is adsorbed on a n-CeO_2 support after reductive treatment if palladium is not present on the surface. If the Pd induces low-temperature CeO_2 reduction, it is likely that CO adsorbs on these reduced CeO_x sites, in addition to Pd sites during the CO titration process. This would result in very high CO adsorption values, and consequently abnormally high Pd surface areas (or dispersions). A high Pd dispersion on the porous TiO_2 support can also explain the high yield obtained from this catalyst. Whilst the high dispersion on this support is likely due to Pd-TiO_2 interactions, it is evident that these interactions differ between p-TiO_2 and n-TiO_2 supports. The Pd dispersions are close to the same on these two supports, while the support surface areas are considerably different, 505 (n-TiO_2) versus 120 (p-TiO_2) m^2/g. Some other unexpected results include the low Pd surface areas on the p-SiO_2 n-SiO_2, MgO supports. Considering the reasonably high yields obtained from palladium on these supports, it would be expected that the palladium surface areas are higher than the measured values. Thus, either the palladium sinters more on these supports compared to the other supports, or a greater fraction of the palladium on the surface of these catalysts is active compared to the palladium on the surface of for example the n-Al_2O_3 (+) support (see Figure 3-2 and Table 3-3). From Figure 3-2 it is evident that there is a correlation between the catalytic activity (product yield) and the palladium surface area (dispersion). In general, a higher dispersion results in a higher yield. However, there are some deviations from this relationship and the correlation is definitely not linear (Figure 3-2). It appears that several supports interact with the palladium and alter the catalytic properties of these catalysts.

3.3.3 Acidic and Basic Sites

In order to further probe the how the properties of the supports affect the palladium dispersion and the catalytic activity of the catalysts, the amounts of acidic and basic sites of the supports were investigated. This was done by measuring the adsorption of NH_3 and CO_2 on the different catalysts (see Table 3-4).

As is evident in Figures 3A and 3B there is no simple correlation between the catalyst dispersion and the acidic or basic sites on the supports. As expected the n-CaO had a large uptake of CO_2 (due to facile $CaCO_3$ formation). The amount of CO_2 adsorbed by the calcium (4.4 ml/g) is more consistent with surface adsorption rather than bulk carbonate formation (~400 ml/g). While moderately basic supports (such as γ-Al_2O_3 and MgO) evidently can give reasonable product yields (Figure 3-1 A), it appears that the Pd dispersions are lower on these compared to less basic or neutral supports (Figure 3-1 B). Considering that the Pd dispersion on the CaO support is very low, avoiding moderately to highly basic supports when preparing well-dispersed Pd catalysts using the base precipitation method may be advisable. It also appears that avoiding highly acidic supports is recommended when preparing well-dispersed palladium catalysts. The support with the highest ammonia adsorption (n-SiO_2) resulted in a catalyst with a palladium surface area below that expected for its support surface area (Figure 3-1 B). However, despite a lower palladium surface area on the n-SiO_2 support, the yield obtained from this catalyst is in the range expected for this catalyst considering its support surface area (Figure 3-1 A). Consequently, the average activity of the palladium on the surface of this catalyst is higher than the activity of for example the palladium on the n-Al_2O_3(+) support (see the turnover numbers in Table 3-3). The second most acidic support, the n-$Al(OH)_3$, also results in a catalyst with higher turnover number than the Pd/n-Al_2O_3(+) catalyst, and the same is true for the most

basic supports (Table 3-3). Consequently, highly acidic or basic supports appear to result in lower Pd dispersions, but the palladium that is on the surface is more active than the palladium on our reference Pd/n-Al_2O_3(+) catalyst. It is easier to see how an acidic support (electron acceptor) can lead to more electrophilic, and thus more reactive, palladium, than how the basic support leads to more active Pd species. For example, a density functional calculation study of Pd atoms on γ-Al_2O_3 [110] found that single Pd atoms interact strongly with tetragonal Lewis acid sites [76]. Evidently, there are some complex interactions between palladium and the supports on the catalysts included in this investigation. Considering the turnover numbers reported in Table 3-3, more active catalysts should result if the dispersion on the γ-Al_2O_3 support can be increased.

3.3.4 Estimated Cost of Selected Catalyst

In the search for a more effective catalyst the economics must also be considered, i.e. cost of the catalyst compared to the yield obtained. For example, this reaction does proceed over Raney nickel, which is a considerably less expensive catalyst. However, the yields over the Raney nickel catalyst are also low per gram of catalyst [1-4] and the reaction is more involved since the catalyst must be activated and the resulting catalyst after reaction is pyrophoric. Consequently, palladium would be the active metal of choice if higher yields and economically viable catalysts can be developed. Although the main cost of the catalysts is due to palladium, the cost of nanoparticle oxide supports can be significant, as can be seen in Table 1. Since the n-Al_2O_3(+) support is the most expensive of the oxide supports used in this study, it is possible that other supports can be competitive with the Pd/n-Al_2O_3(+) catalyst if the cost of the catalyst per g of product is considered. To allow for variations in the price of palladium, as well as the cost of preparing palladium nitrate, a more expensive palladium cost basis ($450/oz) was used for calculating the cost of catalyst per gram of product (Table 4-5), even though the price of

palladium has recently been as lower than $250/oz [77]. At these prices the Pd/p-TiO_2, Pd/n-ZrO_2, and Pd/n-ZnO are catalysts competitive with the Pd/n-Al_2O_3(+) catalyst. At a commercial scale the amount of catalyst used and the conversion of starting material also comes into the economic analysis equation, since a larger amount of catalyst and a lower conversion would result in larger reactor sizes (higher capital costs) for the same production rate. This naturally favors the most active catalyst by minimizing reactor size in addition to palladium usage. Consequently, the lower yields of the Pd/ZrO_2 and Pd/n-ZnO catalysts likely offset any cost savings from the support compared to the Pd/n-Al_2O_3(+) catalyst. Consequently, the Pd/p-TiO_2 is likely the only support that has potential to exhibit better economics than the Pd/n-Al_2O_3(+) catalyst. This said, some of the other support oxides with moderate price and relatively high activities, such as the n-MgO, n-TiO_2, n-CeO_2, n-ZrO_2 and n-ZrO_2+CeO_2 may make their corresponding catalysts competitive with the n-Al_2O_3(+) support through optimization and, perhaps, promoter use.

3.4 Conclusions

Palladium supported on n-ZrO_2, n-ZrO_2(+10% CeO_2), n-CeO_2, n-ZnO, n-MgO, n-TiO_2 and p-TiO_2 supported catalysts all demonstrated high catalytic activities. While none of the catalysts outperformed the activity of the precipitated 5% Pd/n-Al_2O_3(+) catalyst developed in previous research, several of the catalysts outperformed the highest 2g/g yields reported for activated carbon catalysts (Table 3-2).

In general there appeared to be two groups of supports giving highly active catalysts; 1) supports with high surface areas and 2) support oxides known to result in strong Pd-support interactions. For example, supports with very high initial surface areas (more than 450 m^2/g), such as n-TiO_2, n-SiO_2, n-MgO and n-Al_2O_3(+), were generally quite active (>35 g product/g Pd) and high surface area supports (450 > SA > 200 m^2/g), such as porous SiO_2 and Al_2O_3 gave

moderate yields (32 and 24 g/g Pd respectively). The other group of active catalysts includes, for example, palladium supported on n-ZrO_2, n-ZrO_2+n-CeO_2, n-CeO_2, and n-ZnO, which all have relatively low surface areas. As a result of strong metal-support interactions these supports resulted in relatively high Pd surface areas compared to the surface area of the support (10-19% of the total SA), which in turn gave higher yields than expected from the support surface areas (Figure 3-1A). It is also possible that these supports can result in electronic Pd-support interactions that positively affect the catalytic activity. This would explain why the activities for some of the catalysts are higher than what would be expected from the Pd dispersion on these catalysts.

No simple correlation between the catalytic activity and the support surface area or the palladium dispersion could be identified. It is also evident that there is no correlation between the acid or basic sites of the supports and the palladium dispersion or the catalytic activity. Despite the lack of correlation between activity and acidity or basicity, the CaO support with a high CO_2 uptake (basic support) resulted in a catalyst with very low dispersion. Using a precipitation procedure where a base is added to palladium nitrate solution it may therefore be advantageous to avoid highly basic supports. Also, using highly acidic support, such as n-SiO_2, did not result in poor catalysts. While the n-SiO_2 support resulted in a palladium dispersion lower than what would be expected from its surface area, this catalyst had a high turnover frequency.

The lack of linear correlation between the catalytic activity and the palladium surface area indicates that the reaction is structure sensitive, i.e. some palladium species are more active than others. This is particularly evident in the n-Al_2O_3(+)-supported catalysts, where there was no significant difference in product yield between the 5% and the 10% Pd loadings [66]. Our

hypothesis is that the most active palladium species are very small Pd/PdO particles, which may form at corner and edge sites on the supports due to Pd-support interactions. Nanoparticle oxide supports, and to some extent more traditional high surface area supports (such as bimodal γ-Al_2O_3, p-SiO_2 and p-TiO_2), would have a large number of these corner and edge sites. Once these support sites are saturated with palladium, any additional palladium would be deposited on "non-active" support sites, or on top of the active palladium. The number of corner and edge sites on the support may be more important on "non-interacting" supports. On, for example, reducible oxides there are already "active" support sites, which can result in high Pd dispersions and highly active Pd species.

In summary, the search for more active and economically competitive catalysts, identified a few promising supports. In particular, the n-ZnO and p-TiO_2 result in catalysts that are significantly less expensive but with comparable activity to Pd/n-Al_2O_3(+) catalysts. The high surface area n-MgO support also result in a catalyst with reasonably high activity. This support may, thus, prove useful in future catalyst development where the effects of additives are investigated. This is particularly important in cases where the promoters are known to form inactive aluminates with alumina supports.

Table 3-1 Suppliers, properties and price of the supports used in the study

Oxide	Supplier [a]	SA m^2/g [b]	Crystallite Diameter [c] [nm]	Cost [d] $/kg
n-Al_2O_3(+)	NanoScale	695	NA [f]	694.10
n-MgO	NanoScale	685	4	424.60
n-TiO_2	NanoScale	505	NA [f]	277.45
n-SiO_2	NanoAmor	490	15	180.00
n-Al_2O_3(-)	NanoScale	275	NA [f]	68.45
γ-Al_2O_3	Alfa Aesar	260	NA	115.00
p-SiO_2	Alfa Aesar	240	NA [f]	116.00
p-TiO_2	Alfa Aesar	120	NA	112.00
n-CaO	NanoScale	100	20	65.80
n-ZnO	NanoScale	70	10	87.70
n-CeO_2	NanoScale	60	7	197.30
n-ZrO_2+10%CeO_2	NanoAmor	45	20-30	450.00
n-$Al(OH)_3$	NanoAmor	40	15	320.00
n-ZrO_2	NanoAmor	35	29-68	395.00
n-SnO_2	NanoAmor	35	55	270.00
n-CuO	NanoScale	35	8	Unavailable [e]

[a] Suppliers; NanoScale, NanoActive compounds [66]; NanoAmor: [68]:3.Alfa Aersar: [69]
[b] Determined by BET (Nova 1200)
[c] As specified by supplier (determined from XRD). NA = not available/amorphous substance.
[d] Price FOB for 1 kg quantities 3/13/08
[e] Discontinued Product
[f] Amorphous

Table 3-2 Catalyst pretreatment temperatures and catalytic activities for all prepared catalysts

Entry	Catalyst: 5% Pd on	Calc. T [°C]	Yield [g/g cat] ±10%	Yield [g/g Pd]
1	Activated C [1,2]	NA	1.7[4]	36
2	n-Al_2O_3(+) [2]	350	2.5	52
3	n-MgO	350	2.3	46
4	n-TiO_2	350	1.6	31
5	n-SiO_2	350	1.6	35
6	n-Al_2O_3(-) [2]	350	0.3	5.8
7	γ-Al_2O_3 [2]	350	1.5	24
8	p-SiO_2	350	1.6	32
9	p-TiO_2	350	2.6	52
10	n-CaO	350	0.15	2.8
11	n-ZnO	350	2.1	44
12	n-CeO_2	350	1.5	29
13	n-ZrO_2+10%CeO_2	450	2.7	58
14	n-ZrO_2+10%CeO_2	350	2.2	44
15	$Al(OH)_3$	350	0.8	17
16	n-ZrO_2	350	2.3	47
17	n-SnO_2	350	0.5	10
18	n-CuO	350	Fail [3]	NA

[1] Commercial catalyst.
[2] Results from previous work [66]
[3] No measurable amount of product could be recovered
[4] Yield ±20%

Table 3-3 Catalyst surface areas and other support properties

Catalyst 5% Pd	Catalyst SA [m^2]	CO Adsorbed [µmol/g cat]	% Dispersion[1]	Pd SA[1] [m^2/g]	Pd % SA	Pd Diameter [nm]	Product/Pd SA [mg/m^2]	Turnover Number [mol prod. / mol surf. Pd]
C (commercial)[1]	695	110	23.4	5.2	0.7	4	345	90
n-Al_2O_3(+)[2]	180	205	44	9.7	5	2.0	165	70
n-MgO	85	105	22	5.0	6	4.0	45	120
n-TiO_2	210	185	39	8.8	4	2.5	180	50
n-SiO_2	120	65	14	3.1	3	7	585	140
n-Al_2O_3(-)[2]	155	15	3	0.7	0.5	30	420	110
g-Al_2O_3[2]	200	6.5	1	0.3	0.2	68	3870	1000
p-SiO_2	230	20	4	0.9	0.4	22	1685	430
p-TiO_2	115	195	41	9.2	8.0	2.0	280	70
n-CaO	30	4.5	1	0.2	0.7	100	715	180
n-ZnO	35	75	16	3.6	10	6	620	150
n-CeO_2	60	245	52	12	19	1.5	145	30
n-ZrO_2+CeO_2	40	145	31	6.9	17	3.0	420	110
$Al(OH)_3$	55	25	5	1.2	2	18	1090	170
n-ZrO_2	35	95	20	4.5	13	4.5	355	130
SnO_2	20	15	3	0.7	4	30	705	180
CuO	30	1	0.2	0.05	0.2	440	0	0

[1] The Pd dispersion, surface area and average particle diameter and SA have been calculated using a conservative value of 1:1 as the CO:Pd stoichiometry and a surface atom density of 1.27×10^{15} atoms/cm^2. Some research has indicated that 2:1 stoichiometry with surface atom density of 1.44×10^{15} and may be more accurate for small particles [53]

[2] Results from previous work [66]

Table 3-4 Adsorption of NH_3 and CO_2 on the different catalyst supports

Support	NH_3 [sccm[1]/g support]	CO_2 [sccm[1]/g support]
n-Al_2O_3(+)	9.0	0.75
n-MgO	3.4	2.0
n-TiO_2	4.0	0.6
n-SiO_2	53	0.0
n-Al_2O_3(-)	8.3	0.6
γ-Al_2O_3	1.6	1.75
p-SiO_2	5.7	0.0
p-TiO_2	9.9	1.0
n-CaO	2.8	4.4
n-ZnO	14	0.2
n-CeO_2	7.3	0.8
n-ZrO_2+10%CeO_2	2.6	1.1
$Al(OH)_3$	25	0.1
n-ZrO_2	4.7	0.3
n-SnO_2	2.3	0.02
n-CuO	3.3	0.4

[1]Standard cubic centimeter: 1 ml at standard temperature and pressure

Table 3-5 Catalyst cost

Support	Support Cost [$/ g Product] [1]	Cost of product [$ cat./g product] [2]
n-Al_2O_3(+)	0.29	0.57
n-MgO(+)	0.18	0.49
n-TiO_2	0.16	0.62
γ-Al_2O_3	0.09	0.69
p-TiO_2	0.04	0.32
n-ZnO	0.04	0.37
n-CeO_2	0.11	0.54
n-ZrO_2+10% CeO_2	0.20	0.53
n-ZrO_2	0.16	0.48

1 Price FOB for 1 kg quantities 3/13/08

2 At a price of palladium at $450/oz. Calculation excludes cost of derivation to a nitrate precursor

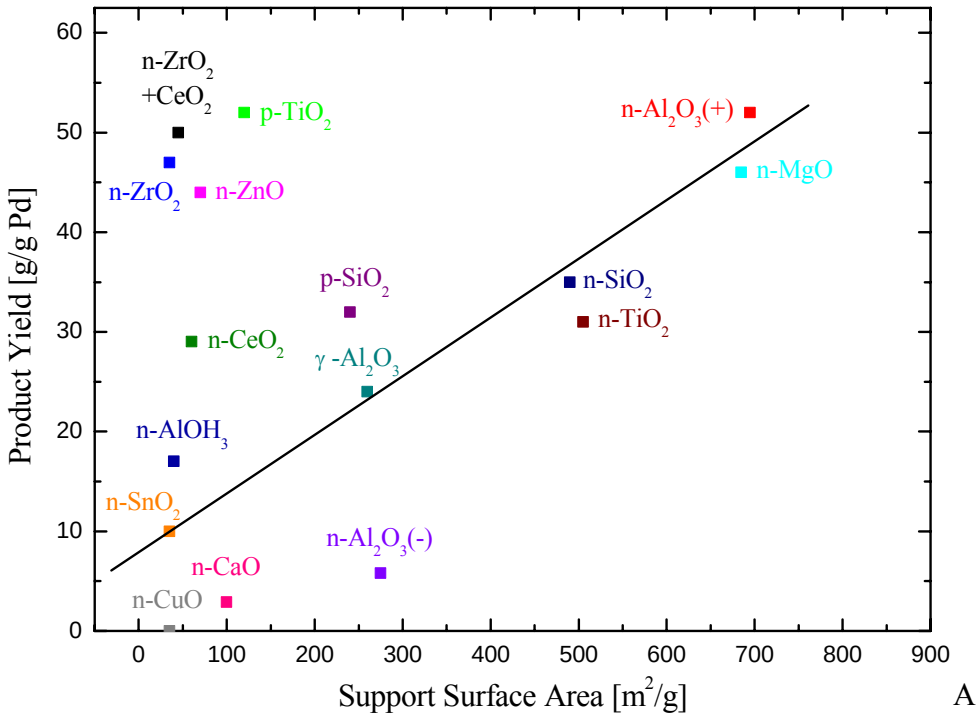

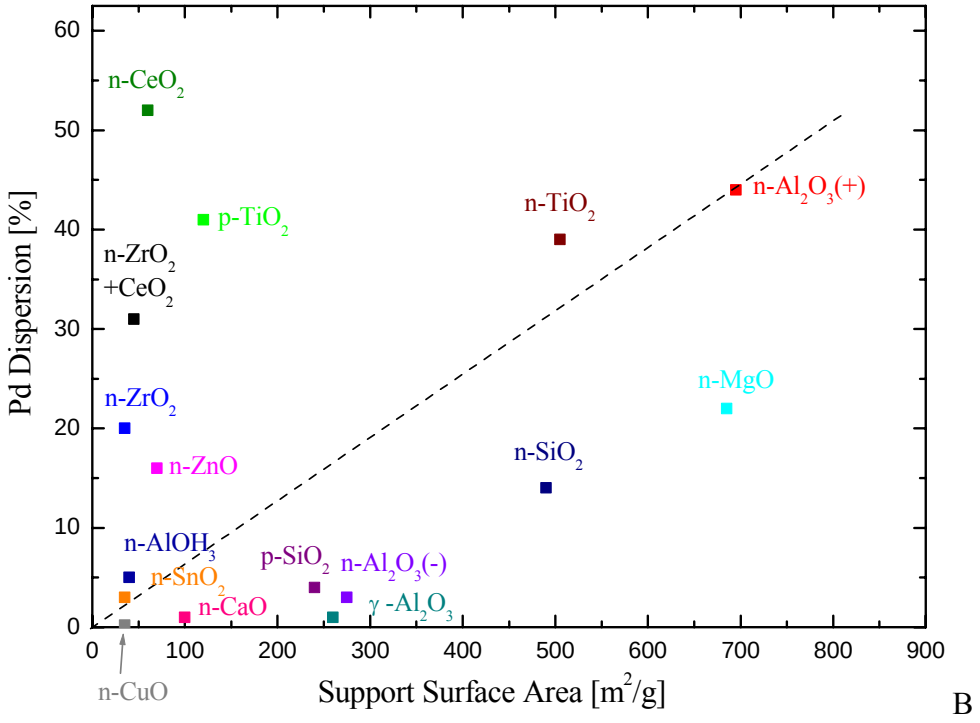

Figure 3-1 Support surface area effects, A) Product yields, B) Pd dispersions

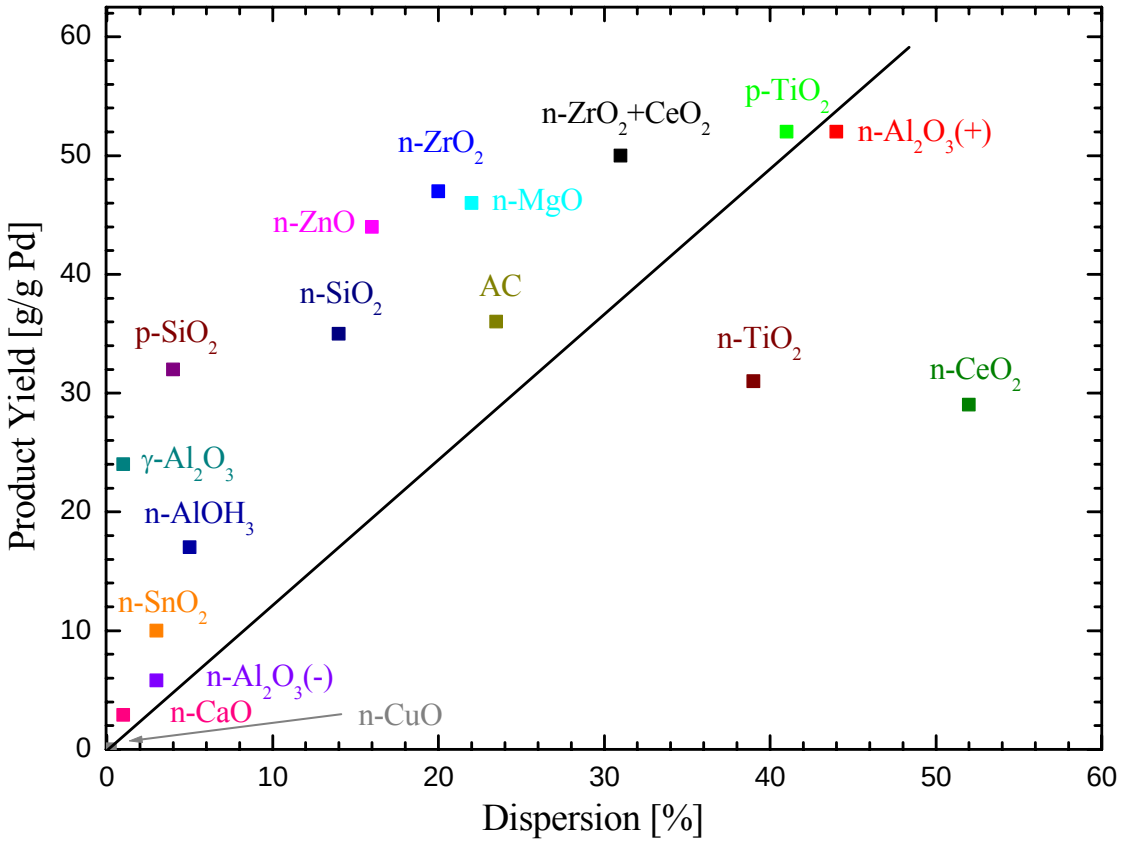

Figure 3-2 Palladium dispersion vs. product yield

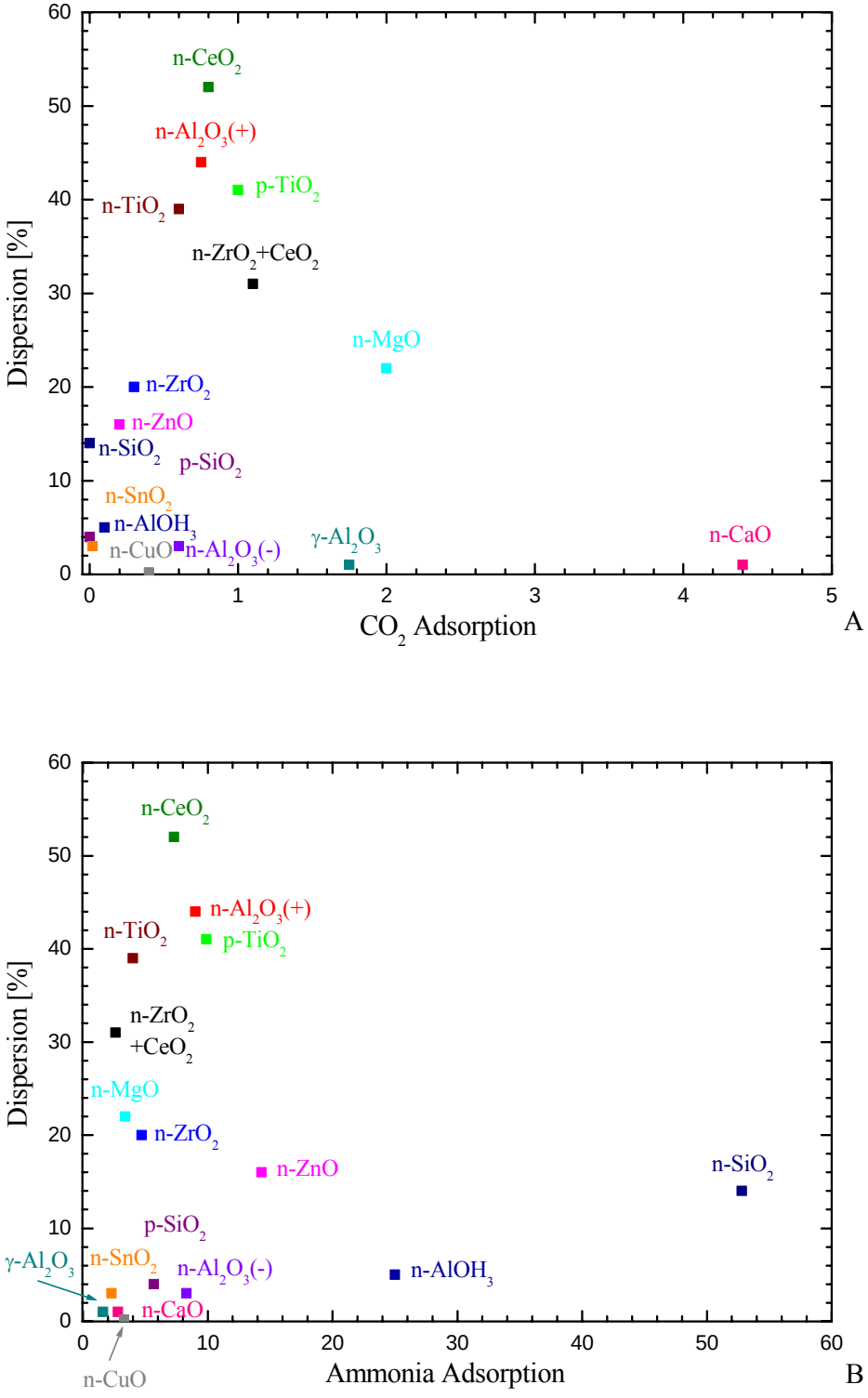

Figure 3-3 Support pH vs. palladium dispersion A) CO_2 adsorption B) Ammonia adsorption

CHAPTER 4
USE OF ZIRCONIA, CERIA, AND ZINC OXIDE AS ADDITIVES IN NANOPARTICLE-OXIDE-SUPPORTED PALLADIUM CATALYST FOR THE OXIDATIVE COUPLING OF 4-METHYLPYRIDINE[1]

4.1 Introduction

Bipyridines possess the ability to coordinate to transition metal cations and form complexes with distinct photochemical and catalytic properties [20,23,42,43]. Bipyridine complexes of ruthenium are especially interesting for applications in organic light-emitting diodes [23] and chemiluminescence detection systems [21,23,24]. Various catalyst systems also use transition metal complexes with bipyridine ligands [25,26], including oxidative carbonylation [27], the Kumada-Corriu reaction [28], and the Suzuki cross-coupling reaction [29]. Their widespread, large-scale use, however, is likely limited by the cost of bipyridine compounds. For instance, 4,4'-dimethyl-2,2'-bipryidine costs in excess of $5,200 per kilogram [31]. Consequently, finding more economical synthesis pathways to bipyridines is desirable. When developing new processes it is also important to consider environmentally friendly reactions. Reactions using no solvents with no byproduct formation, such as halide salts, are preferred.

The oxidative coupling of 4-methylpyridine to 4,4'-dimethyl-2,2'-bipyridine over a palladium is a simple one-step process that uses no solvents nor halogenated precursors (Figure 1-1) with only water and terpyridine as by-products. This reaction thus meets the criteria of an environmentally friendly process. However, the reaction rate is slow, and the catalyst undergoes deactivation during reaction, which limit the product yields [5]. Early research focused on

[1] Luke M Neal, Justin Dodson, Helena Weaver. Manuscript in preparation, used by permission, unpublished copyright (2008)

palladium on carbon (Pd/C) catalysts with yields for 5 wt% and 10 wt% Pd loadings varying between 1.5 to 2.0 g/g catalyst [5, 38-40]. In our previous research it was shown that a 5 wt% palladium precipitated onto nanoparticle alumina [n-Al_2O_3(+)] gives yields in excess of 2.5 g/g catalyst, which is the best performing palladium catalyst reported to date [66]. Several other oxide supports, including nanoparticle magnesia (n-MgO) and nanoparticle TiO_2, give catalysts with reasonable yields after 5 wt% palladium deposition, i.e. yields similar to or higher than the yields obtained from Pd/C catalysts. In addition, catalysts supported on nanoparticle ceria (n-CeO_2), nanoparticle zinc oxide (n-ZnO), and nanoparticle zirconia (n-ZrO_2) were found to produce moderate yields (> 1.5 g/g catalyst) despite the relatively low surface areas of the supports (< 70 m^2/g). The high dispersions on the latter nanoparticle oxides indicate favorable metal-support interactions.

In this paper, the effects of additives on nanoparticle catalysts are investigated. A few selected nanoparticle oxides and "promoter" oxides have been chosen for the study. The n-Al_2O_3(+), n-TiO_2 and n-MgO supports were selected due to their very high surface areas (> 500 m^2/g), and, consequently, strong potential for producing catalysts with high palladium dispersions. The addition of promoter oxides to palladium supported on these nanoparticle oxides could potentially improve the product yields. The strong metal-support interactions of CeO_2, ZnO, and ZrO_2 indicated by previous studies [see Chapter 3] suggest that these materials have potential as efficient additives for palladium catalysts. These materials are commonly used as catalyst promoters or catalyst supports in a number of systems. For example, Pd/CeO_2 catalysts have been studied in CO oxidation reactions [22,42] and in the methane reforming with CO_2 [78]. It has been suggested that CeO_2 interacts strongly in Pd catalysts due to formation of palladium hydroxide at basic sites on the ceria surface [79]. CeO_2 also has oxygen storage

abilities and can serve as an oxygen source to palladium [31]. The formation of Pd-O-Ce bonds promotes high metal dispersion and favors activity at interfacial metal-support sites on Pd-CeO_2 catalysts [80-82]. ZnO promoted Pd catalysts have been used in the water-gas shift reaction with a palladium catalyst [83] and Pd/ZnO are excellent catalyst for the steam reforming of methanol [21,43,84]. In these catalysts, a Pd-Zn alloy appears to form, leading to good metal-support interaction [83] and to improved thermal stability [84]. Pd/ZnO-based methanol reforming catalysts has been shown to have a longer catalyst life than Cu catalysts [41]. Using zirconia as a promoter improves the activity and thermal stability in methane combustion [18], and three-way catalysts (TWC) utilizes both ZrO_2 and CeO_2 to increase the oxygen storage capacity of palladium catalysts [80]. Another application of Pd/ZrO_2 catalysts includes the aromatization of hexane [20]. ZrO_2-supported palladium catalysts have also been applied to dichloromethane oxidation because of their thermal stability and their unique surfaces with acidic, basic, reducing, and oxidizing characteristics [85]. Pd/CeO_2 and Pd/ZrO_2 catalysts have similar oxidizing surface properties [23] and the oxygen storage and mobility, as well as the redox effects make these catalysts particularly interesting for oxidative coupling as the catalytic activity of this reaction appears to be limited by the reoxidation of palladium. Evidence suggests the PdO is the active phase whilst Pd^0 is inactive [5]. Since the catalysts after reaction are recovered with surface palladium in a reduced state and very little, if any, activity, assistance in oxygen transfer between the support and the palladium has potential to result in highly effective catalysts.

When preparing promoted supported catalysts, the additive can be deposited on the support with the active metal, or before the active metal (two step deposition). Therefore, this study also focuses on whether co- or sequential precipitation of additive and palladium on the nanoparticle oxides is the preferred catalyst preparation technique for this reaction. Co-precipitation forms a

uniform distribution of active species [86]. However, the added oxide may cover the active metal and thus hinder the reaction. Sequential precipitation ensures the active metal gets deposited on the externals surface of the additive/support. The disadvantage of sequential precipitation results mainly from the reduction in the surface area of the promoted support versus the base support. Dependent on the additive/support identity this can lead to inhomogeneous active metal dispersion [86]. Furthermore, two calcination treatments are likely to cause damage to the support via sintering

The main objectives in this work were 1) to determine if CeO_2, ZnO, and ZrO_2 are effective additives for n-Al_2O_3(+)-, n-MgO-, and n-TiO_2-supported palladium catalysts and if the promoting effects are dependent on the nanoparticle oxide used, 2) determine which is the more effective preparation method, co- or sequential precipitation of the additive and palladium, and 3) determine if a catalyst with an activity greater than the best catalyst to date, i.e. the 5wt% Pd precipitated onto n-Al_2O_3(+), can be prepared via promoter addition.

4.2 Experimental

4.2.1 Catalyst Preparation

The catalysts were prepared using commercially available nanoparticles supplied by NanoScale Materials Inc[2] [66]. The precipitation method was used to deposit the palladium onto the supports. Using this method, the support was dispersed into an aqueous solution of metal nitrate(s). The mixture was titrated with NaOH to form metal hydroxide(s) on the support [51]. The amount of NaOH corresponded to a 50% stoichiometric excess based on the amount of metal nitrate(s) used. The resulting mixture was aged overnight at room temperature before being

[2] Surface areas: n-TiO2 = 505 m2/g, n-MgO = 685m2/g, and n-Al2O3(+) = 695m2/g,

filtered. The filtered material was rinsed in deionized water overnight and filtered again. Then the material was then dried at 105°C overnight and calcined at 350°C for 3 hours.

All the catalysts had loadings of 5% palladium and 5% additive by weight on metal basis, unless otherwise noted. Two different precipitation methods were used to determine the effect of the additives, co-precipitation and sequential precipitation. In the co-precipitation method, the cerium nitrate, zirconium nitrate, or zinc nitrate was dissolved together with the palladium nitrate in deionized water before the support was added. The metals were then precipitated together onto the support using NaOH. In the sequential precipitation method, the metal oxide additive was deposited first by precipitation onto the support, aged, rinsed and calcined, and then the process was repeated to deposit the palladium. In the sequential precipitation, the amount of palladium is based upon the mass recovered additive/support after calcination.

4.2.2 Reaction Conditions

The reactant, 4-methylpyridine (Acros) was doubly distilled over KOH prior to use. The reaction was run in a 1:10 ratio of catalyst to reactant by weight in a round bottom flask. For all reactions 0.7 g of catalyst was used. The reaction mixture was evacuated followed by introduction of an oxygen atmosphere. The reaction was heated to the boiling point (145°C) under continuous agitation. After refluxing for 72 hours, the flask contents were filtered using a glass micro-fiber filter and washed with chloroform to dissolve the product. The product was obtained by removing the chloroform, water, and unreacted 4-methylpyridine with a rotary evaporator.

4.2.3 Carbon Monoxide Chemisorption

The support surface areas, as received, and the prepared catalyst were performed by multipoint Brunauer-Emmett-Teller (BET) isotherms on a Quantachrome Nova 1200 instrument as described in previous work [66]. Chemisorption measurements were performed in a

Quantachrome ChemBET 3000 instrument and used to characterize active catalyst surface area. The catalysts were reduced with hydrogen at 170 °C for 1 hour, and then outgassed in nitrogen at 170 °C for another hour, followed by titration with CO to characterize the palladium dispersions of the catalysts. A detailed description of the procedure and calculations is giving in previous work [See chapter 3]. A very mild reduction was used to limit sintering of the Pd particles on the surface. This is very important since PdO is believed to be the active phase or a necessary precursor for this reaction.

4.3 Results and Discussion

4.3.1 Catalytic Activity

All prepared catalysts were subjected to activity measurements in the coupling reaction of 4-methylpyridine. The results are summarized in Table 4-1. The Pd/n-Al_2O_3(+) catalyst from previous research has been added for comparison. Included is also a catalyst in which the nano-alumina support was calcined before deposition of palladium to determine the effects of the first calcination treatment in the case of the sequential precipitation method. As is evident from Table 4-1, calcining the n-Al_2O_3(+) support before deposition of palladium resulted in a catalyst with significantly reduced product yield.

4.3.2 Additives

Adding ZnO to the supported palladium catalysts under investigation did not increase the product yields by either deposition method. In the case of the Pd/n-Al_2O_3(+) addition of ZnO had little effect, only a slight, insignificant decrease was observed using the co-precipitation technique. In contrast ZnO appeared to reduce the catalytic activities of the Pd/n-TiO_2 and Pd/n-MgO catalysts. It has been reported that zinc readily forms an aluminate ($ZnAl_2O_4$) with the n-Al_2O_3(+) support under conditions similar to the ones used in the current study [87]. Mixed metal oxides with ZnO may also be expected for the n-TiO_2 and n-MgO, since $ZnTiO_4$ [88] and

$Mg_xZn_{1-x}O$ [89] have been observed. Naturally, compound formation between the support and the additive would reduce the favorable effects of the added metal oxide. In fact, if the additive only interacts with the support and there are no favorable interactions between the added metal oxide and the active metal (palladium), then it may be expected that the additive results in inferior activities. In this case, the additive can block some of the palladium on the surface and it will reduce any favorable palladium-support interactions. Furthermore, it has been observed that ZnO combined with oxide supports can induce reduction of palladium [36]. These phenomena would explain the low activities of the ZnO-promoted catalysts.

Addition of CeO_2 and ZrO_2 to the supported palladium catalysts could in most cases induce a promoting effect. However, the effect of the additive is evidently very sensitive to the preparation method, i.e. whether the Ce- or Zr-precursor is added before or at the same time as the active metal. The only exception to the promoting effects of the additives was the CeO_2 and n-Al_2O_3(+) combination for which a decreased catalytic activity was observed with CeO_2 addition irrespective of preparation method. There is no evident trend in the effects on the catalytic activity of CeO_2 and ZrO_2 addition as well as the preparation method between the supports. Sequentially precipitated CeO_2 appeared to promote the n-MgO- and n-TiO_2-supported catalysts with yield increases of approximately 15% and 35 % respectively. However, the co-precipitation method yielded Pd/CeO_2/n-MgO and Pd/CeO_2/n-TiO_2 catalysts that had lower activities compared to the cases without additives (see Table 4-1). The lack of promoting effect of CeO_2 on the alumina catalysts may be due to CeO_2-Al_2O_3 interactions as in the case of ZnO and $ZnAl_2O_4$ formation. This is supported by the fact that CeO_2 has been reported to induce damage to some supports, particularly alumina [31].

While sequential addition of ZrO_2 resulted in catalysts with lower activities than the catalysts without zirconia for the n-Al_2O_3(+) and n-MgO supports, this preparation method resulted in a more active Pd/n-TiO_2 catalyst. Evidently, co-precipitation of ZrO_2-and PdO-precursors resulted in less active Pd/nTiO_2 and Pd/MgO catalysts. In contrast, ZrO_2 proved to be an excellent promoting additive when co-precipitated with PdO on the n-Al_2O_3(+). The co-precipitated Pd/n-ZrO_2 catalyst gave yields in excess of 3.3 g/g catalyst. This is ~30% more than the highest yield reported to date for this reaction system. The promoting effects of ZrO_2 and CeO_2 strongly indicate that decreasing the extent of PdO reduction, and/or enhancing the supply of oxygen to the reaction surface increase(s) the catalytic activity.

4.3.3 Catalyst Preparation Method

The results in Table 4-1 indicate that the catalytic activities of these catalysts are very dependent on the preparation method (sequential- versus co-precipitation). It appears that, in general, the co-precipitation method results in more active catalysts on n-Al_2O_3(+) supports, compared to the sequential precipitation method. In contrast, it appears that the sequential precipitation method results in more active catalysts on the n-TiO_2 and n-MgO supports. As pointed out in Section 3.1, calcination of the n-Al_2O_3(+) support before palladium deposition results in a significantly less active catalyst compared to the catalyst prepared using the as received n-Al_2O_3(+). This would explain the lower activities of the sequentially precipitated n-Al_2O_3(+)-supported catalysts. In fact, comparing the yield of the sequentially precipitated Pd/ZrO_2/n-Al_2O_3(+) catalyst, it is evident that the ZrO_2 indeed has a promoting effect compared to the catalyst prepared using the precalcined n-Al_2O_3(+).

For the n-TiO_2 and n-MgO supports, the first calcination step does not appear to have the same effect as on the n-Al_2O_3(+). The lower activities of the co-precipitated catalysts, compared to the sequentially precipitated catalysts, may in these cases be due to partial coverage of the surface

palladium by the additives. An unusual effect was noted for the co-precipitated $Pd/CeO_2/n\text{-}TiO_2$ catalyst; significant palladium mirrors were observed on the reaction flask after a completed reaction. This is evidence of palladium being dissolved into the reaction solution from the support and indicates week palladium-support interactions. This is usually only observed in cases where the catalyst has very low activity. Ceria may interact with Pd ions strongly enough to undermine support interactions during co-precipitation, whereas CeO_2 may provide good surface sites for Pd ions once it has been coated onto the surface. In general it appears that the sequential precipitation must be avoided on supports that are significantly damaged during calcination and this may be the main reason for using the co-precipitation method.

4.3.4 Catalyst and Metal Surface Area

Consistent with previous work, it is observed that, in general high dispersions correspond to high activities but that the correlation is not always direct, and does not hold across different catalyst types (Table 4-2). Generally the more active catalyst had higher dispersion than the catalyst with lower activity for a given support but among the higher activity catalyst there is no direct correlation of Pd surface area (SA) or crystallite size and activity. We have hypothesized that while the active Pd/PdO crystallites are quite small, the active Pd species in the catalyst are only a fraction of the total surface Pd. The sequentially prepared $n\text{-}Al_2O_3(+)$-supported palladium catalysts consistently had lower Pd surface areas (%50-70) than the corresponding co-precipitated catalysts. This supports the hypothesis that the support is damaged in the first calcination.

4.4 Conclusions

Several imported observations can be made about the use of ZnO, ZrO_2, and CeO_2 as additives in oxide supported palladium catalyst. When the support is more thermally stable ($n\text{-}TiO_2$, n-MgO) sequential deposition appears to work better. This may result from the additive

partially covering active Pd/PdO phase during co-deposition. In the case of the n-Al_2O_3(+) co-precipitation worked better than the sequential method. This is attributed to damage to the support during calcinations, as a 5% Pd/n-Al_2O_3 demonstrates similar decreases in activity if the support is pre-calcined before palladium deposition.

As an additive, ZnO generally decreased the activity of the catalysts. This is attributed to strong Zn-Pd interactions that either undermine Pd/PdO-support interactions, or disrupt the Pd/PdO phase due to alloying. CeO_2 appeared to promote the reaction in some cases, but did not produce any catalyst significantly superior to the 2.5±.16 g/g catalyst. The ZrO_2 also promoted some of the catalysts (coprecipitated Pd/n-TiO_2 and sequentially precipitated Pd/n-Al_2O_3(+)). In the case of sequentially precipitated Pd/ZrO_2/n-Al_2O_3(+), the highest observed activity per gram catalyst was observed (3.3±.3 g/g catalyst).

Table 4-1 Catalyst activity

Entry	Method	Support	Additive	Yield [g/g catalyst]	Yield [g/g Pd]
1 [1]	Precipitation	n-Al_2O_3(+)	-	2.5	50
2	Precipitation (precalcined)	n-Al_2O_3(+)	-	1.5	30
3	Co-precipitation	n-Al_2O_3(+)	CeO_2	2.1	42
4	Sequential precipitation	n-Al_2O_3(+)	CeO_2	1.6	30
5	Co-precipitation	n-Al_2O_3(+)	ZnO	2.4	47
6	Sequential precipitation	n-Al_2O_3(+)	ZnO	1.6	30
7	Co-precipitation	n-Al_2O_3(+)	ZrO_2	3.5	69
8	Sequential precipitation	n-Al_2O_3(+)	ZrO_2	2.3	45
9 [1]	Precipitation	n-TiO_2	-	1.6	31
10	Co-precipitation	n-TiO_2	CeO_2	1.2	25
11	Sequential precipitation	n-TiO_2	CeO_2	2.4	48
12	Co-precipitation	n-TiO_2	ZnO	0.9	17
13	Sequential precipitation	n-TiO_2	ZnO	1.2	24
14	Co-precipitation	n-TiO_2	ZrO_2	0.8	16
15	Sequential precipitation	n-TiO_2	ZrO_2	2.0	40
16 [1]	Precipitation	n-MgO	-	2.3	46
17	Co-precipitation	n-MgO	CeO_2	0.9	17
18	Sequential precipitation	n-MgO	CeO_2	2.9	54
19	Co-precipitation	n-MgO	ZnO	0.6	12
20	Sequential precipitation	n-MgO	ZnO	1.0	20
21	Co-precipitation	n-MgO	ZrO_2	1.9	38
22	Sequential precipitation	n-MgO	ZrO_2	1.8	36

[1] Results From previous work

Table 4-2 Promoted catalyst dispersion

Catalyst [5/5/90%]	Deposition Metod	μL CO/g Pd
Ce/Pd/n-Al_2O_3(+)	sequential precipitate	3690
Ce/Pd/n-Al_2O_3(+)	co-precipitate	5060
Zn/Pd/n-Al_2O_3(+)	sequential precipitate	2800
Zn/Pd/n-Al_2O_3(+)	co-precipitate	4490
Zr/Pd/n-Al_2O_3(+)	sequential precipitate	2230
Zr/Pd/n-Al_2O_3(+)	co-precipitate	4490
Ce/Pd/n-TiO_2	sequential precipitate	5430
Zn/Pd/n-TiO_2	sequential precipitate	680
Zn/Pd/n-TiO_2	co-precipitate	2220

CHAPTER 5
CHARACTERIZATION OF PALLADIUM CATALYSTS SUPPORTED ON NANOPARTICLE METAL OXIDES FOR THE OXIDATIVE COUPLING OF 4-METHYPYRIDINE[1]

5.1 Introduction

Palladium is one of the more versatile active metals since it can serve as a catalyst in a large number of reactions [9,90-92]. It is a very efficient hydrogenation catalyst that is commonly used in the reduction of many organic species. Palladium is also an excellent oxidation catalyst that has been used in the complete oxidation of CO [92,93], CH_4 [9-11] and volatile organic compounds (VOC)[95-97]. Selective oxidations can also be performed, e.g. conversion of hexane to benzene [18], as well as oxidation of alcohols to aldehydes or ketones [98]. Other applications include steam reforming of methanol and ethanol [62] and conversion of acetylene to ethylene [61]. One important reaction that has received relatively limited attention is the C-H activation and C-C coupling of aromatic systems over palladium catalysts. Of these, the palladium-catalyzed oxidative coupling of 4-methyl pyridine to 4,4'-dimethyl-2,2'-bipyridine is of particular interest. The bipyridine product has the ability to coordinate to transition metal cations and form complexes with interesting properties [2]. For example, some bipyridine complexes have unique photo- and electrochemical properties [20,21,23,24,43,44], while other organometallic bipyridine complexes are very efficient catalyst systems [25-29]. The 4,4'-dimethyl-2,2'-bipyridine is a particularly important bipyridine, since it can be easily modified in the 4 position [23,30]. For example, the oxidation of the methyl groups is facile resulting in 2,2'-bipyridine-4,4'-dicarboxylic acid [30], which can then be reacted further and used to tether the bipyridine, and then later a coordinated transition metal, to a support [99].

[1] Luke M Neal, Samuel D. Jones, Michael Everett, Gar B. Hoflund, Helena Hagelin-Weaver, Manuscript in preparation, unpublished copyright (2008).

Moreover, the oxidative coupling of 4-methylpyridine to 4,4'-dimethyl-2,2'-bipyridine over palladium catalysts is a simple, environmentally friendly, one-step process (Scheme 1), where water and the terpyridine are the only byproducts. This is thus an important alternative to routes utilizing expensive halogenated precursors to form the bipyridine. However, the coupling reaction is slow with relatively low yields [5] so significant improvements would be desirable.

According to the literature, the most commonly used palladium catalyst for the coupling of 4-methylpyridine is palladium on carbon (Pd/C), while commercial palladium on alumina (Pd/Al_2O_3) catalysts had been shown to be practically inactive [1-4]. In contrast, recent research studies have demonstrated that 5% palladium precipitated onto alumina nano particles (NanoScale NanoActive alumina plus) or porous titania (Alfa Aesar TiO_2 catalyst support) results in the highest yields reported to date for this palladium-catalyzed reaction, 2.5 g of product / g of palladium or 50 g / g Pd [66, see Chapter 2]. Previous studies have also shown that catalysts prepared via the wet impregnation method, or via precipitation of palladium onto a nanoparticle alumina support with larger particle sizes, were not active. In contrast, palladium precipitated onto a traditional γ-alumina support was shown to exhibit some, albeit limited, activity [66, see Chapter 2]. Other supports, such as n-MgO, n-ZrO_2, n-ZrO_2 doped with 10% CeO_2, and n-ZnO, can also be used to prepare active catalysts [see Chapter 3]. This represents a wide range of supports with varying properties. To this point, no systematic correlation between Pd dispersion and catalytic activity has been found. Low dispersions most often explain a low yield, but a high dispersion is not necessarily a requisite for a high activity. The most active catalysts were prepared using high surface area supports (>400 m^2/g) or were prepared using oxides which have been shown to exhibit strong metal-support interactions with palladium.

Additionally most of the active catalysts had a high number of acidic sites, but not necessarily any strong basic sites, i.e. little or no CO_2 uptake.

Since no distinct correlation between catalyst properties and catalytic activity has been found, a more thorough catalyst characterization study is therefore needed to determine so called structure-activity relationships, which in turn is necessary to be able to further improve these catalysts. Our hypothesis is that palladium supported on a nanoparticle oxide support has potential to be a very efficient catalyst for the reaction due to the high number of low coordination sites, such as corners and edges of this support [6]. These low coordination sites could result in strong metal support interactions and result in high dispersions and unique catalytic properties. We have found that high surface area supports, both nanoparticle oxides or traditional porous supports, can indeed result in high dispersions. Additionally, supports with strong palladium-support interactions can also give high dispersions and high catalytic activities. To further probe these catalysts they have been subjected to the following catalyst characterization techniques: I) X-ray photoelectron spectroscopy (XPS) to probe the surface composition and chemical states of the Pd phase in the fresh and spent catalyst, II) transmission electron microscopy (TEM) with energy dispersive spectroscopy (EDS) to image the structure and dispersion of prepared catalysts, as well as III) X-ray diffraction (XRD) to determine the particle sizes of the catalyst supports (and to determine if the palladium on the surface can be detected with XRD). The objectives of this work were to characterize the Pd/PdO crystallites in fresh, reduced, and spent catalyst for 1) crystallite size/dispersion, 2) oxidation state and electronic binding energy, and 3) compare binding energies of fresh catalysts with varying activities.

5.2 Experimental

5.2.1 Catalyst Preparation and Reaction

The commercial catalysts, 5% Pd/C (dry, reduced) and 5% Pd/Al_2O_3 were obtained from Alfa Aesar and used (as received or dried at 105°C for 1hr) in the reactions and catalyst characterizations. A number of 5% Pd catalysts precipitated onto nanoparticle oxide supports or porous supports, as described in previous work [66], were also carefully characterized.

The reactions were carried out by placing fresh calcined catalyst and doubly distilled 4-methylpyridine under reflux for 72 hours, as described in previous work [66]. After a complete reaction the catalyst was recovered using a glass micro-fiber filter and washed with chloroform to dissolve the product. The recovered spent catalyst was stirred in additional chloroform and filtered, followed by brief drying at room temperature before it was put in the XPS system.

Reduced catalysts were prepared by reduction in 5% hydrogen in nitrogen for 1 hour at 170°C and, outgassed in nitrogen for at 170 °C an additional hour and then cooled to room temperature with continued nitrogen flow. The sample was kept sealed in nitrogen until immediately before XPS sample preparation

5.2.2 Chemisorption

Fresh catalysts were reduced in 5% H_2 in nitrogen at 170ºC for one hour and then outgassed in nitrogen at 170ºC. Spent catalysts were outgassed in nitrogen at 170ºC for one hour. Selected spent catalysts were also subjected to the same reduction applied to fresh catalysts. These catalysts were then subjected to CO adsorption measurements to determine the Pd surface area. Estimates of the Pd particle sizes were made from these CO adsorption measurements. The details of the calculations for Pd dispersion, surface area and crystallite size are given in previous work [see Chapter 3].

5.2.3 X-ray Photoelectron Spectroscopy

The fresh, spent and reduced catalyst powders were pressed into aluminum cups prior to insertion into the ultra-high vacuum (UHV) chamber (base pressure $1 \cdot 10^{-10}$ Torr). XPS was performed using a double pass cylindrical mirror analyzer (PHI model 25-270 AR). Spectra were taking in retarding mode with a pass energy of 50 eV for surveys and 25 eV for high resolution spectra using a Mg Kα X-ray source (PHI 04-151). Data was collected and then digitally smoothed using a computer interface. A value for the C1s binding energy of 284.6 eV was assigned to correct for static charging [100].

5.2.4 X-ray Diffraction

The XRD data was gathered on a Philips powder X-ray diffractometer using Bragg-Brentano geometry with Cu-Kα radiation (λ = 1.54 Å). Diffraction patterns were obtained for selected calcined, reduced and spent catalysts. The catalyst powders were secured onto a glass side with double-sided sticky tape. Average particle sizes were calculated from the line-broadening of the XRD peaks using the Scherrer equation

$$d = \frac{K \cdot \lambda}{(FWHM \cdot \cos(\theta))}$$

In this equation K is a constant generally taken as unity, λ is the wavelength of the incident radiation, $FWHM$ is the full width at half max and θ is the peak position.

5.2.5 Transmission Electron Microscopy

TEM grids we prepared by dispersing the catalyst into water by ultasonication and then placing a drop of the dispersion onto lacy carbon grids. Micrographs and EDS spectra were taking on a JEOL TEM 2010F, with a 200 kV electron source.

5.3 Results and Discussions

In the discussion of the characterization data obtained it is important to have an idea of a likely reaction mechanism. Therefore, a suggested reaction mechanism is presented here.

5.3.1 Proposed Reaction Mechanism

A reasonable description of the catalytic cycle for the palladium-catalyzed coupling of pyridine is presented in Figure (5-1). The first step is most likely coordination of the pyridine nitrogen to a palladium atom on the surface. Considering that there is a significant difference in yield between pyridine and 4-methylpyridine in these reactions [5], this coordination appears to be very important for the overall reaction. The C-H activation is probably facilitated by an oxygen atom in close proximity to the palladium on the surface. This step is likely the rate-determining step in these reactions. The result of the C-H activation is a hydroxyl group and a pyridine bonded to palladium via a carbon rather than the nitrogen. After two consecutive C-H activations and insertions, a reductive elimination gives a coordinated bipyridine [not shown in Figure (5-1)] which later desorbs to give the product. Also, water is formed from the two surface hydroxyl groups and desorbs leaving an oxygen vacancy on the surface. To close the catalytic cycle the surface oxygen must be regenerated. This step is likely not trivial in the reaction system, since the oxygen is in gas phase above the dispersion of catalyst and liquid reactant.

5.3.2 X-ray Photoelectron Spectroscopy

Even though XPS is considered a surface technique, it must be interpreted carefully for catalysts. This is due to the fact that the photoelectron attenuation length in a solid is ~ 20-40 Å [101], dependent on the kinetic energy of the electron (and thus also its binding energy). Consequently, the XPS probing depth is often greater than 10 atomic layers down into the solid. As catalysis takes place only on the top layer of a catalyst, most of the XPS signal originates from non-active near surface species. Furthermore, the near surface region of a catalyst is very

inhomogeneous both laterally and vertically. Consequently, it is challenging to obtain qualitative data of the surface composition of a catalyst. However, knowing the limitations of the technique very useful information can be obtained from XPS data collected from different catalysts.

The Pd 3d XPS spectra obtained from the palladium catalysts supported on the various alumina supports are presented in Figure (5-2). The commercial Pd/C and Pd/Al_2O_3 catalysts have been included for comparison. The major species on most catalysts, including Pd/C, is located at a binding energy of 336.1 eV, which is reasonably consistent with reference values for PdO (336.3 eV [36]). In fact, values between 335.6 and 337.1 eV have been reported for the Pd $3d_{5/2}$ peak of PdO [102]. In contrast, the major species on the Pd/Al_2O_3 catalyst is located at 334.5 eV. This binding energy is lower than that reported for bulk Pd metal (334.9 eV [100]), but is in agreement with values observed for surface Pd^0 typically seen in high-dispersion catalysts [78]. This observation supports the notion that PdO is the active phase on these catalysts. It also explains why the commercial Pd/Al_2O_3 catalyst exhibits little if any activity in these reactions, while the Pd/C is an active catalyst. As the commercial Pd/Al_2O_3 catalyst, the Pd $3d_{5/2}$ peak obtained from the spent $Pd/n\text{-}Al_2O_3(+)$ catalyst is located at a low binding energy (334.9 eV), which is indicative of Pd metal as has been observed previously for spent catalysts [5]. As pointed out previously, this is likely the main reason for catalyst deactivation in these systems. While the major species is PdO on the prepared fresh catalysts, the Pd 3d peaks obtained from the catalysts supported on the nanoparticle $Al_2O_3(+)$ are considerably broader than those obtained from the $n\text{-}Al_2O_3(-)$- and $\gamma\text{-}Al_2O_3$-supported catalysts. The $Pd/n\text{-}Al_2O_3(+)$ catalyst prepared via the precipitation method not only has a distinct shoulder at 337.8 eV, it also exhibits a small shoulder at 334.5 eV. This suggests that PdO_2 and Pd^0, as well as PdO are present on the surface of this catalyst. While the Pd 3d peaks obtained from the $Pd/n\text{-}Al_2O_3(+)$ catalyst

prepared via impregnation also are broad compared to those obtained from the $Pd/Al_2O_3(-)$ and $Pd/\gamma\text{-}Al_2O_3$ catalysts, the contributions from the PdO_2 and Pd^0 states are considerably smaller on this catalyst compared to the precipitated one. This may explain the observed differences in activity between the impregnated and the precipitated $Pd/n\text{-}Al_2O_3(+)$ catalysts (A summary of the product yields obtained from the catalysts are presented in Chapter 3 Table 3-2). However, it does not easily explain the differences in catalytic activity between the impregnated $Pd/n\text{-}Al_2O_3(+)$ and the precipitated $Pd/\gamma\text{-}Al_2O_3$ catalysts. Evidently, these systems are very complex and it may be that only certain palladium species, perhaps palladium particles below a certain size are active in these catalysts. The main difference between the Pd 3d peaks obtained from the $Pd/Al_2O_3(-)$ and $Pd/\gamma\text{-}Al_2O_3$ catalysts appears to be a small shoulder at low binding energy on the $Pd/\gamma\text{-}Al_2O_3$ catalyst. There may also be an indication of a PdO_2 state on the $Pd/\gamma\text{-}Al_2O_3$ catalyst, but this species is close to the noise level. Since it is known that the dispersions are very low on the $Pd/Al_2O_3(-)$ and $Pd/\gamma\text{-}Al_2O_3$ catalysts, it may be difficult to discern the active species on these catalysts. This may be particularly true in the case of the $Pd/Al_2O_3(-)$, which apparently has a very low number of active sites [66].

The O 1s binding energy region is dominated by the Al_2O_3 oxygen at 531.0 eV on these catalysts (Figure 5-3). The O 1s peak obtained from PdO and the Pd $3p_{3/2}$ peaks cannot be detected on the alumina-containing catalysts, which means that no differences in the O 1s peaks between the catalysts can be observed. However, even on the Pd/C catalyst, where the support has a limited number of oxygens, this region is complex. This is due to the close proximity of the Pd $3p_{3/2}$ and the O 1s peaks. For example, the Pd $3p_{3/2}$ peak of PdO is located at 533.8 eV, while that of Pd metal is located at 532.3 eV and the O 1s peak of PdO is at 530.0 eV [103]. Therefore, on the Pd/C catalyst, which consist of a mixture of Pd metal and PdO, the O 1s from

PdO and the Pd $3p_{3/2}$ peaks from PdO and Pd result in a broad peak that cannot be resolved into the different constituents.

As for the alumina-supported catalysts, the titania-supported catalyst with the broader Pd 3d peaks is the most active (Figure 5-4). In this case it is the catalyst supported on porous TiO_2 rather than the Pd/n-TiO_2, which is the more active catalyst. It is a little surprising that the main difference between the Pd 3d peaks on the Pd/p-TiO_2 and Pd/n-TiO_2 catalysts is a more pronounced shoulder at lower binding energies for the Pd/p-TiO_2 catalyst. The spent Pd/n-TiO_2 catalyst has a very low binding energy, below the 334.5 eV reported for dispersed surface Pd^0. One catalyst was therefore subjected to a reductive treatment, the same reduction treatment as before the CO titration experiments. The Pd $3d_{5/2}$ binding energy of the reduced catalyst, 335.1 eV, is in agreement with the values reported for Pd metal. Consequently, the low binding energy of the spent Pd/p-TiO_2 may be attributed to differential charging caused by the presence of a species covering the Pd surface. This is supported by the fact that sputtering of the spent catalysts, i.e. removal of this surface species, results in a Pd $3d_{5/2}$ binding energy of 334.9 eV, i.e. very close to the binding energy reported for the reduced catalyst. These results further indicate the surface of the spent catalysts do contain decomposed products (Pd fouling) or reactants/products that strongly interact with the palladium (Pd poisoning), which could lead to catalyst deactivation as has been suggested previously [5].

The Pd 3d and O 1s peaks obtained from the fresh catalysts supported on n-ZrO_2, n-ZrO_2+10%CeO_2, and n-CeO_2 are presented in Figures 5-5 and 5-6. The binding energies of the Pd $3d_{5/2}$ peaks are located at 336.6 eV for the Pd/n-ZrO_2 and Pd/n-ZrO_2+10%CeO_2, and at 337.4 eV for the Pd/n-CeO_2 catalyst. These Pd $3d_{5/2}$ binding energies are higher than those observed on the Pd/Al_2O_3 and Pd/TiO_2 catalysts (336.1-336.3 eV, Table 5-1). The high binding energies

indicate the presence of electron deficient Pd(II) species on the surface, which is likely due to strong palladium-support interactions. As pointed out in Section 5.3.1, the coordination strength of 4-methylpyridine to a surface palladium atom likely has a significant effect on the reaction. A more electrophilic palladium, i.e. electron deficient, will have a higher affinity to the electron lone pair of the pyridine nitrogen which leads to a stronger coordination. After coordination, the higher charge on the pyridine nitrogen could facilitate abstraction of the proton to form the C-bonded pyridine on the surface. If this is the case, then increasing the electrophilicity of the palladium(II) on the surface would be expected to increase activity. Although the Pd/CeO_2 catalyst with a Pd $3d_{5/2}$ binding energy of 337.4 eV, is not more active than the $Pd/n\text{-}ZrO_2$ and $Pd/n\text{-}ZrO_2$+10%CeO_2 catalysts with binding energies of 336.6 eV, it appears that catalysts with high Pd 3d binding energies and broad peaks in general are more active than catalysts containing less electrophilic palladium(II) and narrower Pd 3d peaks.

In the case of the reduced Pd/CeO_2 catalyst, the Pd $3d_{5/2}$ binding energy is shifted to lower values (Figure 5-5). However, the binding energy is slightly higher (335.3 eV) than that observed for the reduced Pd/TiO_2 catalyst (335.1 eV). In addition, there is a large shoulder at 336.7 eV, indicating the presence of PdO on this catalyst. While this may in part be due to the brief air exposure after the reduction, it does indicate that either the PdO is difficult to completely reduce, since CeO_2 can assist with oxygen, or any Pd metal on the surface is easily re-oxidized to PdO. Either one of these would be very beneficial to the reaction system under investigation. The same may be true for the $Pd/n\text{-}ZrO_2$ and $Pd/n\text{-}ZrO_2$+10%CeO_2 catalysts, but in this case the Zr 3p peaks overlap with the Pd 3d peaks and obstruct the interpretation of the spectra.

The O 1s binding energy region is naturally dominated by the oxygen atoms from the support (Figure 5-6). In our case the O 1s peaks obtained from the CeO_2 and ZrO_2 nanoparticles are located at 529.1 and 529.7 eV. The value for CeO_2 is in agreement with the literature, while the binding energy for the ZrO_2 is lower than the commonly reported 530.5 eV [100]. However, a value of 529.9 eV has been reported for ZrO_2 [102], which means that using the C 1s peak as the charge reference is reasonable. Furthermore, considering that the O 1s peaks line up for the ZrO_2 nanoparticle, Pd/ZrO_2 and the reduced Pd/ZrO_2 it does not appear likely that the shift is due to differential charging. In general the O 1s peaks obtained from the catalysts are slightly broader than those obtained from the pure supports, due to the presence of the Pd $3p_{3/2}$ peaks (and perhaps the O 1s peak from PdO). It is interesting to note the O 1s peak obtained from the Pd/CeO_2 catalyst is significantly broader than that obtained from the CeO_2 support. It appears that there is a substantial contribution from oxygen-containing species with binding energies of 534 eV and higher on this catalyst. This is probably from the electron deficient PdO species and supports the high binding energy observed for the Pd $3d_{5/2}$ peak on this catalyst.

5.3.2 Transmission Electron Microscopy

The micrographs of the alumina catalysts show a variety of support structures (Figure 5-7). In the n-Al_2O_3(+) catalyst the support appears to be composed of agglomerated "flakes" (Figure 5-7 a). The bimodal γ-alumina (γ-Al_2O_3) contains fine rod/needle structures (Figure 5-7 B). The n-Al_2O_3(-) has larger and more round structure compared to the "flakier" n-Al_2O_3(+). Also, the palladium particles appear much larger on the Pd/n-Al_2O_3(-) compared to the Pd/ n-Al_2O_3(+). The presence of a fine structure in the moderately active γ-Al_2O_3 would be consistent with the presence of some low-coordination edge sites, whilst highly active, flaky nano-Al_2O_3(+) would be expected to have a higher concentration of corner and edge sites. It is also expected

that the largely inactive nano-Al_2O_3(-) with more spherical particles would have very few low-coordination sites. These results are consistent with our hypothesis that the number of low coordination sites on a support correlates with the catalytic activity of the corresponding catalyst.

Comparing the precipitated Pd/n-Al_2O_3(+) and a commercial Pd/C reference, small particles (>2nm) of PdO (identified by EDS) can be observed. It appears that the PdO particles are smaller on the Pd/n-Al_2O_3(+), which is consistent with the CO adsorption data. It is difficult to find Pd on the γ-Al_2O_3 catalyst and in cases where they are visible they appear larger than on the Pd/n-Al_2O_3(+) and Pd/C catalysts. This correlates well with the observed low dispersion on the Pd/γ-Al_2O_3.

5.3.3 X-ray Diffraction

Caution is necessary in interpreting XRD data obtained from catalysts. First of all, it is considered a bulk technique and has attenuation depths on the order of micrometers. XRD thus probes several orders of magnitude deeper than the thickness of the catalyst surface layers. This is a serious limitation, since the reaction over a heterogeneous catalyst occurs at the surface. Furthermore, there must be long-range order in a crystal for a phase to be detected with XRD. XRD is, consequently, insensitive to amorphous phases and the detection limit for small particles is around one nm. For catalysts where a few percent of an active phase is present at the surface of a support, the active phase can be, and often is, invisible with XRD. Despite these limitations, useful information can be obtained from XRD. This is particularly the case when the catalytic activity depends on the structure of the support. Even though the surface structure is likely different from the bulk, the bulk structure can influence surface structure and thus lead catalytic

activities that are dependent on the support structure [2]. XRD can also be used to probe trends between catalysts and can provide useful information when the active surface particles can be resolved. As the palladium oxide is visible on some of the catalyst supports used in this study, XRD was performed on a few selected catalysts.

Despite the high dispersions and the low palladium loadings, the presence of PdO in the fresh 5% Pd/n-Al_2O_3(+) is evident in the XRD spectra obtained from this catalyst (Figure 5-8). The XRD spectrum obtained from the n-Al_2O_3(+) support is included in the figure for comparison. It was known from the supplier that the n-Al_2O_3(+) is a poorly crystalline (actually stated to be amorphous) [67]. However, there is evidently some structure present in the n-Al_2O_3(+) sample, and it is not γ-Al_2O_3[3] which is often the phase present in high surface area alumina supports. The phase present on the n-Al_2O_3(+) support is identified as bohemite (aluminum oxide hydroxide) [4]. This phase is observed in catalysts calcined under 350ºC whilst only γ-Al_2O_3 is observed in samples calcined at 450ºC. The low palladium oxide signal and overlapping features with γ-Al_2O_3 or bohemite makes it difficult to determine the peak widths of the palladium oxide. Consequently, calculating the particle sizes using the Scherrer equation is challenging at best for these catalysts. However, on the precipitated sample calcined at 450ºC a PdO particle size of ~4.0 nm was calculated using the PdO[5] (122) peak. The low signal to noise of this peak limits the accuracy of the peak fitting, but considering the XRD limits in catalysis this is at least a number that can be used for comparison with other catalysts.

[2] A classic example is the influence of monoclinic versus tetragonal ZrO2 in the methanol steam reforming or methanol synthesis over Cu-based catalysts [104-105].
[3] JCPDS # 10-0425
[4] JCPDS # 21-1307
[5] JCPDS # 43-1024

The same difficulties in determining PdO particle sizes using the Scherrer equation arise for the fresh Pd/n-CeO_2 catalyst on which the main PdO peaks (101) and (002) is obscured by the (200) peak of the CeO_2[6] support (Figure 5-10) and no other peak due to PdO can be resolved. Of the catalysts analyzed using XRD, the p-TiO_2-supported catalysts were the only ones where determining the Pd and PdO particle sizes using the Scherrer equation was trivial (Figure 5-11). On fresh and spent Pd/p-TiO_2 catalysts, the estimated PdO and Pd particle sizes were ~4.0 and 4.6 nm respectively. As expected, this is a little higher than the particle sizes calculated based on the measured Pd surface areas, i.e. 2.4 nm for reduced Pd/p-TiO_2 catalysts. This is expected since XRD measurements normally give larger particle sizes compared to other techniques. It is due to the fact that amorphous phases cannot be detected with XRD and that the detection limit of XRD is particle sizes on the order of one nm. Of particular interest is that no PdO is observed in the spent catalyst. While the presence of amorphous PdO cannot be excluded, this indicates that the reaction over these catalysts reduces not only the surface PdO, but also the bulk PdO. This is a very important observation since complete reduction of PdO to Pd metal on the catalyst surface likely results in a species that is much more difficult to reoxidize than a PdO particle with a Pd surface layer. Again, this explains why supports with mobile oxygens, such as CeO_2 and ZrO_2, can result in very active catalysts.

5.4 Conclusions

The correlation between the fine structures observed in TEM and the catalytic activity is consistent with the hypothesis that low coordination sites on the support results in high catalytic activities. The particle sizes observed in TEM/EDS correlate well with the measured dispersions of the catalyst. XRD gives slightly larger particle sizes but is still reasonably consistent with the

[6] JCPDS# 43-1002

chemisorption measurements. This indicates that the CO chemisorption data gives reasonable estimates of dispersion and particle size.

XPS and XRD suggest that the PdO on the fresh catalyst is completely (both surface and the crystalline bulk) reduced to Pd metal at the end of the reaction. This is consistent with deactivation of the catalyst by complete reduction of the active PdO phase. Additionally, differential charging in the XPS spectra obtained from the spent p-TiO_2 catalyst indicates the presence of a contaminant/surface species on the palladium surface. The differential charging is diminished by sputtering, which indicates removal of the surface species. This in turn is consistent with deactivation by Pd/PdO surface fouling or poisoning by an unidentified byproduct, the desired product itself, or an unknown contaminant.

In XPS the most active catalysts exhibited broadening of the Pd 3d peaks (Pd/n-Al_2O_3(+) and Pd/p-TiO_2) and/or binding energies higher than expected for PdO (Pd $3d_{3/2}$ greater than 336.3 eV) (Pd/n-ZrO_2 and Pd/n-CeO_2). This is consistent with more electrophilic Pd(II) being responsible for activity.

Table 5-1 Palladium 3d binding energy for fresh, reduced and spent catalyst

Catalyst	Pd $3d_{5/2}$	O 1s
Fresh Palladium 5%		
n-Al_2O_3(+) 450ºC	336.3	531.0
n-Al_2O_3(+) 450ºC (impregnated)	336.3	531.0
n-TiO_2	336.4	529.9
n-MgO	336.2	531.0
n-Al_2O_3(-)	336.1	531.0
γ-Al_2O_3	336.2	531.0
p-SiO_2	336.1	532.1
p-TiO_2	336.3	529.8
n-ZnO	336.1	529.8
n-CeO_2	337.4	529.1
n-ZrO_2	336.6	529.7
n-ZrO_2+10%CeO_2	336.6	529.4
Reduced Palladium		
p-TiO_2	335.1	529.3
n-ZnO	334.5	529.9
n-ZrO_2	334.6	529.7
Alfa Aesar	334.5	531.0
Spent Palladium		
n-Al_2O_3(+) 350ºC	334.7	531.1
p-TiO_2	334.1	529.2
p-TiO_2 (sputtered)	334.9	529.4
n-ZrO_2+10%CeO_2	334.6	529.3

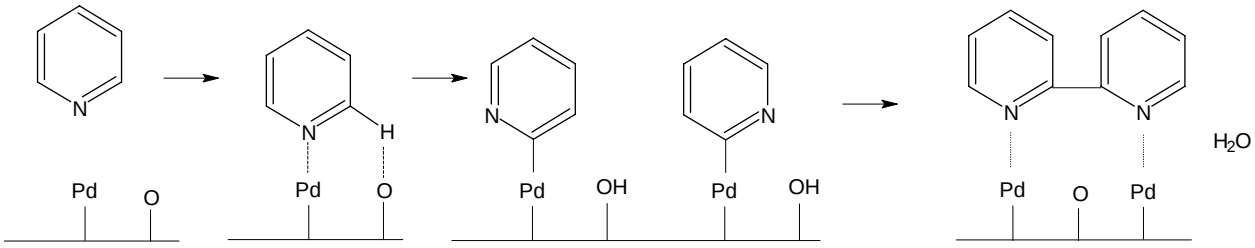

Figure 5-1 Proposed oxidative coupling reaction mechanism

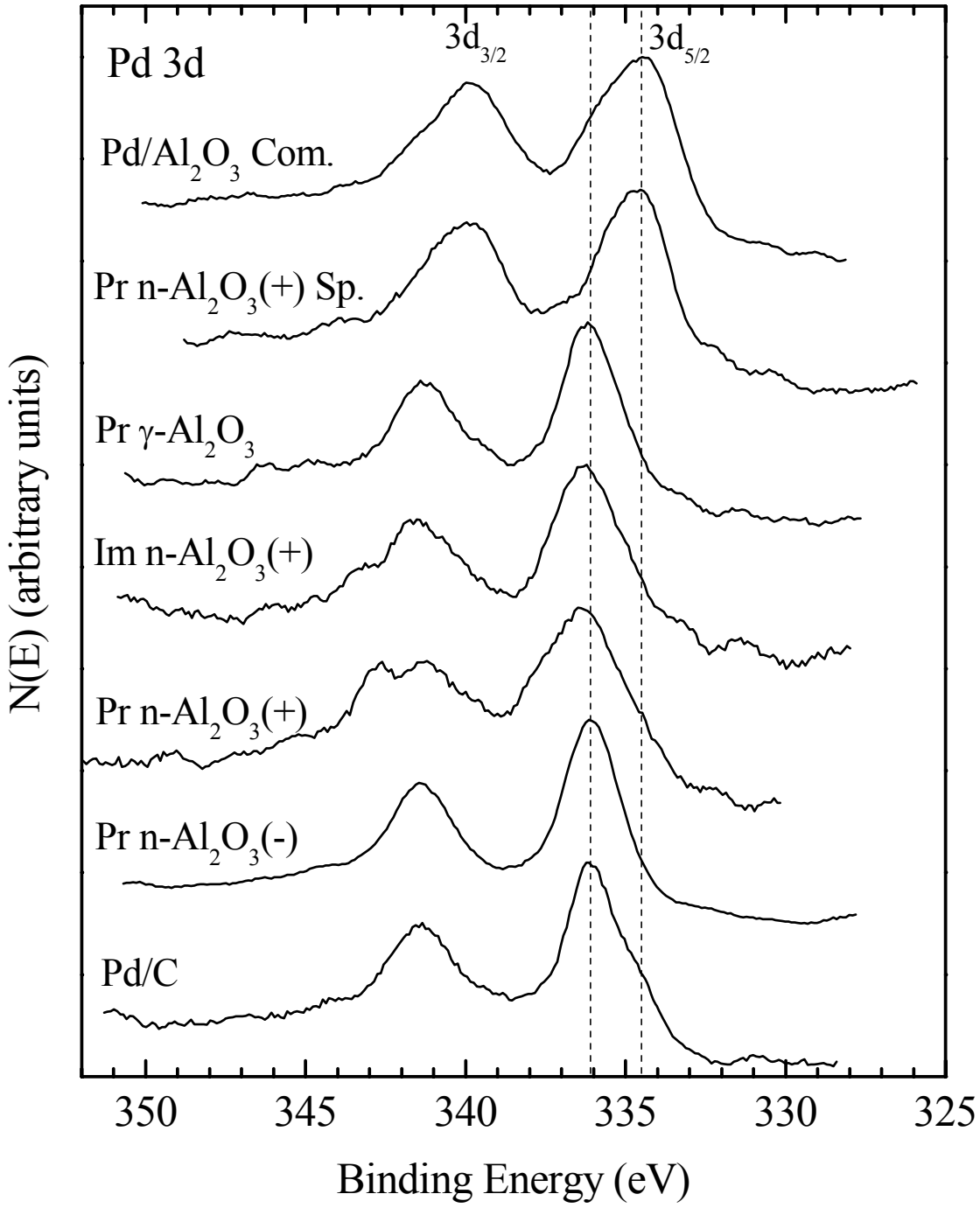

Figure 5-2 Palladium 3d spectra of palladium/nano-alumina catalysts

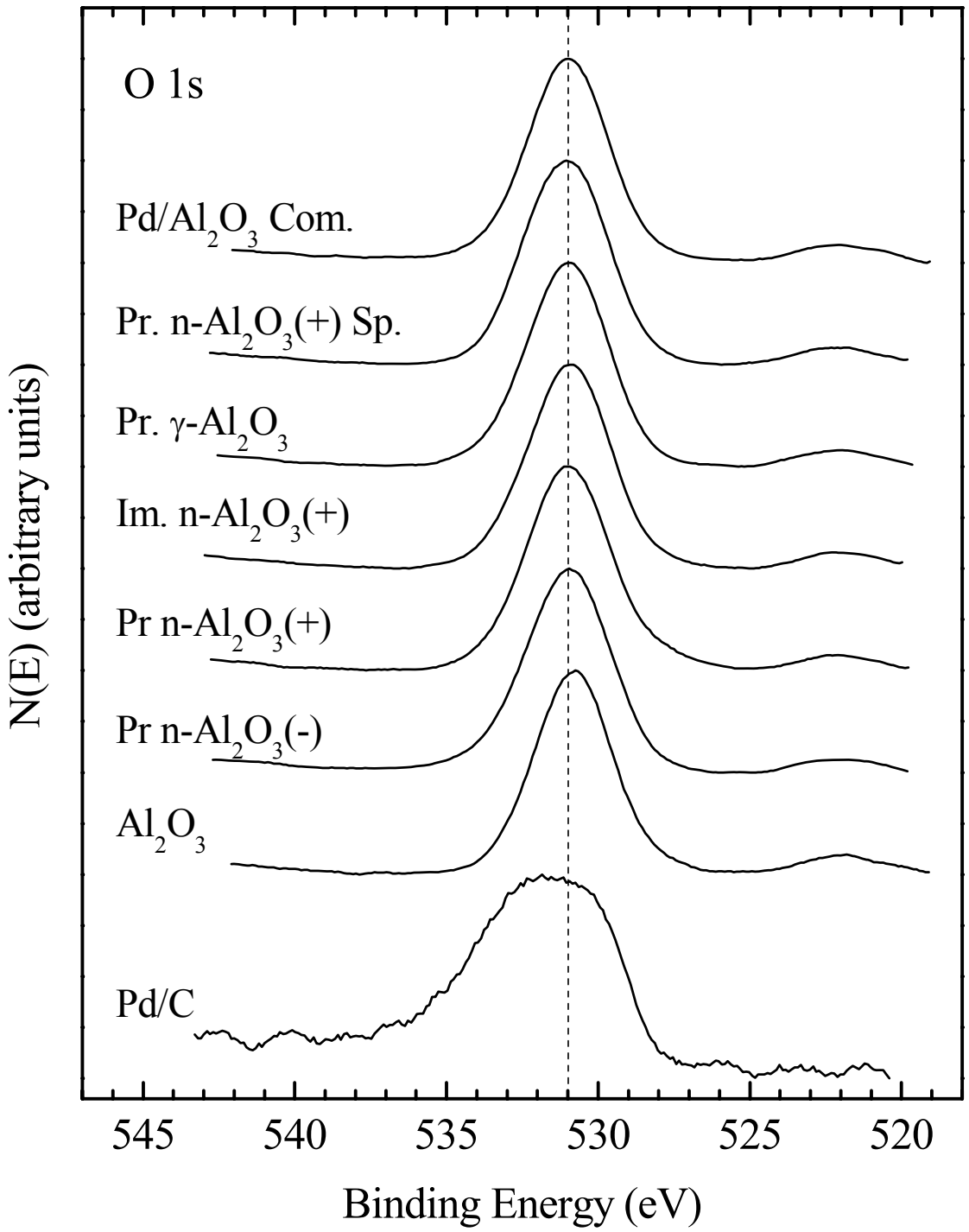

Figure 5-3 Oxygen 1s spectra of palladium/nano-alumina catalysts

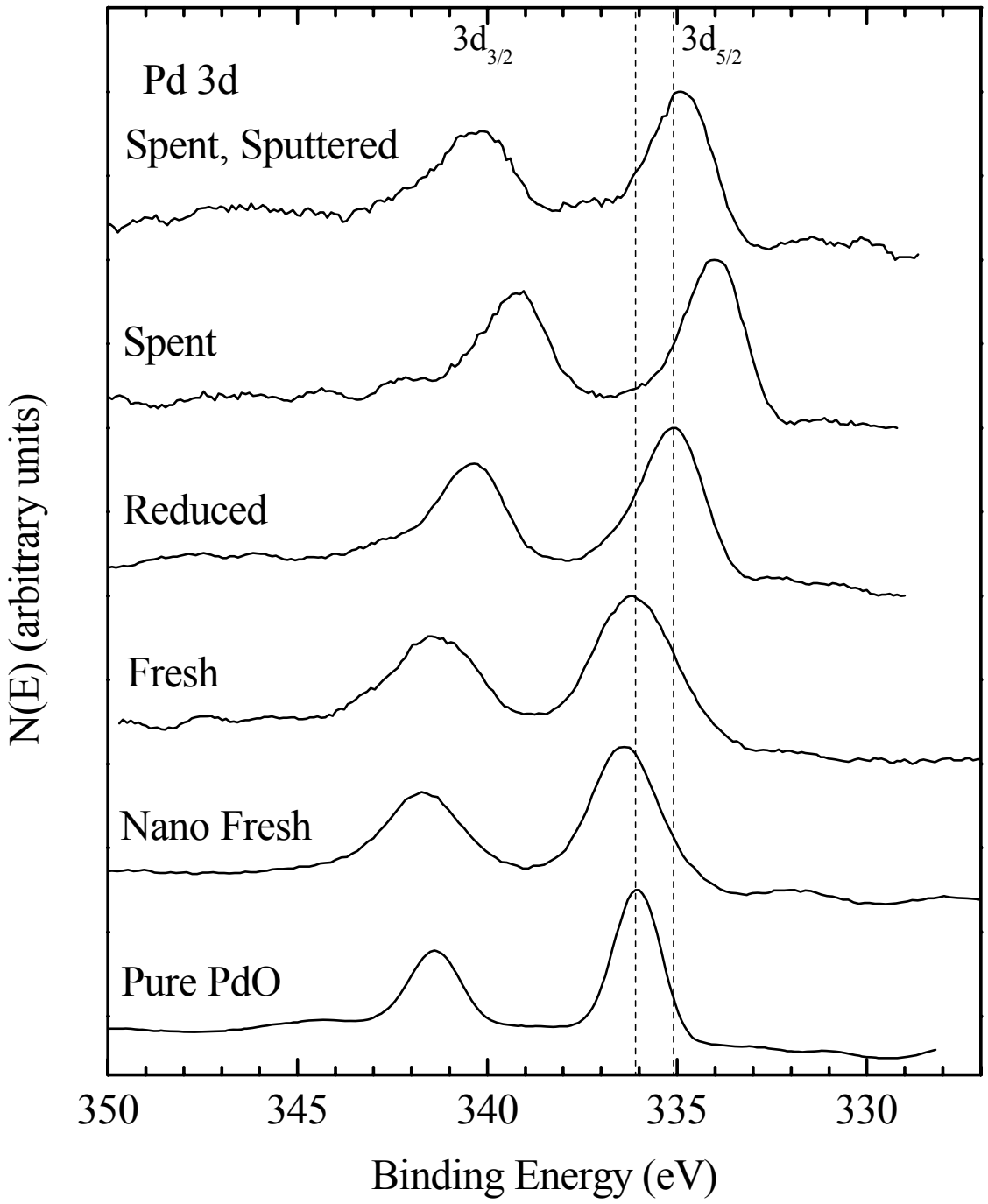

Figure 5-4 Palladium 3d spectra of palladium/titania catalysts

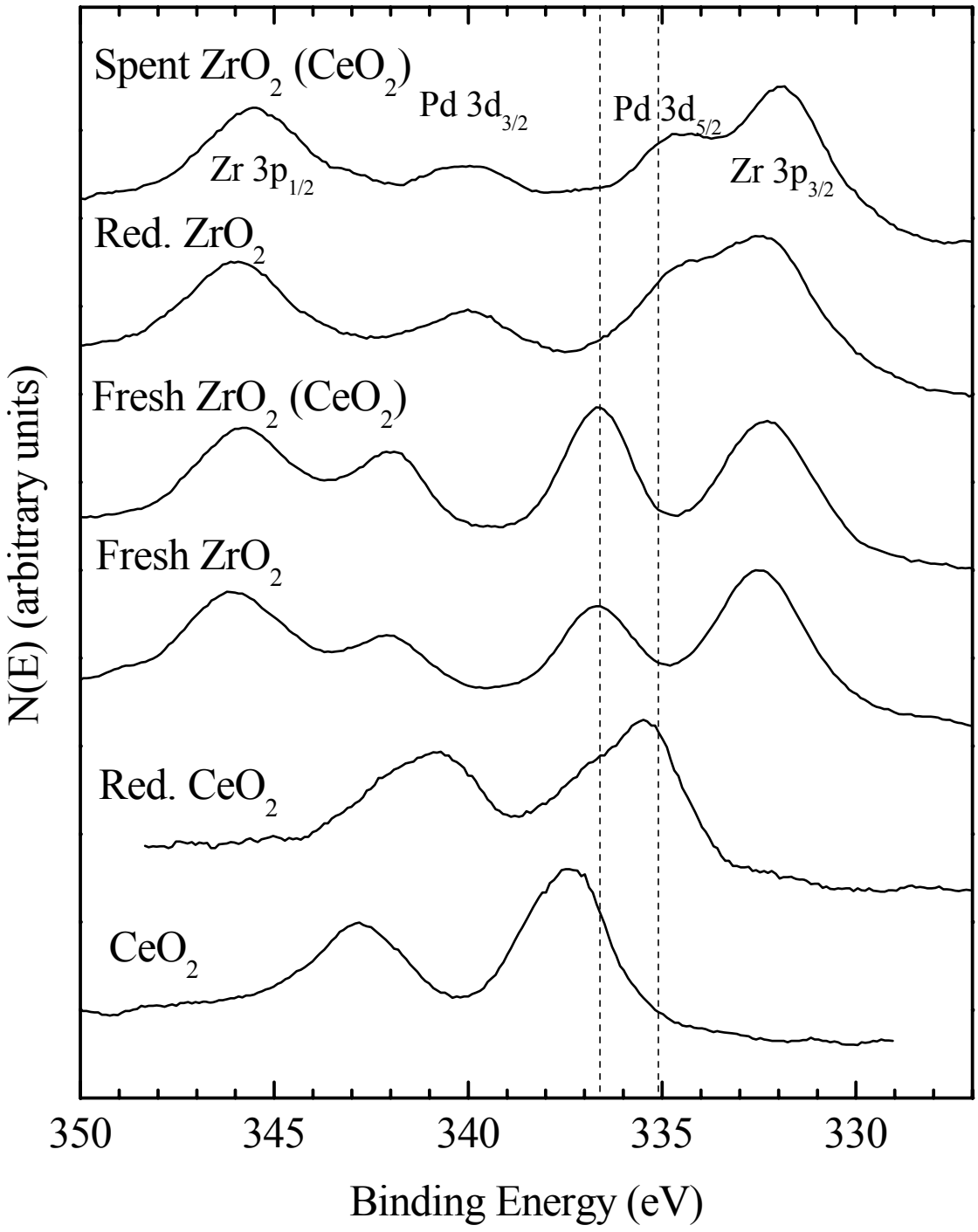

Figure 5-5 Palladium 3d spectra of palladium on nano- zirconia and ceria catalysts

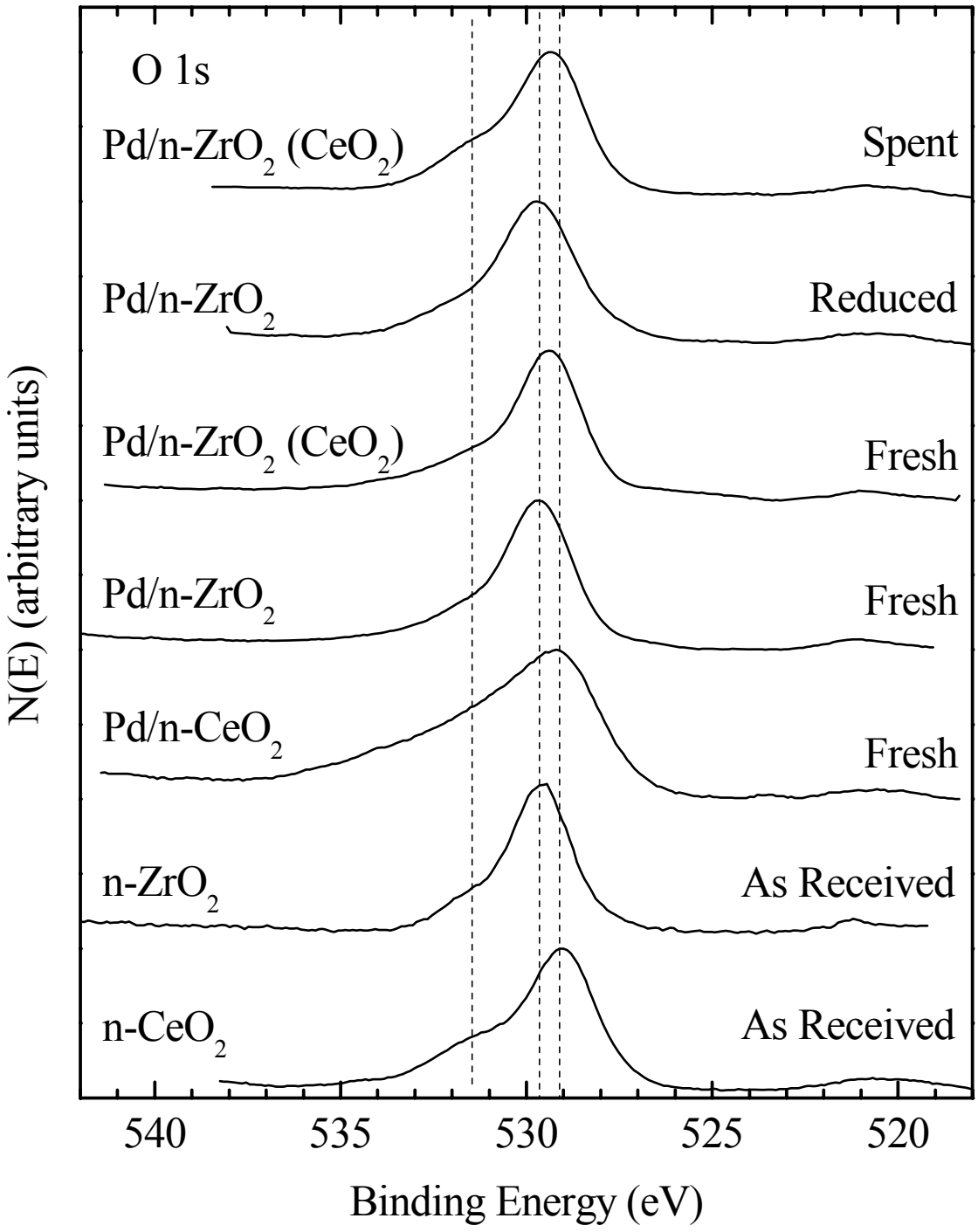

Figure 5-6 Oxygen 1s spectra of palladium on nano- zirconia and ceria catalysts

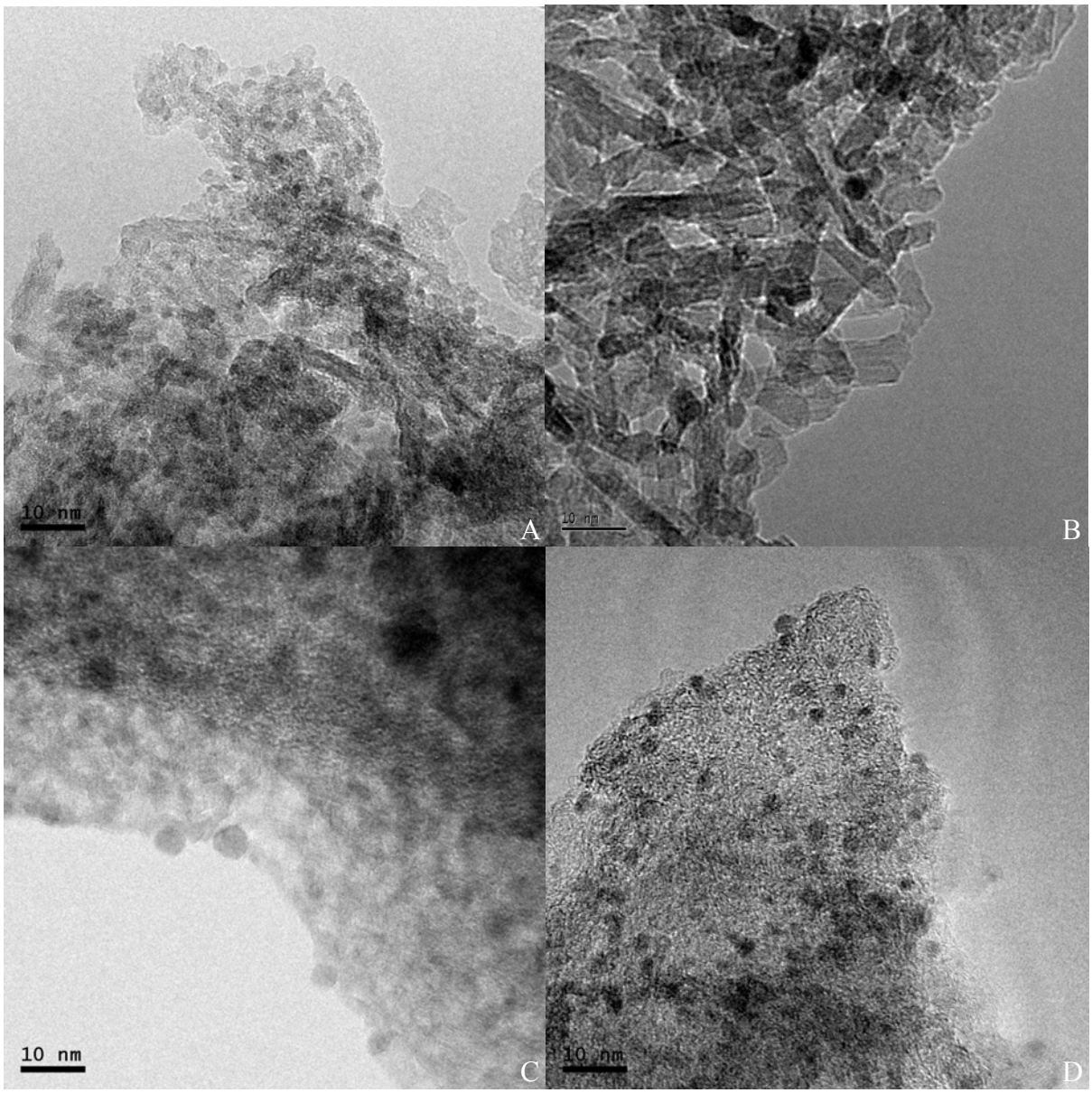

Figure 5-7 TEM of select catalysts A) Pd/n-Al2O3(+), B) Pd/γ-Al2O3, C) Pd/n-Al2O3(-) and D) Pd/C.

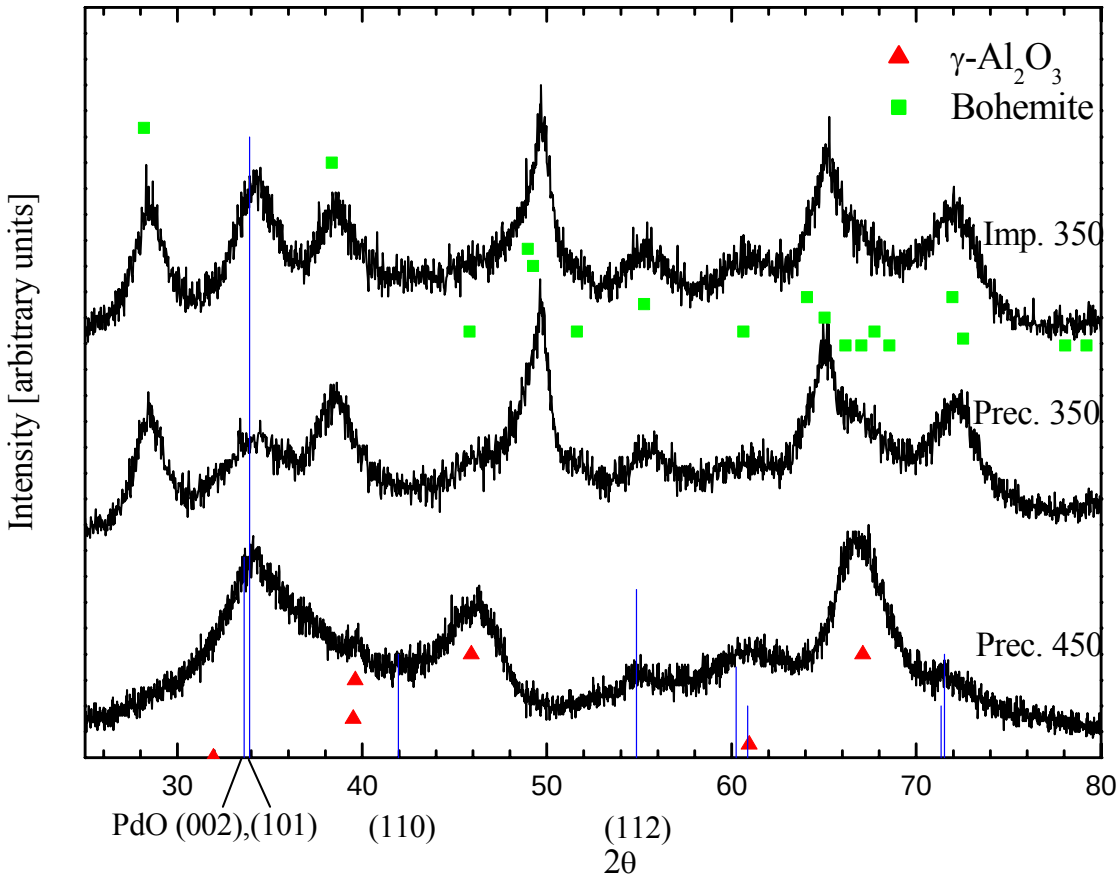

Figure 5-8 Powder XRD of n-Al_2O_3(+) catalysts[7]

[7] PdO(JCPDS # 43-1024), bohemite (JCPDS # 21-1307), γ-Al_2O_3 (JCPDS # 10-0425)

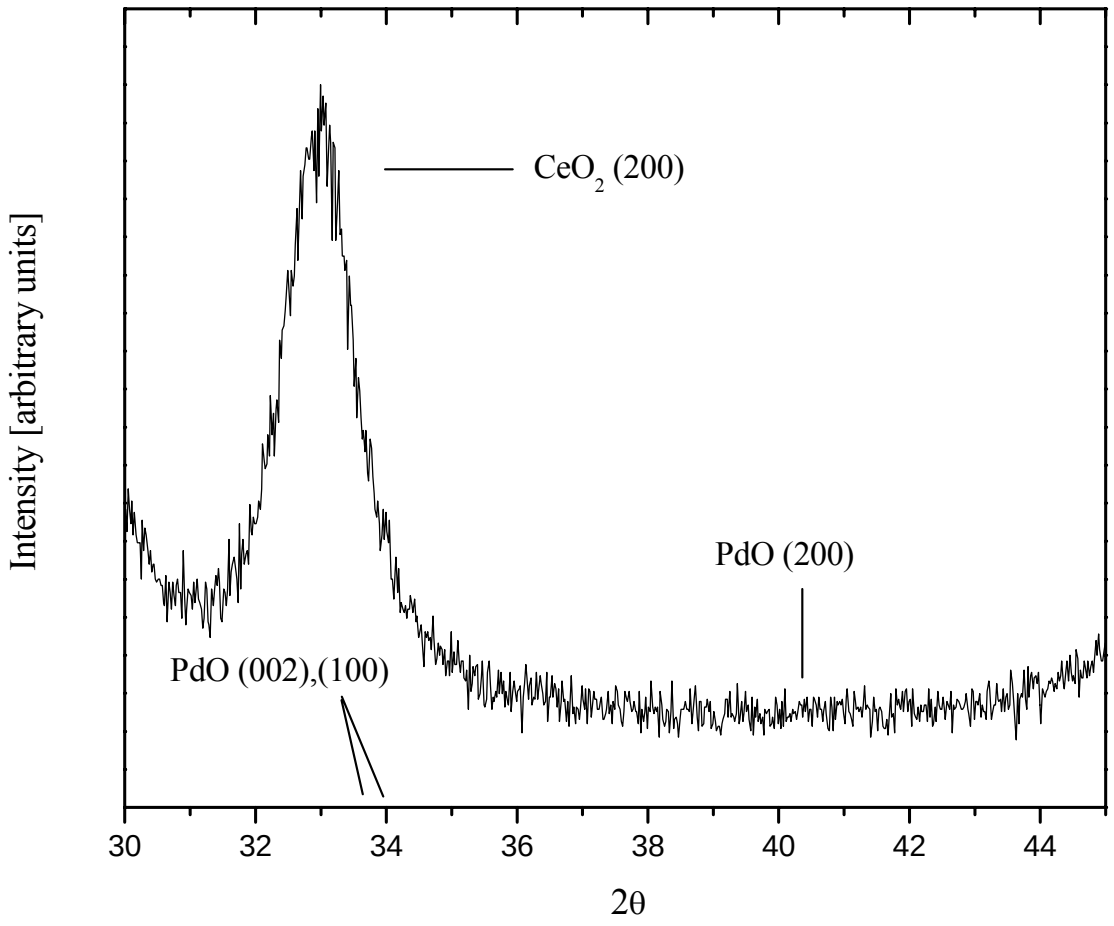

Figure 5-9 Powder XRD of palladium on ceria catalyst

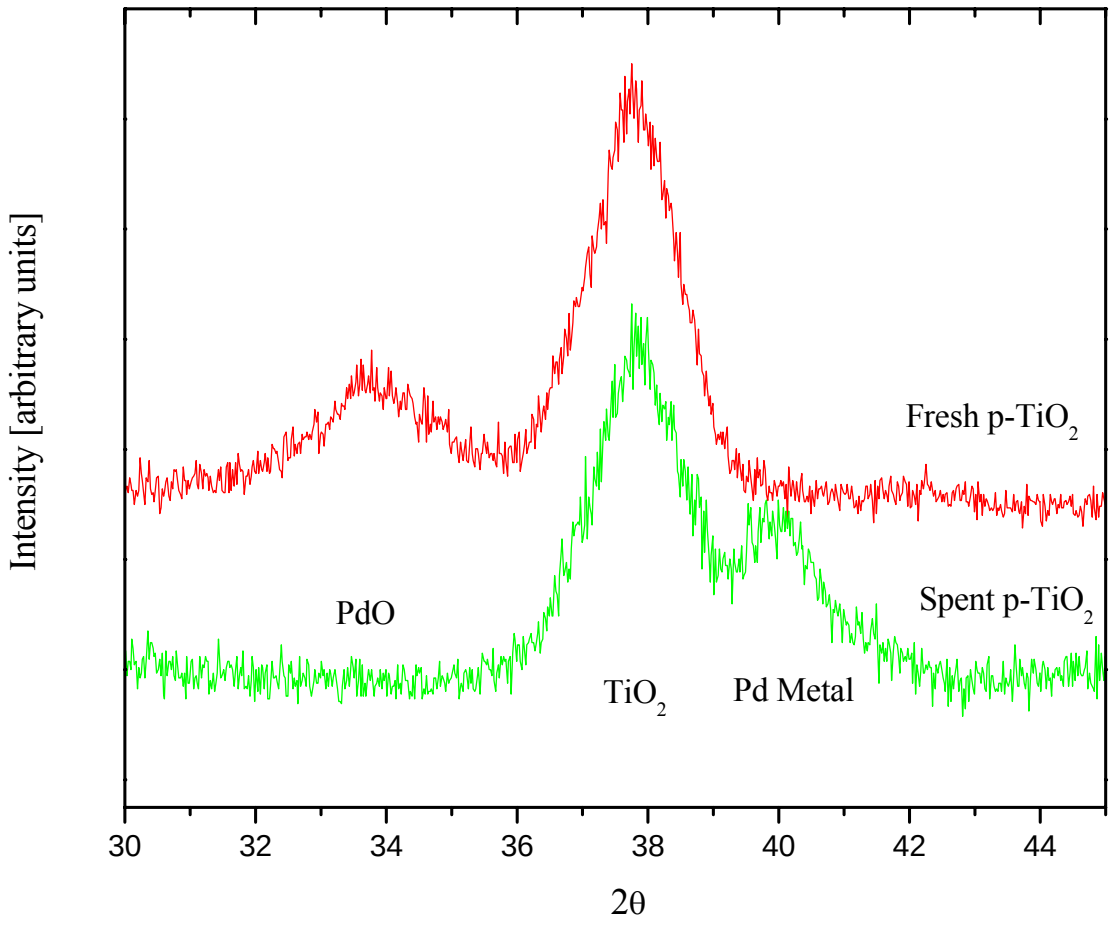

Figure 5-10 Powder XRD of spent and fresh palladium on porous titania

CHAPTER 6
OPTIMAZATION OF METAL-OXIDE-SUPPORTED PALLADIUM CATALYST FOR THE OXIDATIVE COUPLING OF 4-METHYLPYRIDINE[1]

6.1 Introduction

Bipyridines are important compounds since they can coordinate to transition metal ions and form complexes with interesting properties [20-22,41,42]. Some of these complexes have been studied for their photochemical properties, such as Ru-based bipyridine complexes [20,23,42-44], while other transition metal complexes have been used in various catalyst systems, e.g. Pd, Rh and Mo based systems [25-38,99]. However, bipyridines, such as the commonly used 4,4' dimethyl-2,2'-bipyridine, are prohibitively expensive for large-scale commercial use. They cost in excess of $5,200/kg [31], with smaller quantities selling for significantly higher prices per unit weight ($13-20/g depending on quantity [5-50 g batches] and purity [31,47,106]. Consequently, more efficient routes to bipyridines using relatively inexpensive starting materials are desired.

The simplest pathway to 4,4'-dimethyl-2,2'-bipyridine is the oxidative coupling of 4-methylpyridine using palladium catalysts [5] or Raney nickel [1-4]. Over both catalysts this is a one-step process in which the bipyridine is formed directly from the pyridine reactant without the use of solvents or costly halogenated precursors (Scheme 6-1). However, the reactions are slow and in both cases the catalyst deactivates, yielding only a few grams of product per gram of catalyst at best [1-5]. While Raney nickel is less expensive compared to palladium catalysts, it is more hazardous to handle as it is pyrophoric when dry and releases toxic vapors when ignited [107]. Additionally the potential for recycling after reaction is low for the Raney nickel.

[1] Reproduced from Manuscript in preparation Luke M Neal, Helena Weaver, Unpublished copyright (2008)

Therefore, Pd/C has been the catalyst of choice in the literature. Compared to the commonly used Pd/C our previous research has produced catalysts with higher and more consistent activities [66, see chapter 2]. The best catalysts to date for unpromoted catalysts are a 5% palladium precipitated onto alumina nanoparticles [n-Al_2O_3(+)] and a 5% palladium precipitated onto porous titania [p-TiO_2], which both gave yields in excess of 2.5 g of product per g of catalyst or 50 g/g Pd [66, see chapters 2 and 3], with yields in excess of 3.3 g/g catalyst (66 g/g Pd) being observed when 5% ZrO_2 (metal basis) is added to 5% Pd/n-alumina by co-precipitation [see Chapter 4]. This is to be compared with the maximum isolated yield of ~2 g/g of catalyst (40 g/g pd) reported for a 5% Pd/C, [37]. While the prepared catalysts supported on p-TiO_2 and n-Al_2O_3 are superior to the traditional Pd/C catalyst, it is our belief that further optimization is possible.

Since the major cost of palladium catalysts is the high price of the palladium, the most cost-effective catalyst is likely the one giving the highest yield per gram of palladium. The price of the support can also influence the cost-effectiveness of the palladium catalysts, particularly in the case of nanoparticle oxide catalysts in which the support can cost up to $700 per kg [68]. Consequently, to optimize the cost-efficiency of these catalysts it is important to optimize the yield per unit weight of palladium and to investigate supports other than the n-Al_2O_3(+), which has proven to be the best support to date. For this reason supports, such as n-MgO, n-TiO_2, and p-TiO_2, were included in the optimization study.

In addition to the selection of active metal and support, there are a number of factors that can influence the catalytic activities of heterogeneous catalysts. These include, for example, 1) catalyst composition, i.e. loading of active metal on the support or addition of promoters, 2) catalyst preparation method, such as technique and order of depositing the active metal and

additive on the support, as well as calcination temperatures or other pretreatments, and 3) reaction conditions, which includes reactant to catalyst ratios and reaction time.

Previous results have demonstrated that 10% and 5% loadings on n-Al_2O_3(+) give approximately the same yield per gram of catalyst despite similar dispersions and significantly higher Pd surface areas per gram of catalyst [66]. In fact, it has been shown that the Pd surface areas of the various catalysts tested are not strongly correlated to catalytic activity. Thus, it is expected that lower loadings of Pd have potential to produce similar yield per g catalyst, which corresponds to significantly higher yields per g Pd and a more cost-effective catalyst.

Previous research has revealed that the precipitation method is superior to the impregnation method. Of these the precipitation method involves more steps to be optimized. For example, in the early work a simple 50% stoichiometric excess of NaOH base (based on the amount of metal nitrate in solution) was added to precipitate Pd(II) out of solution as $Pd(OH)_2$ onto the support. It is possible that the resulting pH of the mixture after titration can affect the catalytic properties. This is particularly true for highly acidic or basic supports. The base used for precipitation may also influence the catalytic activity. In addition to the titration, the current procedure for catalyst precipitation requires multiple days to age and rinse the catalyst. The goal of the current study is to determine the effects of final precipitation pH as well as the aging and rinsing time on the catalytic properties.

In the earlier studies a reactant catalyst ratio of 10:1 (by weight) was used [66]. The bipyridine product is predicted to poison the catalyst, and, consequently, it is expected that a higher ratio of reactant to catalyst would increase the reaction yield per gram of palladium by diluting the concentration of inhibiting products. The disadvantage with this is that the actual conversion of reactant to product is likely to be lower at the higher reactant-to-catalyst ratio.

This means that in a commercial process the reactor cost would prohibit very high reactant to catalyst ratios due to the increase in reactor size. However, since it is possible that a higher ratio could significantly increase the yield, it is important to optimize this ratio. Another variable to optimize is the reaction time. The current procedure calls for a 72-hr reaction. With a more active catalyst, it is possible that such a long reaction time is not necessary to reach a reasonable yield.

The main objectives in this work is to 1) optimize the Pd loading for selected supports, 2) optimize precipitation methodology and 3) optimize reaction conditions, i.e. reactant-to-catalyst ratios and reaction time.

6.2 Experimental

6.2.1 Catalysts preparation

The catalysts were prepared using the precipitation method and commercially available nanoparticles supplied by NanoScale Materials Inc [67] or traditional porous supports from Alfa Aesar [69]. These supports were characterized in previous work [Chapter 3, Table 3-1 and Table 3-4].

In the precipitation method, the support was dispersed into a solution of palladium nitrate. The porous oxide pellets were ground before dispersion. The mixture was then titrated with a NaOH solution, which formed $Pd(OH)_2$ on the support [51]. The amount of NaOH used in for initial optimization corresponded to 50% stoichiometric excess based on the amount of Pd nitrate. For the optimization of the final precipitation pH, the dispersions were titrated with NaOH until a pH of 9 or 11 was obtained. The pH was measured with an Orion pH meter equipped with a ROSS Sure-Flow probe. For most catalysts the resulting mixture was aged overnight at room temperature before it was filtered. The recovered catalysts were rinsed by stirring in water overnight, followed by another filtration. For some catalysts the aging and/or

rinsing step was omitted. The catalysts were then dried overnight at 105°C and calcined at 350°C for 3 hours. Additionally, the calcination step was omitted for select catalysts to determine if it is necessary to heat the catalyst at higher temperatures before reaction to obtain reproducible results. Other catalysts were calcined at temperatures higher than 350°C.

6.2.2 Reaction Conditions

The 4-methylpyridine (Acros) was doubly distilled over KOH prior to use. In a typical reaction run 0.7 g of catalyst was placed in a round bottom flask along with 7 g of the distilled 4-methylpyridine for a reactant-to-catalyst ratio of 10:1. The reaction mixture was evacuated and an oxygen atmosphere introduced before it was heated to the boiling point (145°C). The reaction proceeded under reflux for 72 hours. For some catalysts 1 g of catalyst and 5 g of 4-methylpyridine or 0.5 g catalyst and 10 g of 4-methylpyridine were used to obtain reactant-to-catalyst ratios of 5:1 or 20:1 (by weight) respectively. For reaction time optimization the reaction mixture was removed from reflux after 24 or 48 hours. After reaction the flask contents were filtered using a glass micro-fiber filter and washed with chloroform to dissolve the product. The chloroform, water and unreacted 4-methylpyridine were removed using a rotary evaporator.

6.2.3 Palladium Dispersion

Chemisorption measurements to characterize active surface area of the catalysts and the number of acidic and basic sites were performed on a ChemBET 3000 instrument from Quantachrome Inc. The palladium surface area was measured by CO titration after reduction in hydrogen. The reductions were performed using mild conditions (170°C in a stream of 5% hydrogen) to minimize sintering of the formed Pd phase and to be close to the temperatures experienced by the catalysts during reaction. An explanation of the calculations used for Pd surface area and crystallite size are provided in previous work [see Chapter 3]. The surface areas

of supports, as received, were characterized in previous work [66] using a Quantachrome Nova 1200 instrument.

6.3 Results and Discussion

6.3.1 Palladium Loading

It was previously shown that reducing the palladium loading from 10% to 5% has little effect on the yield per g catalyst for the n-Al_2O_3(+) [66]. As is evident from Table 6-1 this is also true when going from palladium loadings of 5% to 2.5%. As a result, the product yield per gram of palladium is doubled every time the loading is reduced by half. Consequently, a 2.5% Pd loading gives four times as much product per gram of palladium as a 10% Pd loading. As is evident from Table 6-1 the palladium surface area decreases with the palladium loading. This means that the catalyst with the highest palladium surface area also gives the lowest product yield per gram of palladium, and consequently the lowest turnover frequency, i.e. the lowest amount of product formed per surface palladium for this set of catalysts. The turnover frequencies increase with decreasing palladium loading on these catalysts down to ~2.5% Pd loading (Table 6-1). The turnover frequency of the 2.5% Pd/n-Al_2O_3(+) catalyst (130) is the highest observed on these catalysts and is considerably higher than those of the 10%, 5% and 1% Pd/n-Al_2O_3(+) catalysts (35, 70, and 55 respectively). While the yield per gram of catalyst is reasonably constant between palladium loadings of 2.5-10%, a 1% palladium loading results in a dramatic decrease in the yield per gram of catalyst. In this case, the turnover frequency is also considerably reduced from the highest values observed for the 2.5% Pd loading (Table 6-1). Evidently, at the low 1% loading the amount of active palladium available at the surface is decreased compared to the available surface palladium on the 2.5% and 5% catalysts. Again it is evident that there is no direct correlation between the measured Pd surface area and the catalytic activity. Even though PdO is the active phase, it is not expected that the mild reduction used

before the CO titration measurements to determine the Pd surface area would lead to discrepancies of this size. Also, considering the high dispersions on all these catalysts, it is not likely that there are large differences between bridged and linearly bound CO on the surface, which would lead to difficulties in accurately determining the Pd surface areas using our instrument. The observed results may be due to a particle size dependence of the catalytic activity on these catalysts. If only palladium particles below a certain particle size are active, then as larger particles are formed the catalytic activity per Pd surface area would decrease with higher palladium loadings. Another explanation would be a limited number of "activating" support sites, i.e. palladium interacting with these specific support sites would result in much more active palladium species than palladium interacting with other sites on the support. If this is the case, then the 1% Pd loading would not be sufficient to fill up ("saturate") all these active support sites on the n-Al_2O_3(+). It appears that Pd loadings of ~2.5% for the n-Al_2O_3(+) support is optimal. This catalyst produces the highest yields of desired product per g of Pd.

In contrast to the Pd/n-Al_2O_3 catalyst, the p-TiO_2-supported palladium catalyst does have some sensitivity to loading. This indicates that some supports either do not exhibit a clear "saturation" or that the saturation Pd loading is higher on this support. The turnover number still significantly decreases as loading increases. However, it appears that optimal loadings, may vary from supports.

6.3.3 Reactant-to-Catalyst Ratios

As expected, the low 5:1 reactant-to-catalyst ratios resulted in decreased yields per gram of catalyst (palladium), while the 20:1 ratio had limited improvement in some cases (Table 6-2). However, since less reactant is used per gram of catalyst for the 5:1 ratio compared to the 20:1 ratio, the conversions were 2 to 3 times higher for the 5:1 compared to the 20:1 ratio. If the sole or major source of catalyst deactivation was poisoning of active sites by the product or by-

product (the terpyridine) it would be expected that the reactions were more sensitive to the reactant-to-catalyst ratios. While some effect is indeed observed, since the yield of product per gram of palladium is different for the various reactant-to-catalyst ratios, this is evidently not the major source of deactivation in these reactions.

The results from the reactant-to-catalyst ratios indicate that a ratio of ~10:1 appears reasonable unless unreacted started material is recycled at the end of the reaction, in which case a ratio of 20:1 or higher can be used to increase the yields. However, if the goal is to produce more product per gram of catalyst, it is likely better to adjust another parameter that has a larger influence on the product yield.

6.3.4 Titration pH

When preparing a 5% Pd catalyst on 1.9 g of n-Al_2O_3(+) or p-TiO_2 a typical pH of the resulting dispersion after titration with 50% stoichiometric excess base (based on the palladium(II) nitrate) was ~10.5-11 (Table 6-3, Entries 1-2). In the case of nano-silica supports (n-SiO_2) the resulting dispersion had a pH of ~9.0-9.5 after titration (Table 6-3, Entry 3). The pH of the n-Al_2O_3(+) dispersion increases relatively slowly near the end of its titration. In contrast, the pH of the p-TiO_2 and n-SiO_2 dispersions increase rapidly near the end of their titrations, if the amount of base corresponds to a 50% excess of the palladium(II) nitrate in the solution. This indicates that the acidity of the support significantly influences the pH of the solution for these supports. Consequently, titration based upon a 50% excess NaOH based on the stoichiometric amount needed to precipitate Pd(II) as $Pd(OH)_2$ may not be adequate for reproducibility on p-TiO_2 and n-SiO_2 supports. This is particularly true when using hygroscopic materials, such as sodium hydroxide and palladium nitrate dihydrate, for which the compositions of commercial preparations vary. Consequently, weighing of these materials is inherently imprecise, which is problematic since small changes in the concentrations of these materials can

lead to large variations in the final pH for dispersions in which there is a steep slope in the pH near the end of the titration. For low Pd loadings on acidic supports monitoring the pH during precipitation is even more important, since the final pH may be significantly lower than the desired pH to complete the $Pd(OH)_2$ precipitation. This may explain the lower yields obtained from a 2.5% loading on p-TiO_2 when the pH is not monitored.

Titration to a pH of 11 during the preparation of the n-SiO_2 catalyst did increase the yield modestly and improved reproducibility (Table 6-3). Additionally, no discernable brown color was observed in the filtrates during the recovery and rinsing processes. The pale brown tint due to palladium compounds was often seen in the first and/or second filtrate when the amount of NaOH was based on a 50% stoichiometric excess required for the Pd(II) concentration used in the preparation of the Pd/n-SiO_2 catalysts.

Monitoring the pH is also important at higher pH values. At a pH of 12 a large portion of the p-titania catalyst cannot be recovered from the mixture supports by filtration or centrifugation. It is possible that at very high base concentrations the support is etched, i.e. it begins to dissolve into the basic solution. Another possibility is that the high pH is far from the isoelectric point, with the result that aggregates are broken up and the suspension produced contains particles too small to be filtered. These phenomena make processing difficult at this pH.

6.3.5 Pre-reaction Treatment

It was found that unaged catalysts gave inconsistent results with large differences in activity. Aging and rinsing the catalysts did increase both Pd dispersion and yield (Table 6-4). The aging process may be important in allowing $Pd(OH)_2$ to be transported on the surface of the support from the solution. For the Pd/n-Al_2O_3(+) catalyst calcination of the sample did improve activity moderately with temperatures up to 350ºC, compared to the yields obtained from the catalyst dried at 105ºC. Calcination of up to 550ºC induced only minor deactivation of the

catalyst (Table 6-4). The small increase in yield with calcination temperature (between drying at 105ºC and calcining at 350ºC) may due to the removal of further water from the catalyst from either a $Pd(OH)_2$ or a $PdO \cdot H_2O$ phase. It could also be removal of water from the "alumina" support, since powder XRD measurements have shown that the n-Al_2O_3(+) contains a bohemite (AlOOH) phase before calcinations (See chapter 5). For the Pd/p-TiO_2 dried at 105 ºC, significant mirroring of the reactant flask and a dark brown product color is observed, which indicates leaching of the palladium from the support. Calcination at 450ºC gives a moderate decrease in activity while calcinations at 550ºC gives a greatly reduced activity of less than one half the 2.6 g/g seen for 5% Pd/p-TiO_2 calcined at 350ºC.

6.4 Conclusions

In this study it was determined that calcinations up to 350ºC increases activity and reproducibility of the catalysts over uncalcined samples. In the case of Pd/p-TiO_2 calcination at 550ºC gave approximately half the yield of a catalyst calcined at 350ºC, while higher calcination temperatures did not have a significant effect on the n-Al_2O_3(+) catalyst. Additionally it was found that higher reactant-to-catalyst ratios increased activity based on product yield per unit weight of catalyst, but above 10:1 by mass the increase is not significant. It was also found that the yield per gram of catalyst obtained from the Pd/n-Al_2O_3(+) is insensitive to loading between 2.5% and 10% on a metal basis, while Pd/p-TiO_2 does exhibit an increase in yield per gram of catalyst with increased Pd loading. While further work is likely to produce improved catalysts, the 2.5% Pd precipitation onto n-Al_2O_3(+) and the 5% Pd on p-TiO_2 are the best catalysts to date with activities of 2.7±0.27 (105±10% g/g Pd) and 2.6±0.26 g product /g catalyst respectively.

Table 6-1 Effects of palladium loading on catalyst properties and catalytic activities.

Pd/n-Al_2O_3(+)	Loading	g product/g catalyst	g Product /g Pd	% Dispersion	Pd SA [m^2/g]	Turnover Frequency[2]
n-Al_2O_3(+)	1.0%	0.66	66	72	2.8	55
n-Al_2O_3(+)	2.5%	2.7	108	48	4.7	130
n-Al_2O_3(+)[1]	5.0%	2.5	49	43	8.4	70
n-Al_2O_3(+)	10.0%	2.4	24	38	15	35
p-TiO_2	1.0%	0.9	90	56	2.2	95
p-TiO_2	2.5%	1.6	64	44	4.3	85
p-TiO_2[1]	5.0%	2.6	52	44	8.6	70
p-TiO_2[1]	10.0%	3.2	32	35	16	50

[1]Result from previous work [See chapter 3]
[2]Defined at mol product/mol surface Pd

Table 6-2 The effects of catalyst reactant ratio on the catalytic activities of Pd/ n-Al_2O_3 and Pd/p-TiO_2.

Catalyst	Reactant : Catalyst ratio	g product/g palladium	% conversion
5% pd on n-Al_2O_3	5:1	32	23
	10:1	51	25
	20:1	63	16
5% Pd on pTiO2	5:1	34	34
	10:1	46	23
	20:1	49	13

Table 6-3 Effects of titration pH on the activities of selected catalysts.

Entry	Catalyst	Titration pH	Product yield [g/g Pd]
1	5% Pd/n-Al_2O_3[1]	10.4	52
2	5% Pd/p-TiO_2[1]	11.1	52
3	5% Pd/n-SiO_2[1]	9.5	32
4	5% Pd/n-Al_2O_3	11.0	43
5	5% Pd/p-TiO_2	11.0	46
6	5% Pd/n-SiO_2	11.0	40
7	5% Pd/n-SiO_2	9.0	27

[1]Results from previous work [66]

Table 6-4 Effects of catalyst pretreatments on the activities and dispersion of 5% Pd precipitated on nano alumina (+) or porous titania.

Catalyst	g product/g palladium	% Dispersion
nano-Al_2O_3(+)		
Pretreatment:		
Unaged	51	
Unaged (repeat)	27	20
Unrinsed	25	
Dried at 105ºC	45	43
Calcined 350ºC	53	35
Calcined 450ºC	49	40
Calcined 550ºC	47	
p-TiO_2		
Dried at 105ºC	54*	
Calcined 350ºC	52	44
Calcined 450ºC	48	41
Calcined 550ºC	25	12

*Evidence of Pd leaching and/or catalyst contamination in product

CHAPTER 7
CONCLUSIONS

The research presented here was performed to study an important type of catalyst (supported palladium) and its use for producing a useful chemical (4,4'-dimetyl-2,2'-bipyridine). Additionally, the use of nanoparticles for enhancing catalytic activities was studied. The objectives of this work, included: 1) showing that nanoparticle oxides are viable supports for palladium catalysts in the production of 4,4'-dimetyl-2,2'-bipyridine via oxidative coupling of 4-methylpyridine, 2) determining what support/catalyst properties are responsible for activity, 3) developing an economically viable catalyst.

7.1 Summary of Results

In the initial study, the use of two nanoparticle aluminas (n-Al_2O_3) and a traditional porous alumina as supports were studied. The wet impregnation method of deposition on the n-Al_2O_3(+) gave poor activities. The yield obtained from a 5% loading of palladium precipitated onto n-Al_2O_3(+) is significantly higher than the same loading on carbon (49 ± 4 vs. 33 ± 6 g/g Pd). In addition to nanoparticle alumina, several other nanoparticle catalysts were determined to be active for the oxidative coupling reactions including nanoparticle ceria (n-CeO_2), titania, silica, magnesia, zirconia (n-ZrO_2), and ceria-doped zirconia, with activities ranging from (30-54 g/g Pd), while nanoparticle calcium oxide, copper oxide, aluminum hydroxide and tin oxide had little or no activity (less than 17 g/g Pd). Additionally porous silica, titania (p-TiO_2) and alumina (γ-Al_2O_3), were also active. The porous titania catalyst was of particular interest as it gives activities similar to the n-Al_2O_3(+) support (49 ± 4 g/g Pd). This indicates that a porous oxide with strong Pd/support interactions and/or high surface area (and, perhaps, a relatively high density of corner and edge sites) may be able to match nanoparticle oxide supports in activity for the oxidative coupling reaction.

The two main factors in catalyst optimization are cost and activity. The n-Al_2O_3(+) as well as n-ZrO_2 and p-TiO_2 catalyst were shown to have excellent activities compared to the standard palladium on carbon catalyst. However the n-ZrO_2 and p-TiO_2 are significantly less expensive than the n-Al_2O_3(+). It was determined that low loadings of palladium (2.5%) can be as active as higher loadings (5% and 10%) on the n-Al_2O_3(+) support. As the cost of palladium is the major cost in catalyst preparation, a lower loading with the same yield as a higher loading, represents a significantly cheaper catalyst. Also, it was determined that the use of ZrO_2 and CeO_2 as additives could boost the activity of a catalyst by up to 40% (up to yields of 3.1 ± 0.3 g/g catalyst for 5/5/90% coprecipitated Pd/Zr/Al_2O_3).

7.2 Nanoparticles Oxides as Palladium Support

7.2.1 Viability

At the outset of this research it was hypothesized that nanoparticle alumina oxides may be more active supports for palladium compared to traditional porous supports when used in the oxidative coupling of 4-methylpyridine. Palladium dispersed onto a high quality nanoparticle alumina [n-Al_2O_3(+)] via precipitation indeed gives excellent yields; 2.5 ± 0.15 g/g catalyst at a 5% Pd loading with a maximum yield of 105 g/g Pd at a loading of 2.5% Pd (metal basis) on the [n-Al_2O_3(+)]. This exceeds the highest reported activities for this catalyst in literature of (40 g/g Pd on Carbon [38] see Table 2-1). Additionally, palladium on other nanoparticle supports including nano- magnesia, zirconia, zirconia (with 10% ceria doping), and zinc oxide were found to have activities that exceeded reported values for Pd/C. Thus, in terms of activity per mass of catalyst and mass of palladium nanoparticle oxides were found to be viable catalyst supports.

7.2.2 Traditional Porous Supports

In addition to nanoparticle oxides, it was found that palladium dispersed on traditional porous supports were also active, with 5% Pd/p-Al_2O_3, Pd/p-SiO_2, and Pd/p-TiO_2 prepared by precipitation giving yields of 1.2,1.6, and 2.6 ±10% g/g catalyst respectively. (It is particularly noteworthy that Pd/alumina catalysts had been reported as inactive in literature [1]. However, this may be attributed to the use of pre-reduced catalysts). While only the activity of the p-TiO_2 was significant (in that it greatly exceeds the activity of commercial Pd/C; 2.6 ± 0.25 vs. 1.6 ± 0.3 g/g Pd), further study of porous catalyst supports is needed.

7.2.3 Nanoparticle vs. Porous Supports

The high activity of at least one porous oxide support catalyst (2.6±0.25 g/g catalyst for Pd/p-TiO_2) combined with the low activity of several nanoparticle supports raises the question of whether nanoparticles have a significant advantage over porous oxides. At current market prices porous oxides can be significantly cheaper than nanoparticles ($112.0/kg for p-$TiO_2$ [69] vs. $694.10/kg for n-$Al_2O_3$(+)[66]). Thus, at 5% loadings the p-TiO_2 is more cost effective than n-Al_2O_3(+), since the yields are almost the same: 2.6 ± 0.15 g/g and 2.5± .25 g/g catalyst, respectively). At a 2.5% loading of Pd the Pd/n-Al_2O_3(+) catalyst is more active per unit weight of catalyst compared with the 2.5% Pd/p-TiO_2. For Pd market prices of ~$15/g, the Pd content alone would cost ~ $0.75/ gram catalyst at 5% loading and $0.38/g catalyst at 2.5% which is less than the difference in support cost. However, the palladium nitrate precursors (for a 50g or less purchases) sell for large premiums over the market value of the actual Pd metal content ($60/g palladium[1]). Additionally, it seems likely that the cost of producing nanoparticle oxides will decrease as the technology becomes more developed and the scale of production increases.

[1] Based upon 50 g of palladium nitrate dihydrate at $1,170 (39% Pd) from Alfa Aesar #11035 [69]

Consequently, while porous oxides supports certainly deserve further study, nanoparticles oxides have greater promise for making the most cost effective catalyst.

7.3 Factors in Catalyst Activity and Deactivation

7.3.1 Palladium Dispersion and Surface Area

Perhaps the most striking result in this work is the lack of strong correlation between measured Pd dispersion and/or surface area. This seems to hold across multiple catalyst supports and within different loadings on the same support. If these results are reasonable measurements of the PdO surface area, then this has some important implications in that they indicate a structure sensitivity (which will be discussed shortly). However, the limitations of the CO chemisorption measurement must, certainly, be taken into account. It is possible that the CO to Pd ratio is not constant in the range of Pd particle sizes measured. If, for example the Pd:CO stoichiometry changes from near 2:1 to near 1:1 for palladium particles when going from loadings of 2.5% to 10% on the n-Al_2O_3(+) support, then the dispersions would be 96% vs. 38% Pd rather than the 48 ± 8 % vs. 38 ± 6% reported. Furthermore, it is possible that the palladium dispersion is altered significantly during reduction due to sintering, and that the degree of sintering could be much higher on some supports than others. More detailed studies, possibly incorporating a combination of XRD and/or TEM and possibly ISS (Ion Scattering Spectroscopy) would be useful in future studies to address these uncertainties. However, it seems unlikely that sintering and stoichiometry can fully account for the wide variances seen in the dispersion of active catalyst. For example, catalysts with measured dispersions of less than 5% (such as 5% Pd/p-SiO_2 and γ-Al_2O_3) were shown to give yields that are as high as 1/3 to 1/2 of the yields obtained from catalysts with dispersions and Pd surface areas that are more than eight times greater.

7.3.2 Structure Sensitivity

The low apparent correlation between the measured palladium surface area and the catalytic activity very strongly suggest that the reaction is structure sensitive[2], as a structure insensitive reaction would exhibit a direct correlation between the number of surface palladium atoms and the catalytic activity. In this work, it was not possible to conclusively identify what structures are responsible for activity. At first glance, the low correlation between activity and dispersion or palladium surface area suggests that the structure sensitivity is not related to particle size (which varies with dispersion), but this may be misleading. The turnover number varies significantly between catalysts, and in some low dispersion catalysts is very high (1000 vs. 70 for 5% Pd/γ-Al_2O_3 vs Pd/n-Al_2O_3(+). It is likely that only a small fraction of the surface Pd/PdO is active in any given catalyst. Because the measured dispersion can only give an average particle size, the presence of a minor fraction (in terms of SA) of smaller particles in the low dispersion catalyst can not be discounted. That the activity does seem to increase with dispersion, in the higher dispersion range (>10%), suggests that if there is a size dependence, it is the smaller Pd/PdO particles that are responsible for activity. Structure sensitivity could also be related to the support (as discussed in the next section).

The proposed mechanism (see Chapter 5) does suggest several factors that could contribute to structure sensitivity. The catalyst would need to hold oxygen and Pd atoms in a configuration that allows for formation of a Pd-N bond / C-H-O bond transition state. The structure should also be stable enough to allow oxygen to be removed and added. Additionally the active structure must be large enough to accommodate two adsorbed pyridines. Using FTIR with

[2] A detailed discussion of structure sensitivity and its various modes can be found in Masel [36]

pyridine[3] as an adsorbate, could prove useful in identifying active catalyst sites and their related structures. Use of nanoparticle-supported catalysts, were the active Pd/PdO phase is expected to be on the surface (rather than in pores) would be particularly suited for such a study.

7.3.3 Support Properties

The study of the wide range of active and inactive catalyst supports can give some insight into the properties that lead to catalytic activity. Firstly, very high surface area supports are likely to give high catalytic activities. The higher surface areas may be indirect indications of higher concentrations of edge and surface sites, which could be more active than oxide surfaces with lower surface areas. The interactions with low coordination sites could either influence the Pd/PdO structure or result in strong coordination of Pd ions to these sites and consequently forming more electrophilic palladium species. If these low coordination sites are interacting strongly with the Pd/PdO in this catalyst, these support sites would be expected to adsorb probe molecules such as CO_2 and pyridine. Consequently, the use of FTIR/TPD would likely give valuable insights into the concentration and nature of such sites.

Such a study would also be useful in more fully probing acid and basic sites on the bare supports. The concentrations of these acid and base sites alone, did not give much insight into activity or dispersion. However, the effectiveness of precipitation vs. impregnation strongly implies that acid/base properties are important (in that $Pd^{+2}/Pd(OH)_2$ is attracted to the support at some pH). The lack of any measured strong basic sites on the porous and nano silica together with their relatively high activities (1.6± 0.15 and 1.7 ± 0.2 g product/ g catalyst at a 5% Pd loading, which is comparable to Pd/C), would suggest that any interacting sites are acidic in nature. In addition to FTIR studies, laboratory preparation of nanoparticles, in which the

[3] Pyridine is a common adsorbate molecule in FTIR used for probing acid sites. Pyridine would seem likely to give useful information about PdO adsorption sights in this reaction.

particles properties could be adjusted slightly, would be useful in probing the interactions between palladium and low-coordination and/or acid sites.

Supports such as ZnO, TiO_2, ZrO_2, and CeO_2 reveal strong interactions with Pd/PdO. These interacting oxides may be active due to an ability to supply oxygen to the reaction and/or they may also cause electronic interactions with Pd/PdO at the surface. These interactions may be similar to the edge and corner sites-Pd/PdO interactions on the high surface area supports. The XPS indicates relatively high binding energy Pd^{2+} states on some high surface areas oxides, as well as on oxide with strong metal support interactions (SMSI) (In the case of Pd/n-Al_2O_3(+) a Pd^{4+} like binding energy is observed). This may indicate similar behaviors of these SMSI and high surface area support surfaces. However, the effects of ZrO_2 and CeO_2 on metal redox and oxygen storage properties reported in literature [23,80,85], along with their abilities to enhance the activity of the Pd catalyst when used as additives, would suggest that, for these two oxides, the ability to supply oxygen is related to their activity promotion.

7.3.4 Deactivation

Several possibilities for deactivation were suggested in this work. It was determined that adding water to the reaction mixture decreased activity. This suggests that water can inhibit the reaction, possibly by competing with pyridine for catalyst sites. However, the diminished activity was not sufficient to attribute deactivation solely to the presence of water. Observation of differential charging in XPS of the spent p-TiO_2 catalyst that is diminished by sputtering indicates the presence of a contaminant on the palladium surface. This points to fouling or poisoning by either an unidentified byproduct, or possibly the desired product itself. XPS and XRD also suggest that the PdO on the fresh catalyst is completely reduced to Pd metal at the end of the reaction. Since pre-reduced catalysts have been shown to be ineffective in this reaction [5], it seems likely that a completely reduced Pd phase would not be active. Water

contamination, carbon fouling or product poisoning, and Pd reduction could be addressed by regeneration of the catalyst in oxidative conditions. For such a treatment, Pd/metal oxide supported catalyst, and particularly those with ZrO_2 and CeO_2 as supports or additives in this reaction are very promising, although the thermal stability of some of the nanoparticle supports would be a concern.

7.4 Final Remarks

In general, it has been shown that nanoparticle oxides can be used to make highly active catalysts, although some traditional oxide supports may be competitive. Additionally, important insight into the activity of nanoparticle catalysts has been obtained. Either a high concentration of corner and edge sites or strong oxide-palladium interactions give active catalysts. This activity may result from more electrophilic palladium/palladium oxide particles as a result of strong metal-support interactions on these types of catalysts. More broadly, excellent alternative catalysts to palladium on carbon have been developed for the oxidative coupling of 4-methylpyridine. This includes both a nanoparticle catalyst (2.5% Pd/n-Al_2O_3+) and a traditional porous support catalyst (5% Pd/p-TiO_2) (2.7 ± 0.27 and 2.6 ± 0.26 g/g catalyst).

7.4.1 Future Work

The work presented here has highlighted several avenues for future study. Certainly, further optimization of catalyst formulation and production is necessary to fully exploit the economic possibilities of this system. For example, further study of the CeO_2 and ZrO_2 as supports and additives would be in order. Given their effectiveness as additives in 5% Pd/n-Al_2O_3 and 5% Pd/n-TiO_2, their use in the highly active 2.5% Pd/alumina and 5% Pd/p-TiO_2 is very promising. Furthermore, now that several promising catalysts have been developed, a study focusing on the reactivation of catalyst can be performed. This would include for example

heating in an oxygen-rich environment, steam oxidation, or the use of an oxygen plasma to burn off the carbon on the surface and reoxidize the Pd metal to PdO.

Additionally, several, more expansive, studies into fundamentals of this system seem in-order. Production of nanoparticles in which sizes could be controlled, would allow more controlled studies of the importance of support structure. Use of a combination of extensive XRD, ISS, and/or TEM would be useful in obtaining better estimates of Pd dispersion, particularly in the unreduced PdO state. Perhaps the most interesting prospect, though, is the use of FTIR. The use of CO_2 and pyridine as probe molecules in FTIR/TPD could give valuable insight into the nature of support sites, and help determine what is responsible for the activities of palladium deposited on supports with these sites. Furthermore, pyridine may be used to directly probe the adsorption sites on Pd catalyst. Nanoparticle-supported Pd catalysts may be particularly well suited for this, as it seems likely that a relatively high fraction of Pd/PdO particles would be on the surface relative to a porous catalyst.

7.4.2 Broader Impact

As discussed in numerous parts of this work, the oxidative coupling of 4-metlypyridine is important, as bipyridines have a wide variety of applications [20-29]. Reducing their cost would have a great impact on the economic viability of many catalyst systems. Additionally, a catalyst active for oxidative-coupling 4-methylpyridine could be applied to other systems such as the coupling of unsubstituted and substituted pyridines, benzenes, as well as other heterocyclic systems, which are all important for the synthesis of fine chemicals. Because of the simple nature of the reaction and the omission of solvents and halogens, these catalysts could have a great impact on environment as well as the cost of some fine chemicals.

The impact, however, is not limited to oxidative coupling reactions. Pd catalyst are used in a wide number of systems [7-19], and their use in other oxidation reactions (particularly the low-

temperature oxidation of CO and CH_4 [12,13,16-18]), as well as methanol reforming and water gas shift reactions [21,43,62,63,84] are particularly important. The catalysts developed in this work increase our knowledge of these important Pd/PdO systems, but this work may have a more practical application. Many of the catalysts were found to have excellent dispersions, despite relatively simple methods of preparations, and their high activities in this reaction may, possibly, correlate to higher activities in other systems, particularly oxidation reactions. More broadly, the use of precipitation on nanoparticles may be applicable to a wide range of active metals and their corresponding reaction systems.

7.4.3 Best Catalyst for Oxidative Coupling of 4-Methylpyridine

The practical goal of this work was to develop a more economically viable catalyst for the oxidative coupling of 4-methylpyridine. While further work is likely needed to produce improved catalysts, the 2.5% Pd precipitation onto n-Al_2O_3(+) and the 5% Pd on p-TiO_2 are the best catalysts to date with activities of 2.7±0.27 g product /g catalyst (105±10% g/g Pd) and 2.6±0.26 g product /g catalyst(52g/g Pd) respectively. While the viability of one vs. the other is related to the cost of the Pd precursor, in small batch quantities, of palladium nitrate, the 2.5% Pd/n-Al_2O_3(+) catalyst is currently the most cost effective.

LIST OF REFERENCES

1. G.D.F. Jackson, W.H.F. Sasse, C.P. Whittle, Aust. J. Chem. 16 (1963) 1126

2. P.E. Rosevear, W.H.F. Sasse, J. Heterocycl. Chem. 8 (1971) 483.

3. P.E. Rosevear, W.H. Sasse, Patent App. No. 40930/72, 1973, p. 1.

4. S. Munavalli, M. Gratzel, Chem. Ind. (1987) 722

5. H. Hagelin, B. Hedman, I. Orabona, T. Åkermark, B. Åkermark, C.A. Klug, J. Mol. Catal. A 164 (2000) 137.

6. L. Guczi, A. Beck, A. Horváth and D. Horváth, Top. Catal. 19 (2002) 157

7. L. S. Escandón, S. Ordóñez, A. Vega, F. V. Díez, J. Haz. Mat. 153(2008) 742

8. M. Schmal, M. Souza, V. Alegre, M. da Silva, D. Ce´sar,C. Perez, Catal. Today 118 (2006) 392.

9. P. Gélin and M. Primet, Appl. Catal. B 39 (2002) 1-37, and references therein.

10. T.V. Choudhary, S. Banerjee and V.R. Choudhary, Appl. Catal. A 234 (2002) 1-23, and references therein.

11. D. Ciuparu, M.R. Lyubovsky, E. Altman, L.D. Pfefferle, A. Datye, Catal. Rev. Sci. Eng. 44 (2002) 593-649.

12. K. Sekizawa, H. Widjaja, S. Maeda, Y. Ozawa, K. Eguchi, Catal. Today 59 (2000) 69.

13. K. Sekizawa, H. Widjaja, S. Maeda, Y. Ozawa, K. Eguchi, Appl. Catal. A 200 (2000) 211.

14. Y. Li, Y. Fan, H. Yang, B. Xu, L. Feng, M. Yang, Y. Chen, Chem. Phys. Lett. 372 (2003) 160.

15. T. Kawakami, Y. Ooka, H. Hattori, W. Chu, Y. Kamiya,T. Okuhara Appl. Catal. A (2007) (In press)

16. O. Pozdnyakova, D. Teschner, A. Wootscha, J. Kröhnert, B. Steinhauer, H. Sauer, L. Tothc, F.C. Jentoft, A. Knop-Gericke, Z. Paál, R. Schlög, J. Catal. 237 (2006) 17.

17. H. Zhu, Z. Qin, W. Shan, W. Shen, J. Wang, J. Catal. 233 (2005) 41.

18. R Zhou, B Zhao, B. Yue, Appl. Surf. Sci. 254 (2008) 4701.

19. D. Ciuparu, A Ensuque, F. Bozon-Verduraz, Appl. Catal. A 326 (2007) 130.

20. C. Kaes, A. Katz and M.W. Hosseini, Chem. Rev. 100 (2000) 3553.

21. V. Balzani, G. Bergamini, F. Marchioni and P. Ceroni, Coord. Chem. Rev. 250 (2006) 1254-1266.

22. C.D. Clark, M.Z. Hoffman, Coord. Chem. Rev. 159 (1997) 359-373.

23. R.C. Evans, P. Douglas and C.J. Winscom, Coord. Chem. Rev. 250 (2006) 2093-2126.

24. L. Gámiz-Gracia, A.M. García-Campaña, J.J. Soto-Chinchilla, J.F. Huertas-Pérez and A. González-Casado, Trends Anal. Chem. 24 (2005) 927-942.

25. N.M.L. Hansen, K. Jankova and S. Hvilsted, Eur. Polym. J. 43 (2007) 255-293.

26. D.L. Feldheim, C.J. Baldy, P. Sebring, S.M. Hendrickson, C.M. Elliott, J. Electrochem. Soc. 142 (1995) 3366.

27. H.Ishii, M Goyal, M Ueda, K. Takeuchi and M. Asai, Applied Catalysis A 201(2000) 101.

28. F. Tsai, B. Lin, M. Chen, C. Mou and S. Liu, Tetrahedron 63 (2007) 4304.

29. W. Wu, S. Chen and F. Tsai, Tetrahedron Lett. 47(2006) 9267.

30. A. Launkonis, D. Lay, A. Mau, A. Saragesor and W. Sasse, Aust. J. Chem. 39 (1986), 1053-1062.

31. 4,4'-dimethyl 2,2'-bipyridine, GFS Chemicals: http://gfschemicals.com/statics/productdetails/cHJvZHVjdGRldGFpbHMxMjc=.html, accessed 10/2/2008

32. L.A. Summers, Adv. Heterocycl. Chem. 35 (1984) 281.

33. G. Cravotto, M. Beggiato, A. Penoni, G. Palmisana, S. Tollari, J. Lévêque, W. Bontrath, Tetrahedron Lett. 46 (2005) 2267.

34. M. Heller, U Schubert, J. Org. Chem. 67 (2002) 8269.

35. R. I. Masel, Principles of Adsorption and Reaction on Surfaces. Wiley: New York (1996).

36. B. D. Cullity, S. R. Stock, Elements of X-ray Diffraction, 3rd Ed. Prentice-Hall: New York (2001).

37. J.F. Moulder, W.F. Stickel, P.E. Sobol, K.D Bomben, Handbook of X-ray Photoelectron Spectroscopy, Physical-Electronics Inc.: Eden Prairie, MN (1995).

38. P.K. Ghosh and T.G. Spiro, J. Am. Chem. Soc. 102 (1980) 5543.

39. P.A. Adcock, F.R. Keene, R.S. Smythe, and M.R. Snow, Inorg. Chem. 23 (1984) 2336.

40. G. Sprintschnik, H.W. Sprintschnik, P.P. Kirsch, and D.G. Whitten, J. Am. Chem. Soc. 99 (1977) 4947.

41. G.R. Newkome, A.K. Patri, E. Holder, U.S. Schubert, Eur. J. Org. Chem. (2004) 235.

42. U.S. Schubert and C. Eschbaumer, Angew. Chem. Int. Ed. 41 (2002) 2892-2926.

43. V. Balzani, A. Juris, M. Venturi, S. Campagna, S. Serroni, Chem. Rev. 96 (1996) 759.

44. K. Kalyanasundaram, Coord. Chem. Rev. 1982, 46, 159-244.

45. 4,4'-dimethyl 2,2'-bipyridine, GFS Chemicals: http://gfschemicals.com/chemicals/gfschem-127.asp, accessed 07/13/07.

46. 2-amino-4-methylpyridine, Fluka >98%, Sigma-Aldrich: https://www.sigmaaldrich.com/catalog/search/ProductDetail/FLUKA/08630, accessed 08/30/07.

47. 4-Methylpyridine 98% , Fluka, Sigma-Aldrich: http://www.sigmaaldrich.com/catalog/search/ProductDetail/FLUKA/80240. accessed 08/30/07.

48. K.W.R. de França, M. Navarro, É. Léonel, M. Durandetti, and J.-Y. Nédélec, J. Org. Chem. 67 (2002) 1838.

49. G.B. Hoflund, Z. Li, W.S. Epling, T. Göbel, P. Schneider and H. Hahn, React. Kinet. Catal. Lett. 70 (2000) 97.

50. NanoActive Aluminum Oxide Plus and NanoActive Aluminum Oxide, NanoScale: http://nanoactive.interkan.net/content/nanoactive_materials/nanoactive_home.asp, accessed on 03/07/07.

51. B. Didillon, E. Merlen, T. Pagès, D. Uzio, Stud. Surf. Sci. Catal. 118 (1998) 41-54.

52. T. Lear, R. Marshall, J.A. Lopez-Sanchez, S.D. Jackson, T.M. Klapötke, M. Bäumer, G. Rupprechter, H.-J. Freund and D. Lennon, J. Chem. Phys. 133 (2005) 174706.

53. P. Canton, G. Fagherazzi, M. Battagliarin, F. Menegazzo, F. Pinna, and N. Pernicone, Langmuir 18 (2002) 6530.

54. R.G. Heidenreich, J.G.E. Krauter, J. Pietsch and K. Köhler, J. Mol. Catal. A 182-183 (2002) 499.

55. F. Zhao, K. Murakami, M. Shirai and M. Arai, J. Catal. 194 (2000) 479.

56. A. Biffis, M. Zecca, M. Basato, Eur. J. Inorg. Chem. (2001) 1131.

57. G. Dyker, Angew. Chem. Int. Ed. 38 (1999) 1698-1712.

58. D. Schröder and H. Schwarz, Angew. Chem. Int. Ed. 34 (1995) 1973-1995.

59. G.M. Badger and W.H.F. Sasse, Adv. Heterocycl. Chem. 2 (1963) 179.

60. J Co´nsul, I. Costilla, C. Gigola, I. Baibich, Appl. Catal. A 339 (2008) 151.

61. J. Hong, W. Chu, M. Chen, X. Wang, T. Zhang, Catal. Commun. 8 (2007) 593.

62. A. Casanovas, J. Llorca, N.S. Homs, J. Fierro, P. de la Piscina, J. Mol. Catal. A 250 (2006) 44.

63. S. Liu, K. Takahashi, K. Fuchigami, K. Uematsu, Appl. Catal. A 299 (2006) 58.

64. A. Garron a, K La´za´r , F. Epron/App Cat B: Env. 59 (2005) 57-69.

65. M. Garcia,1 A. Martinez-Arias, L Salamanca, J. Coronado, J. Anderson, J. Conesa, J. Soria, J. Catal. 187 (1999) 474.

66. L.M. Neal, H.E. Hageline-Weaver, J. Mol. Catal. A, 284 (2008) 141. (included, in part, in chapter 2)

67. NanoScale Materials Inc., http://nanoactive.interkan.net/content/nanoactive_materials/nanoactive_home.asp, accessed on 10/01/08.

68. Nanostructured & Amorphous Materials Inc., http://www.nanoamor.com/__nanoparticles accessed on 10/01/08.

69. Alfa Aesar, http://www.alfa.com/alf/index.htm, accessed on 10/01/08.

70. E.D. Park, S.H. Choi, J.S. Lee, J. Phys. Chem. B 104 (2000) 5586,

71. A.D. Silva, M.L. Patitucci, H.R. Bizzo, E. D'Elia and O.A.C. Antunes, Catal. Commun. 3 (2002) 435.

72. D.R. Bryant, J.E. McKeon, B.C. Ream, J. Org. Chem. 33 (1968) 4123.

73. T. Ohishi, J. Yamada, Y. Inui, T. Sakaguchi, M. Yamashita, J. Org. Chem. 59 (1994) 7521.

74. H. Hagelin, J.D. Oslob, B. Åkermark, Chem. Eur. J. 5 (1999) 2413.

75. T. Caputo, L. Lisi, R. Pirone, G. Russo, Appl. Catal. A 348 (2008) 42.

76. A. Marquez, J. Sanz, Appl. Surf. Sci. 238 (2004) 82.

77. 5y Palladium Price, Kitco, http://www.kitco.com/charts/popup/pd1825nyb_.html accessed 10/01/08.

78. C.E. Gigola, M.S. Moreno, I. Costilla, M.D. Sanchez, Applied Surface Science 254 (2007) 325.

79. W. Shen, Y. Matsumura, J. Mol. Catal. A. 153 (2000) 165.

80. J. Kaspar, P. Fornasiero, M. Graziani, Catalysis Today 50 (1999) 285.

81. J.M. Padilla, G. Del Angel, J. Navarrete, Catalysis Today 133-135 (2008) 541.

82. A. Trovarelli, C. de Leitenburg, M. Boaro, G. Dolcetti, Catal. Today 50 (1999) 353.

83. L. Bollmann, J. L. Ratts, A. M. Joshi, J. of Catal. 257 (2008) 43.

84. S. Liu, K. Takahashi, H. Eguchi, K. Uematsu, Catal. Today 129 (2007) 287.

85. L.M. Martinez T, C. Montes de Correa, J.A. Odriozola, M.A. Centeno, Catal. Today 107-108 (2005) 800.

86. F. Pinna, Catal. Today 41 (1998) 129.

87. S. Jones, L.M. Neal, H. E. Hagelin-Weaver, App. Catal. B 84 (2008) 631.

88. C.T. Wang , J.C. Lin, App. Surf. Sci. 254 (2008) 4500.

89. R.N. Gayen, S.N. Das, S. Dalui, R. Bhar, A.K. Pal J. Crystal Growth 310 (2008) 4073

90. P.M. Maitlis, "The Organic Chemistry of Palladium", Academic Press, New York, 1971.

91. J.Tsuji, "Palladium Reagents and Catalysis: Innovation in Organic Synthesis," Wiley, Chichester, UK (1995).

92. J.-L. Malleron, J.-C. Fiaud and J.-Y. Legros, "Handbook of Palladium-Catalyzed Organic Reactions", Academic Press Limited, London, UK, 1997.

93. A.K. Santra and D.W. Goodman, Electrochim. Acta 47 (2002) 3595-3609.

94. S.-H. Oh and G.B. Hoflund, J. Catal. 245 (2007) 35-44.

95. M. Hosseini, S. Siffert, H.L. Tidahy, R. Cousin, J.-F. Lamonier, A. Aboukais, A. Vantomme, M. Roussel, B.-L. Su, Catal. Today 122 (2007) 391-396.

96. P. Papaefthimiou, T. Ioannides, and X.E. Verykios, Appl. Catal. B 13 (1997) 175-184.

97. E.M. Cordi and J.L. Falconer, J. Catal. 162 (1996) 104-117.

98. M. Besson, P. Gallezot, Catal. Today 57 (2000) 127-141.

99. C. A. Páez, N. J. Castellanos, F. Martínez O., F. Ziarelli, G. Agrifoglio, E A. Páez-Mozo, and H. Arzoumanian, Catal. Today 620 133–135 (2008) 619–62.

100. C.D. Wagner, W.M., Riggs, L.E Davis, J.F. Moulder and G.E. Muilenberg, Eds., Handbook of X-ray Photoelectron Spectroscopy, Perkin-Elmer Corp.: Eden Prairie, MN, (1979).

101. J.C. Rivière, S. Myhra, Eds., Handbook of Surface and Interface Analysis, Marcel Dekker: New York, (1998), 57-158.

102. National Institute of Standards and Technology, NIST on-Line XPS Database http://srdata.nist.gov/xps/intro.aspx [Accessed 10/28/08]

103. M. Brun, A. Berthet, J.C. Bertolini, J. Electron Spectrosc. Relat. Phenom. 104 (1999) 55

104. K. T. Jung, A. T. Bell, Catal. Lett. 80(2002)63-68

105. M.D. Rhodes, A.T. Bell, J. of Catal. 233 (2005) 198.

106. 4,4'-dimethyl 2,2' –bipyridine http://www.sigmaaldrich.com/catalog/search/ProductDetail/ALDRICH/245739 accessed 09/19/08

107. Raney nickel, Fluka # 8344 bipyridine http://www.sigmaaldrich.com/MSDS accessed 09/19/08

BIOGRAPHICAL SKETCH

Luke Michael Neal was born in Peoria, Illinois, to George and Sue Neal in 1981. He was raised in the town of Morton, Illinois where he attended Morton Community High School. After graduating high school in 1999 he attended the University of Illinois at Urbana-Champaign, where he pursued a bachelor's degree in chemical engineering. During his undergraduate education, he worked summers at the USDA National Center for Agriculture Utilization Research (NCAUR) in Peoria, Illinois. While there, he assisted in research into the purification of soy hull proteins and the use of the corn-ethanol byproduct, zien as a bioplastic. After the graduating from the University of Illinois in 2003, he continued to work as a science aide for NCAUR while advancing his education with coursework at Bradley University in Peoria.

In fall 2004, he came to Gainesville, Florida, to pursue a doctorate of philosophy in chemical engineering at the University of Florida. His research focused on use of nanoparticle oxides in catalyst. Much of this work was devoted to nanoparticle supported palladium oxide for use as an oxidative coupling catalyst. Additionally he contributed to research into nanoparticle nickel catalystss for biomass to hydrogen conversion and the use of nanoparticle iron and cobalt oxides for the catalytic decomposition of carbon monoxide into carbon nanotubes.